Metallic nanoantennas for Field-Enhanced Spectroscopy and Microscopy: from Visible to TeraHertz

Javier Aizpurua

Centro de Física de Materiales CSIC-UPV/EHU

and Donostia International Physics Center (DIPC),

Donostia-San Sebastián, Spain

Summer School on Plasmonics
September 13-17, 2009
Porquerolles Island, Côte d'Azur, France

Outline

- Basics: Localized Plasmons

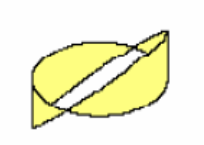

- Optical antennas for SERS

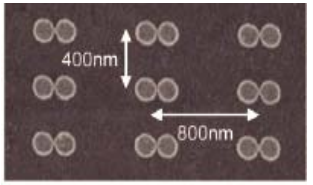

- Infrared antennas for SEIRA

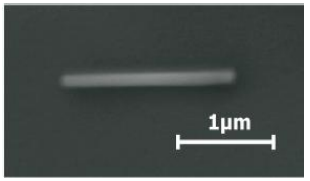

- Substrate-Enhanced Infrared Near-Field Microscopy

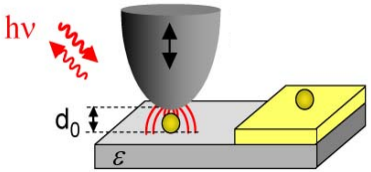

- THz Near-field Nanoscopy

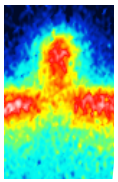

Radio Frequency Antennas

Half wave
dipole antennas

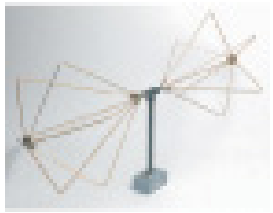

Biconical antenna

Monopole antenna

Combilog antenna

Yagi-Uda antenna

Horn antenna

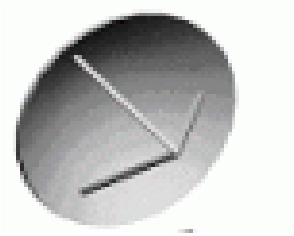

Parabolic antenna

Active loop antenna

Scaling down in size ← Scaling down in wavelength

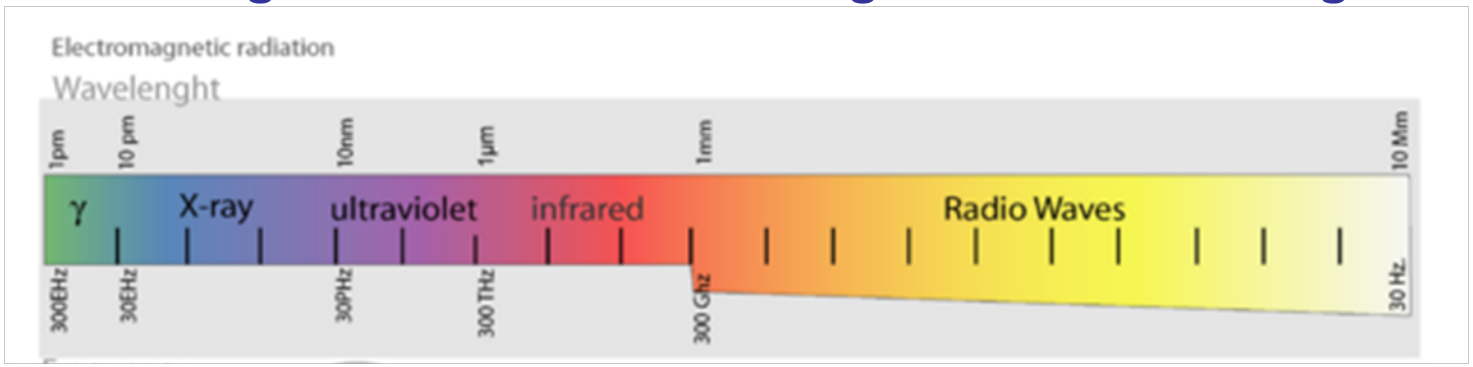

Visible light → Optical antenna → Nanoantenna

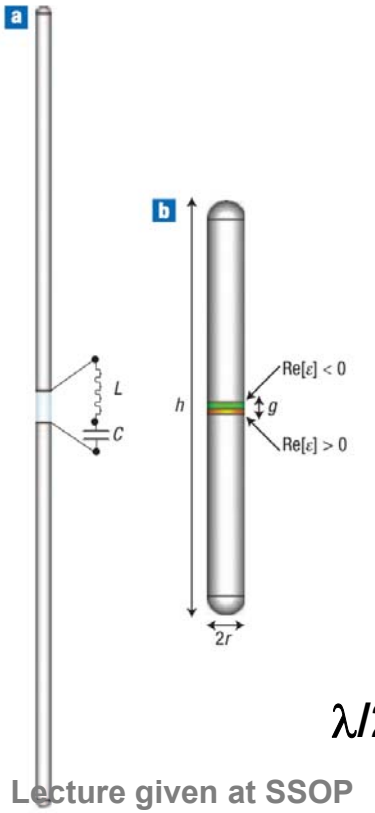

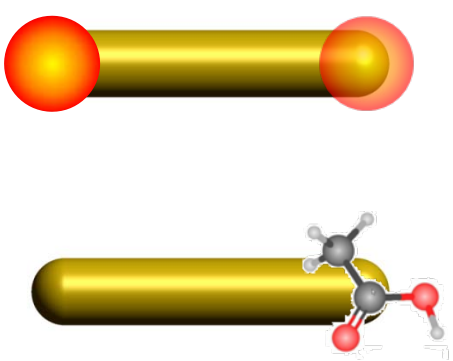

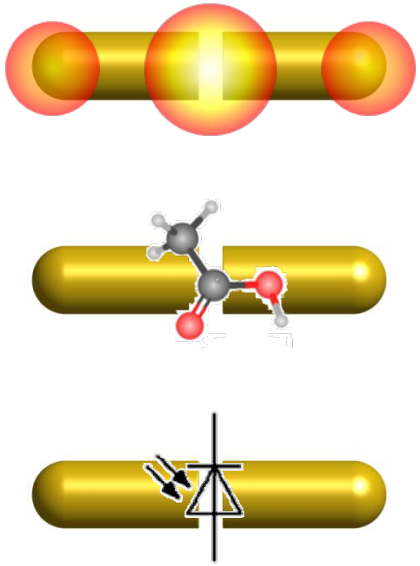

λ/2 nanoantenna

J. Aizpurua, Lecture given at SSOP Porquerolles, Sept. 2009

The simplest optical antenna: a metallic particle

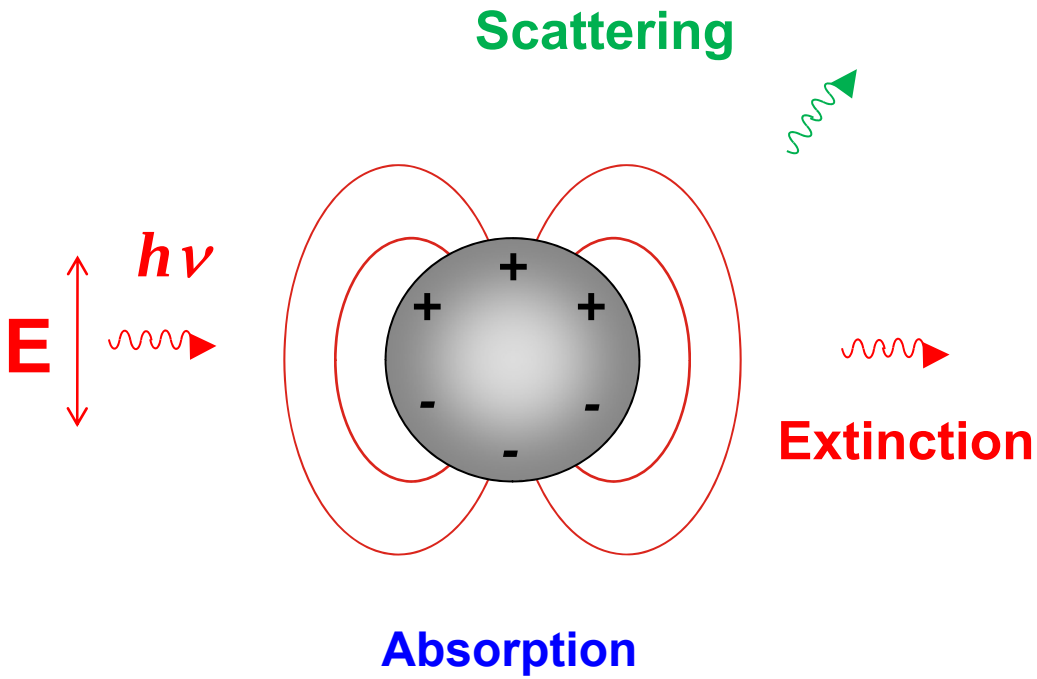

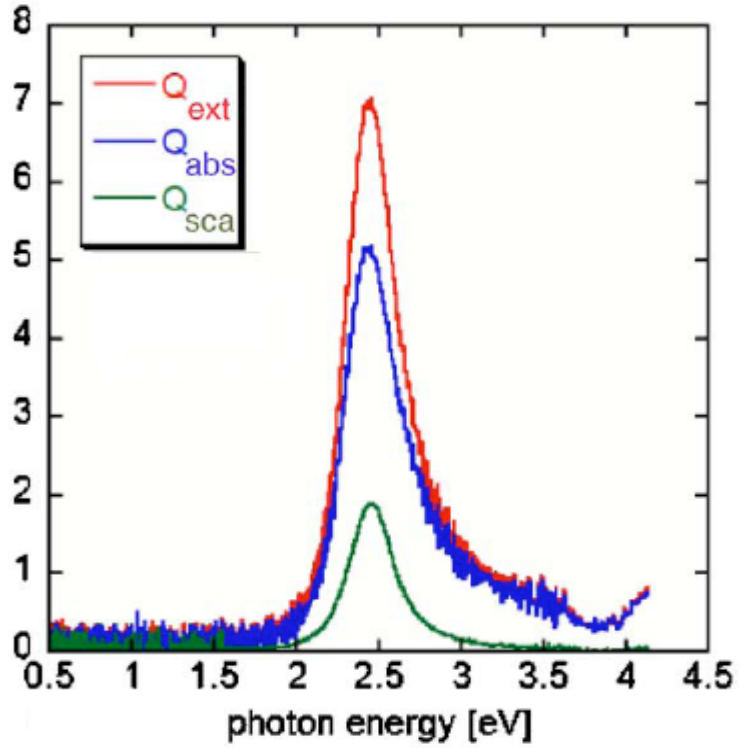

Enhancement of absorption and emission:
Bringing effectively the far-field into the near-field

J. Aizpurua, Lecture given at SSOP Porquerolles, Sept. 2009

Metal particle plasmons

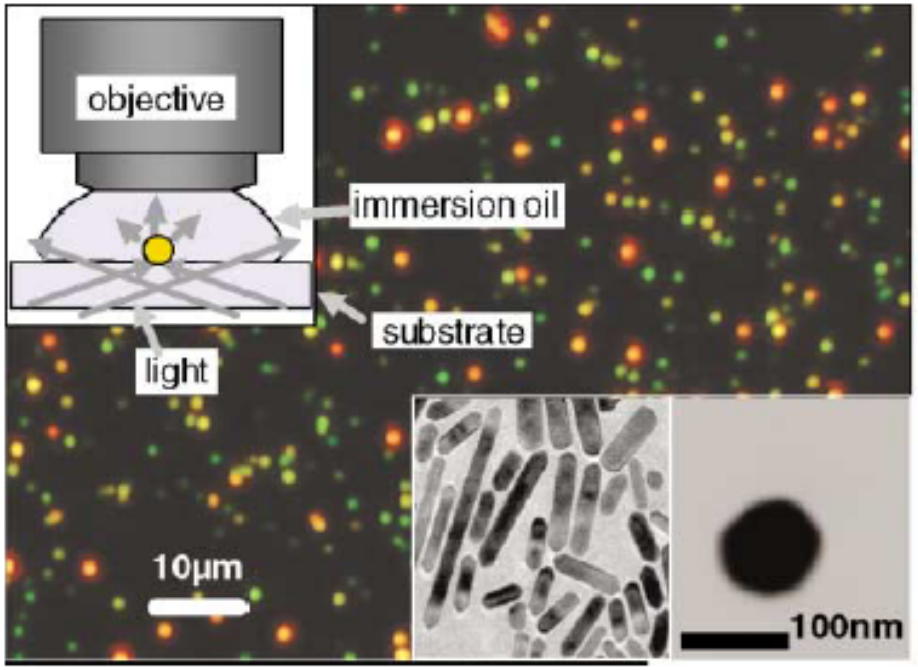

FIG. 2 (color). True color photograph of a sample of gold nanorods (red) and 60 nm nanospheres (green) in dark-field illumination (inset upper left). Bottom right: TEM images of a dense ensemble of nanorods and a single nanosphere.

Standard textbooks:

- Kreibig, Vollmer, Optical properties of metal clusters, Springer1995
- Bohren, Huffmann, Absorption and scattering of light by small particles, Wiley 1983

Metallic nanorod as a λ/2 optical antenna

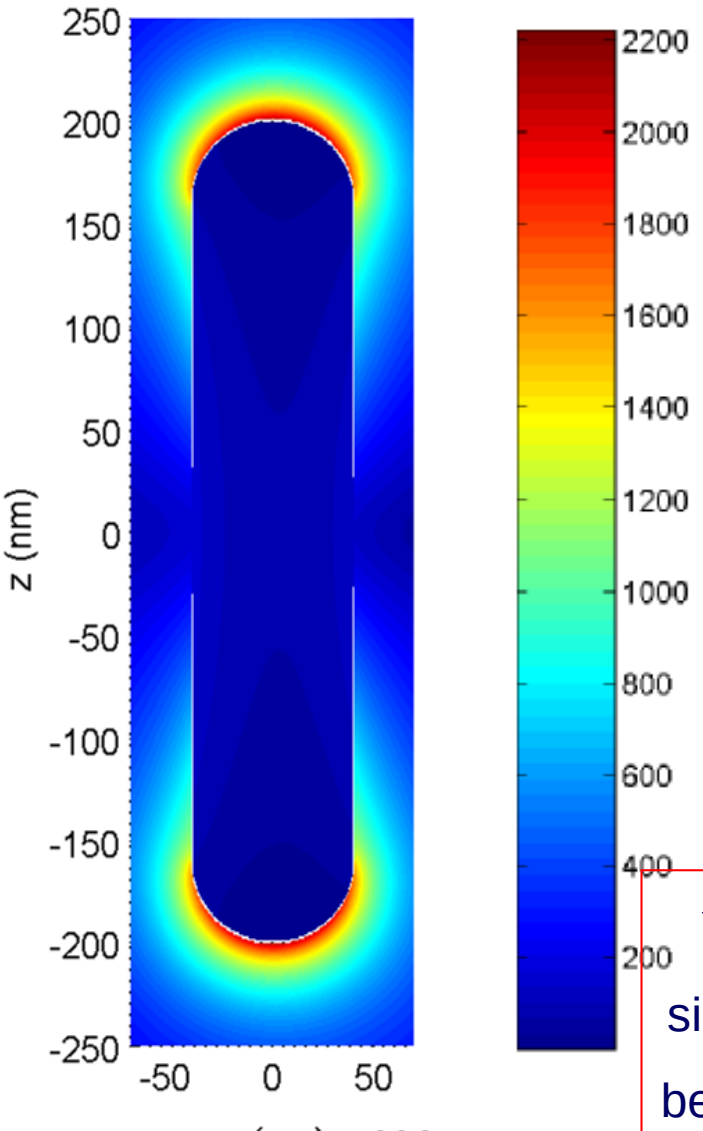

In analogy to a λ/2 radiowave antenna, we call a nanosized rod-like metallic structure a λ/2 optical antenna .

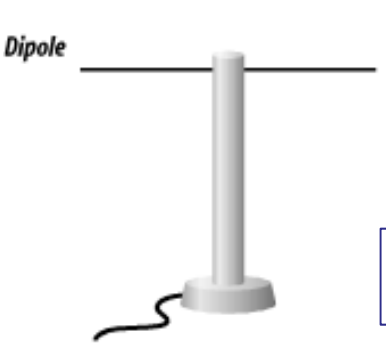

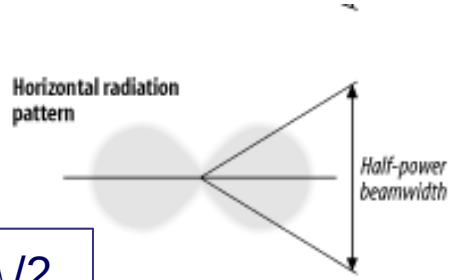

L=λ/2

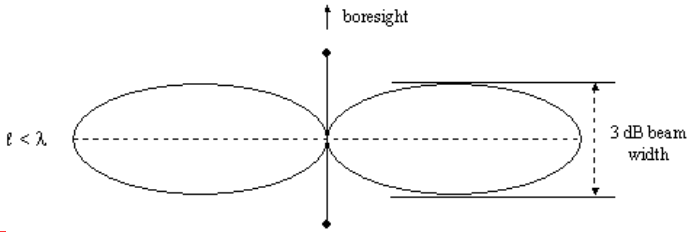

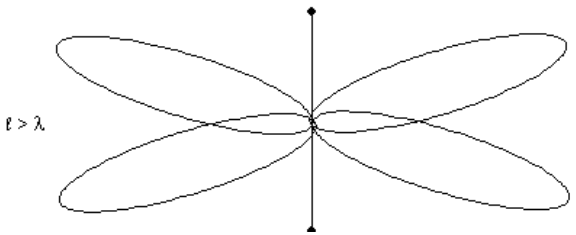

YES BUT, it is just similar, and not equal because of plasmons.

Bulk plasmons

A plasmon is a collective oscillation of the conduction electrons

Bulk plasmon:

The rigid displacement of the electrons induces a dipolar moment and an electric field opposing the displacement

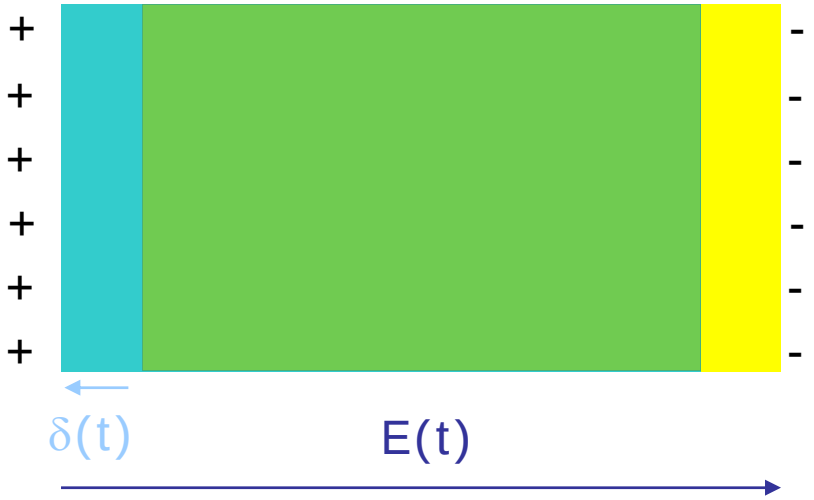

Newton's equation for $\delta(t)$:

Electron density

$$nm_e \frac{d^2}{dt^2}\delta(t) = -enE(t) = -4\pi n^2 e^2 \delta(t)$$

=> Harmonic oscillator

$$\omega_p = \sqrt{\frac{4\pi n_e e^2}{m_e}}$$

All the electrons are involved in the oscillation. The energy of those oscillations in typical metals might be triggered out by external probes.

Surface plasmons

Electromagnetic surface waves which exist at the interface between 2 media whose ε have opposite sign.

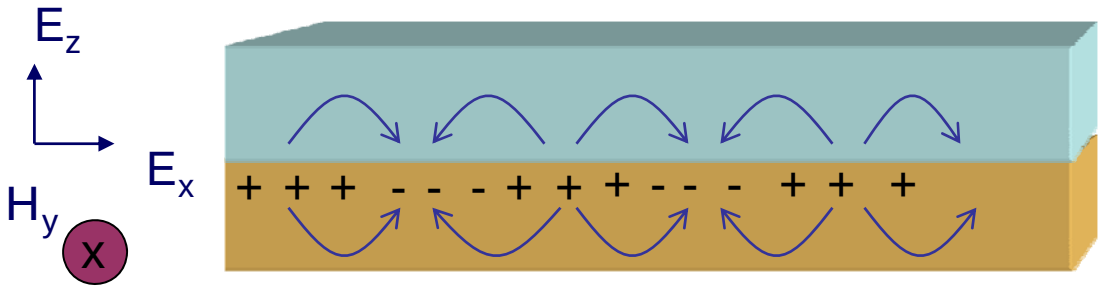

Metal ($\varepsilon_1=\varepsilon_1'+i\varepsilon_1''$)

Dielectric ($\varepsilon_2=\varepsilon_2'+i\varepsilon_2''$)

$$E^{(1)} = E_o^{(1)} e^{i(k_x x-\omega t)-\alpha^{(1)}|z|} \qquad k_x = k_x' + ik_x'' = \sqrt{\frac{\varepsilon_1\varepsilon_2}{\varepsilon_1+\varepsilon_2}}\left(\frac{\omega}{c}\right)$$

Dispersion relation

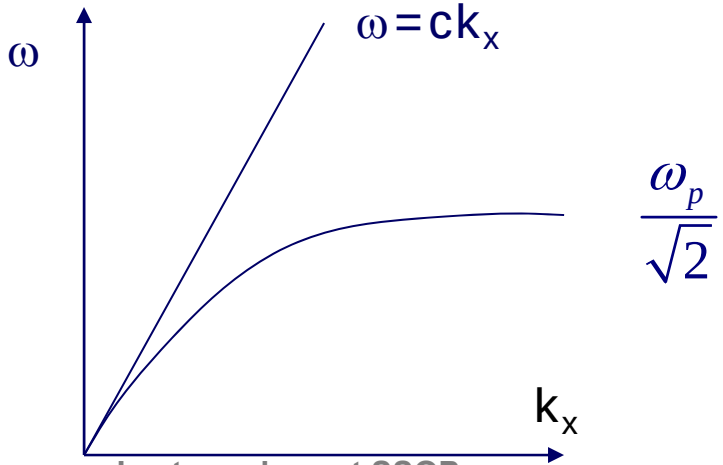

Drude model $\varepsilon' = 1 - \dfrac{\omega_p^2}{\omega^2}$

Surface plasmons $\omega_s = \dfrac{\omega_p}{\sqrt{2}}$

PHYSICAL REVIEW VOLUME 106, NUMBER 5 JUNE 1, 1957

Plasma Losses by Fast Electrons in Thin Films*

R. H. RITCHIE
Health Physics Division, Oak Ridge National Laboratory, Oak Ridge, Tennessee
(Received February 7, 1957)

The angle-energy distribution of a fast electron losing energy to the conduction electrons in a thick metallic foil has been derived assuming that the conduction electrons constitute a Fermi-Dirac gas and that the fast electron undergoes only small fractional energy and momentum changes. This distribution exhibits both collective interaction characteristics and individual interaction characteristics, and is more general than the result obtained by other workers. Describing the conduction electrons by the hydrodynamical equations of Bloch, it has been shown that for very thin idealized foils energy loss may occur at a value which is less than the plasma energy, while as the foil thickness decreases below $\sim v/\omega_p$ the loss at the plasma energy becomes less than that predicted by more conventional theories. The net result is an increase in the energy loss per unit thickness as the foil thickness is decreased. It is suggested that the predicted loss at subplasma energies may correspond to some of the low-lying energy losses which have been observed by experimenters using thin foils.

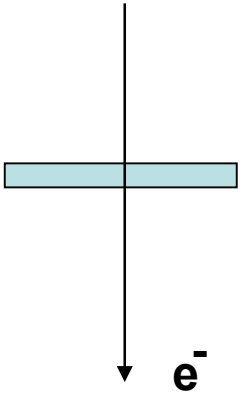

$$P(k_\perp,\omega)\rightarrow\frac{e^2a}{\hbar\pi^2v^2}\left\{\frac{\mathrm{Im}(1/\epsilon)}{(k_\perp^2+\omega^2/v^2)}-\frac{2k_\perp}{a(k_\perp^2+\omega^2/v^2)^2}\mathrm{Im}\left(\frac{(1-\epsilon)^2}{\epsilon(1+\epsilon)}\right)\right\}$$

Now let us define

$$P(k_\perp,\omega)=\{aP_\infty'(k_\perp,\omega)+P_b(k_\perp,\omega)\},$$

Now let us define

$$P(k_\perp,\omega)=\{aP_\infty'(k_\perp,\omega)+P_b(k_\perp,\omega)\},$$

where P_∞' is the transition probability per unit foil thickness in an infinite foil and P_b is the term introduced by the boundary effect. Then one may write, inserting the expression for ϵ,

$$P_b=\frac{e^2}{\pi^2\hbar v^2}\frac{2k_\perp}{(k_\perp^2+\omega^2/v^2)^2}\cdot\frac{g\omega_p^4}{\omega}\cdot\left\{\frac{\frac{1}{4}\omega_p^2}{(\omega^2-\frac{1}{2}\omega_p^2)^2+g^2\omega^2}-\frac{\omega_p^2}{(\omega^2-\omega_p^2)^2+g^2\omega^2}\right\}. \quad (25)$$

One notes that the effect of the boundary is to cause a decrease in loss at the plasma frequency and an additional loss at $\omega=\omega_p/\sqrt{2}$. Call the probabilities for these

Surface plasmons

Electromagnetic surface waves which exist at the interface between 2 media whose ε have opposite sign.

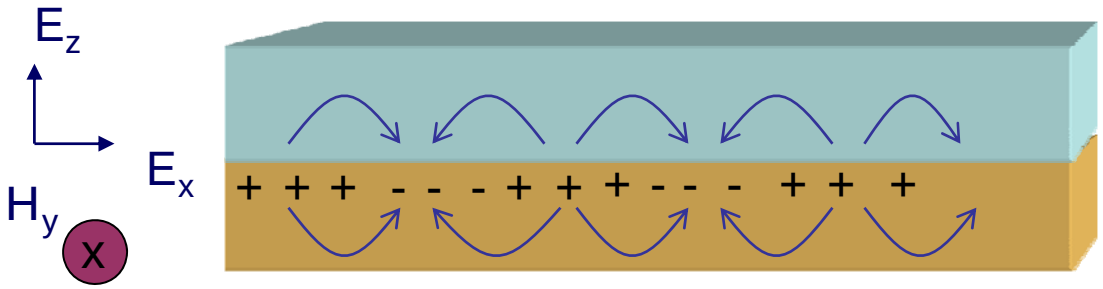

$$E^{(1)} = E_o^{(1)} e^{i(k_x x - \omega t) - \alpha^{(1)}|z|} \qquad k_x = k_x' + ik_x'' = \sqrt{\frac{\varepsilon_1 \varepsilon_2}{\varepsilon_1 + \varepsilon_2}} \left(\frac{\omega}{c}\right)$$

Dispersion relation

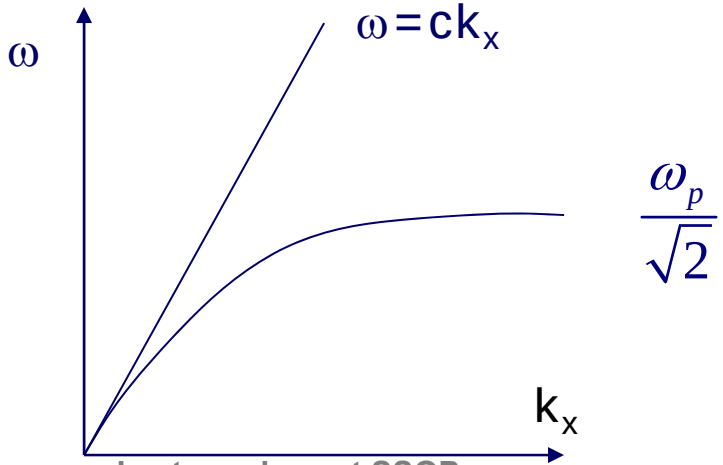

Drude model $\varepsilon' = 1 - \dfrac{\omega_p^2}{\omega^2}$

Surface plasmons $\omega_s = \dfrac{\omega_p}{\sqrt{2}}$

Methods of SPP excitation

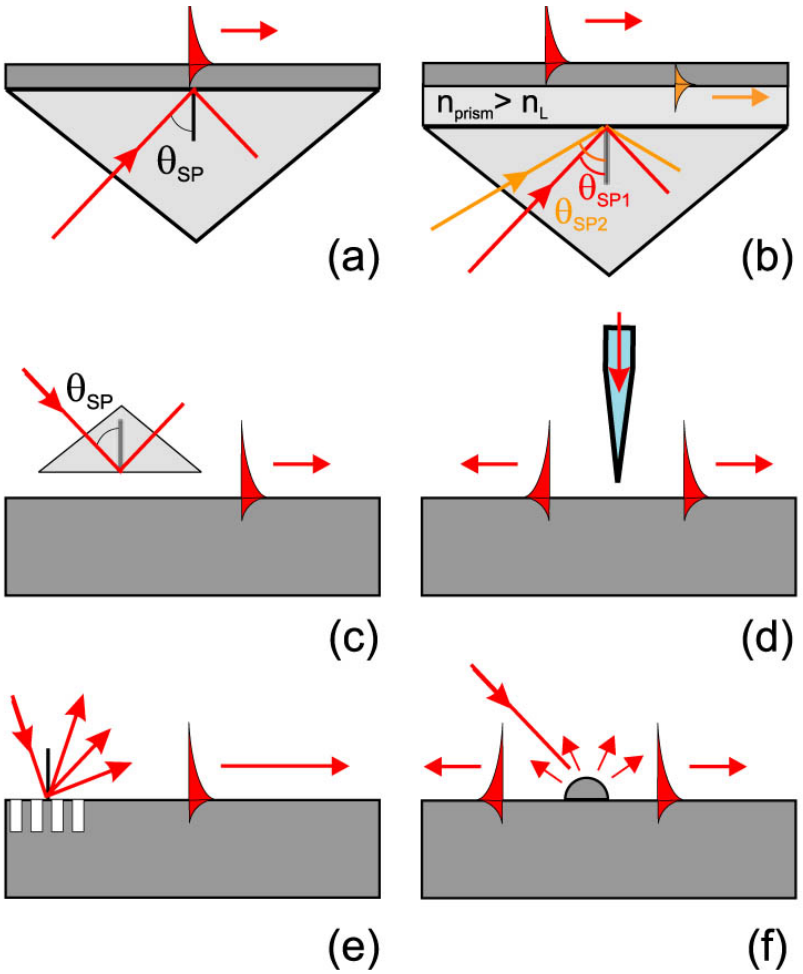

$n_{prism} > n_L$!!

SPP excitation configurations: (a) Kretschmann geometry, (b) two-layer Kretschmann geometry, (c) Otto geometry, (d) excitation with an SNOM probe, (e) diffraction on a grating, and (f) diffraction on surface features.

J. Aizpurua, Lecture given at SSOP Porquerolles, Sept. 2009

Nano-optics with localised plasmons

Characteristics

- Confined fields:
  - *Nanooptics*
- Enhanced field:
  - *Lighting rod effect*
- Tunability:
  - *Geometry*
- Coupling:
- Wavelength range:
  - *Visible ➔ Infrared*

Resonances dependence

with size

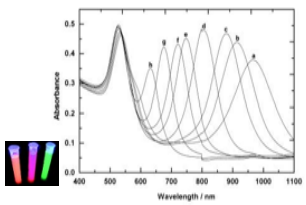

with shape

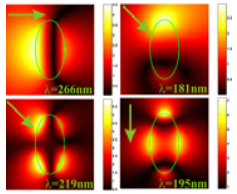

with material

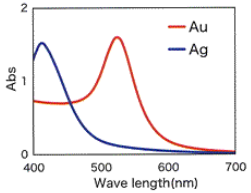

with coupling

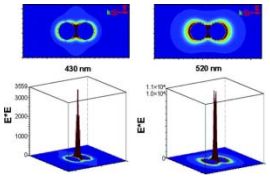

Plasmon polariton

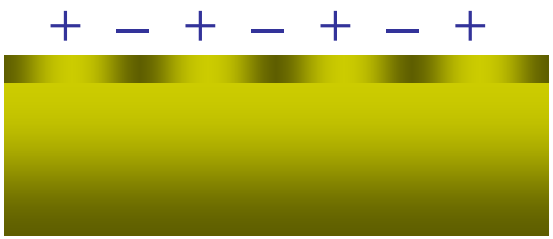

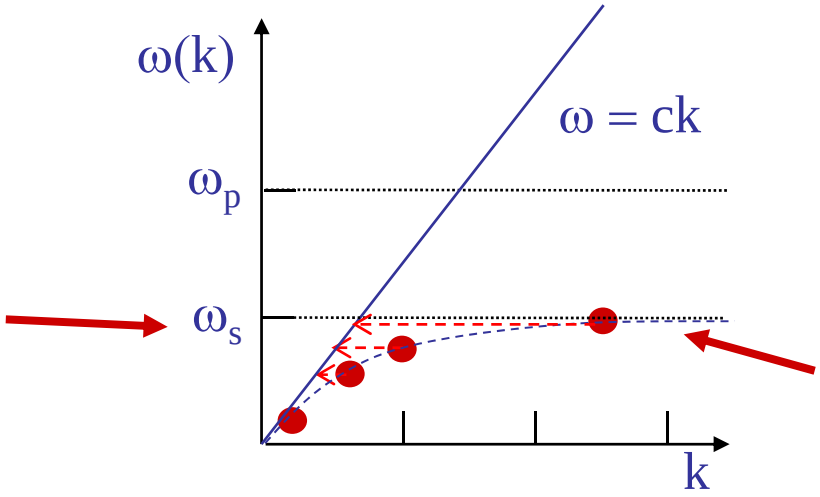

Confined plasmon

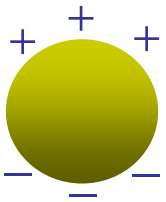

J. Aizpurua, Lecture given at SSOP Porquerolles, Sept. 2009

Light-particle interaction

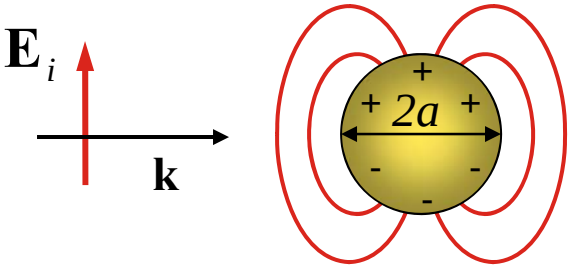

Quasi-static case: λ >> a

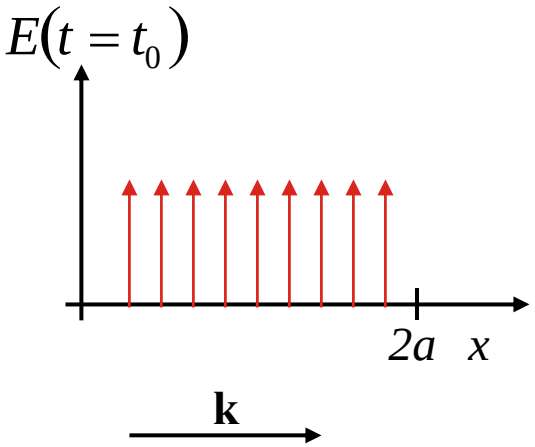

General case: λ <= a

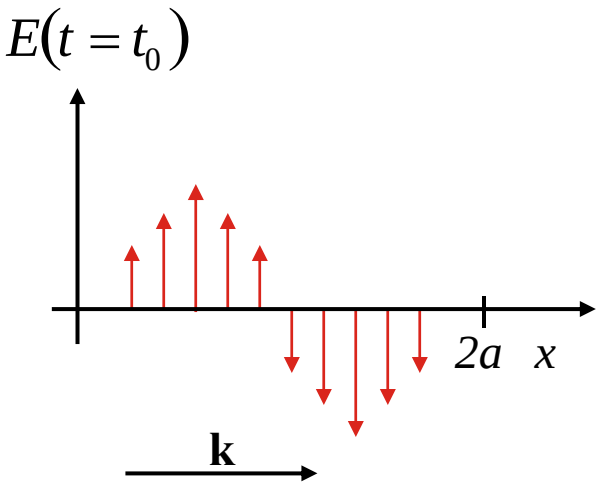

Phase shifts in the particles:
retardation, multipole excitations

Homogeneous polarization:
All points of an object respond simultaneously to the incoming (exciting) field.

⇒ Helmholtz eq. reduces to Laplace equation:

$$\nabla^2 \Phi = 0$$

⇒ el. field: $\mathbf{E} = -\nabla \Phi$

Small sphere

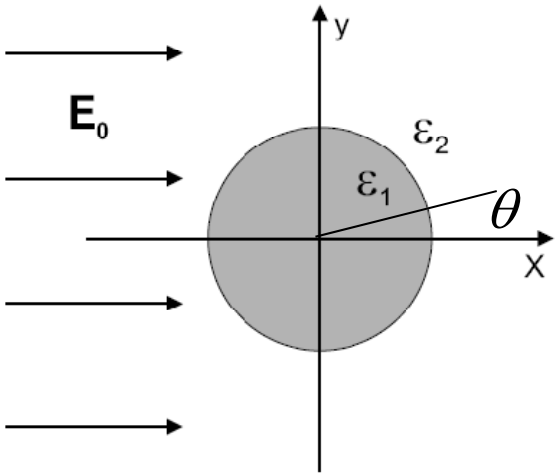

The electric fields inside (E_1) and outside (E_2) the sphere can be obtained from the scalar potentials $\Phi = \Phi(r, \theta, \varphi)$

$$\mathbf{E}_1 = -\nabla\Phi_1 \quad \text{with} \quad \nabla^2\Phi_1 = 0$$

$$\mathbf{E}_2 = -\nabla\Phi_2 \quad \text{with} \quad \nabla^2\Phi_2 = 0$$

$$\Phi_2 = \Phi_{scatter} + \Phi_0$$

Solve Lapace equation in spherical coordinates:

$$\frac{1}{r^2 \sin\theta}\left[\sin\theta\frac{\partial}{\partial r}\left(r^2\frac{\partial}{\partial r}\right) + \frac{\partial}{\partial\theta}\left(\sin\theta\frac{\partial}{\partial\theta}\right) + \frac{1}{\sin\theta}\frac{\partial^2}{\partial\varphi^2}\right]\Phi(r,\theta,\varphi) = 0$$

Boundary conditions:

$$\frac{\partial\Phi_1}{\partial\theta} = \frac{\partial\Phi_1}{\partial\theta} \quad (r = a)$$

continuity of the tangential electric fields

$$\varepsilon_1\frac{\partial\Phi_1}{\partial r} = \varepsilon_2\frac{\partial\Phi_2}{\partial r} \quad (r = a)$$

continuity of the normal component of the electric displacement

Small sphere

Homogeneous electric field along x-direction: $\Phi_0 = -E_0 x = -E_0 r\cos\theta$

The following potentials satisfy the Laplace equation and boundary conditions:

$$\Phi_1 = -E_0 \frac{3\varepsilon_2}{\varepsilon_1 + 2\varepsilon_2} r\cos\theta$$

$$\Phi_2 = -E_0 r\cos\theta + E_0 \frac{\varepsilon_1 - \varepsilon_2}{\varepsilon_1 + 2\varepsilon_2} a^3 \frac{\cos\theta}{r^2}$$

From $\mathbf{E} = -\nabla\Phi$ **we obtain**

$$\mathbf{E}_1 = E_0 \frac{3\varepsilon_2}{\varepsilon_1 + 2\varepsilon_2} (\cos\theta\ \mathbf{e}_r - \sin\theta\ \mathbf{e}_\theta) = E_0 \frac{3\varepsilon_2}{\varepsilon_1 + 2\varepsilon_2}\ \mathbf{e}_x$$

$$\mathbf{E}_2 = E_0(\cos\theta\ \mathbf{e}_r - \sin\theta\ \mathbf{e}_\theta) + \frac{\varepsilon_1 - \varepsilon_2}{\varepsilon_1 + 2\varepsilon_2} \frac{a^3}{r^3} E_0\ (2\cos\theta\ \mathbf{e}_r + \sin\theta\ \mathbf{e}_\theta)$$

The field is independent of the azimuth angle φ which is a result of the symetry implied by the direction of the applied electric field.

Small sphere

Small sphere: $$\Phi_2 = -E_0 r\cos\theta + E_0 \frac{\varepsilon_1 - \varepsilon_2}{\varepsilon_1 + 2\varepsilon_2} a^3 \frac{\cos\theta}{r^2}$$

Dipole: $$\Phi_{dipole} = \frac{p}{4\pi\varepsilon_2}\frac{\cos\theta}{r^2}$$

⇨ The field outside the sphere is the superposition of the applied field and the field of an ideal dipole at the sphere origin

The dipole moment is given by

$$\mathbf{p} = 4\pi\varepsilon_0\varepsilon_2 a^3 \frac{\varepsilon_1 - \varepsilon_2}{\varepsilon_1 + 2\varepsilon_2}\mathbf{E}_0$$

Generally the dipole moment is defined by $\mathbf{p} = \varepsilon_0\varepsilon_2\alpha\mathbf{E}_0$

⇨ **Polarizability of the sphere:** $$\alpha = 4\pi a^3 \frac{\varepsilon_1 - \varepsilon_2}{\varepsilon_1 + 2\varepsilon_2}$$

Small sphere

We can describe the light scattering of a small sphere by plane wave scattering at an ideal point dipole with dipole moment derived on the previous slides. The dipole field is given by:

$$\mathbf{E}(\mathbf{r}) = \frac{1}{4\pi\varepsilon_0}\frac{e^{ikr}}{r}\left\{k^2\left[(\mathbf{n}\times\mathbf{p})\times\mathbf{n}\right] + \frac{1}{r}\left(\frac{1}{r} - ik\right)\left[3\mathbf{n}(\mathbf{n}\cdot\mathbf{p}) - \mathbf{p}\right]\right\}e^{i\omega t} \qquad \text{with} \quad \mathbf{n} = \frac{\mathbf{r}}{r}$$

Near-field zone:

$kr << 1$ $(r << \lambda)$

$$\mathbf{E}(\mathbf{r}) = \frac{1}{4\pi\varepsilon_0}\frac{3\mathbf{n}(\mathbf{n}\cdot\mathbf{p}) - \mathbf{p}}{r^3}e^{-i\omega t}$$

electrostatic dipole field

harmonic time dependency

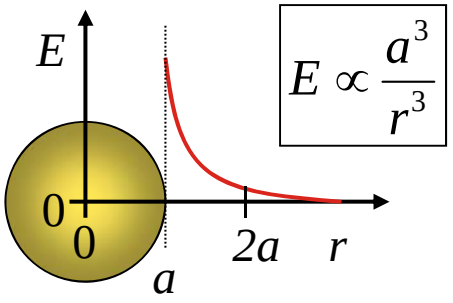

$$E \propto \frac{a^3}{r^3}$$

Radiation zone:

$kr >> 1$ $(r >> \lambda)$

$$\mathbf{E}(\mathbf{r}) = \frac{(\mathbf{n}\times\mathbf{p})\times\mathbf{n}}{r}\frac{k^2}{4\pi\varepsilon_0}e^{i(kr-\omega t)}$$

propagating wave

Far- and near-field calculations for a sphere $a << \lambda$

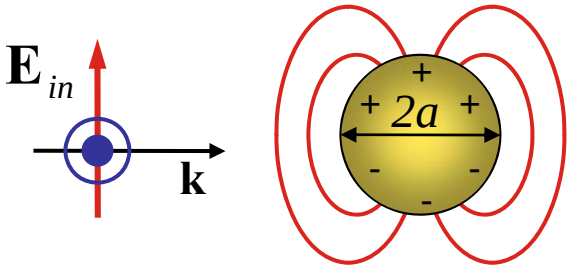

Near-field scattering

$$I = \left| \mathbf{E}_{in} + \mathbf{E}_{particle} \right|^2$$

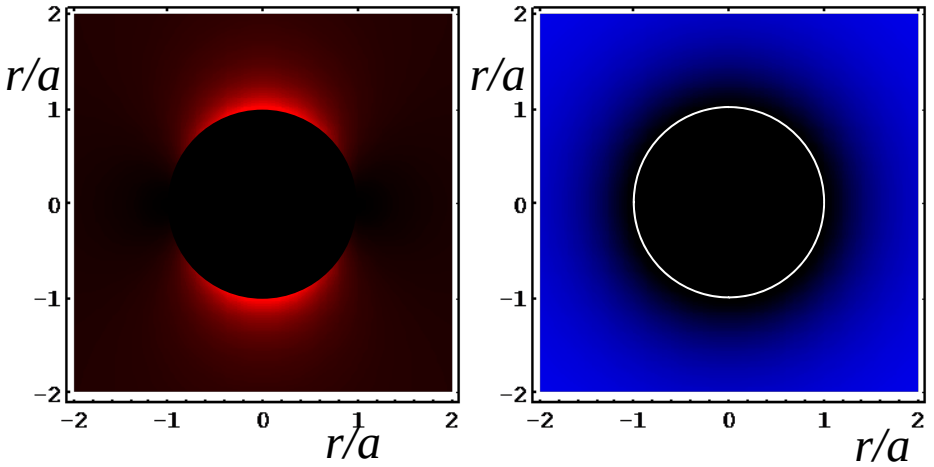

Pointing vector is not always radial

Far-field scattering
(transverse fields)

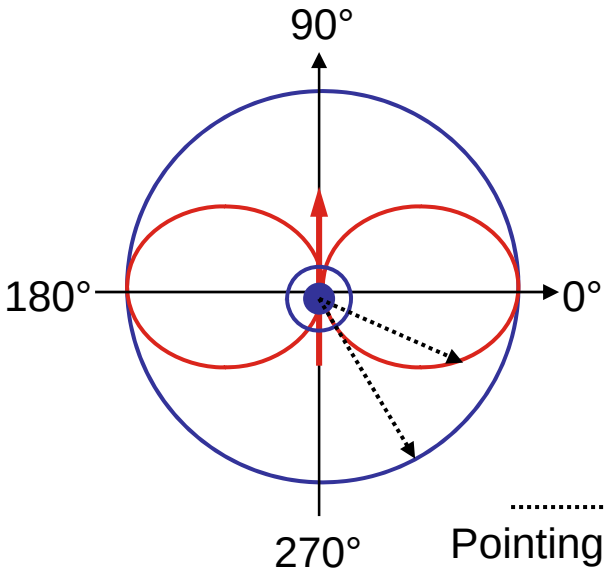

Pointing vector always radial!

Optical cross sections of small spheres

Integrating the Poynting vector $\mathbf{S}_{sca}$ ($\mathbf{S}_{abs}$) over a close spherical surface we obtain the totally scattered (absorbed) power P_{sca} (P_{abs}) from which we can calculate the scattering (absorption) cross section $C_{sca} = P_{sca}/I_i$ ($C_{abs} = P_{abs}/I_i$):

Scattering cross section:

$$C_{sca} = \frac{8\pi}{3} k^4 a^6 \left| \frac{\varepsilon - \varepsilon_m}{\varepsilon + 2\varepsilon_m} \right|^2 = \frac{k^4}{6\pi} |\alpha|^2$$

$$\Rightarrow \quad C_{sca} \propto \frac{a^6}{\lambda^4}$$

Absorption cross section:

$$C_{abs} = 4\pi k a^3 \, \mathrm{Im}\left\{ \frac{\varepsilon - \varepsilon_m}{\varepsilon + 2\varepsilon_m} \right\} = k \, \mathrm{Im}\{\alpha\}$$

$$\Rightarrow \quad C_{abs} \propto \frac{a^3}{\lambda}$$

- stronger scattering at shorter wavelength (Rayleigh scattering, blue sky)

- for large particle extinction is dominated by scattering whereas for small particles it is associated with absorption

- scattering of single particles <10nm is difficult to measure (low signal/noise and low signal/background)

Dielectric function of metals and polar crystals

Metal
collective free electron oscillations (plasmons)

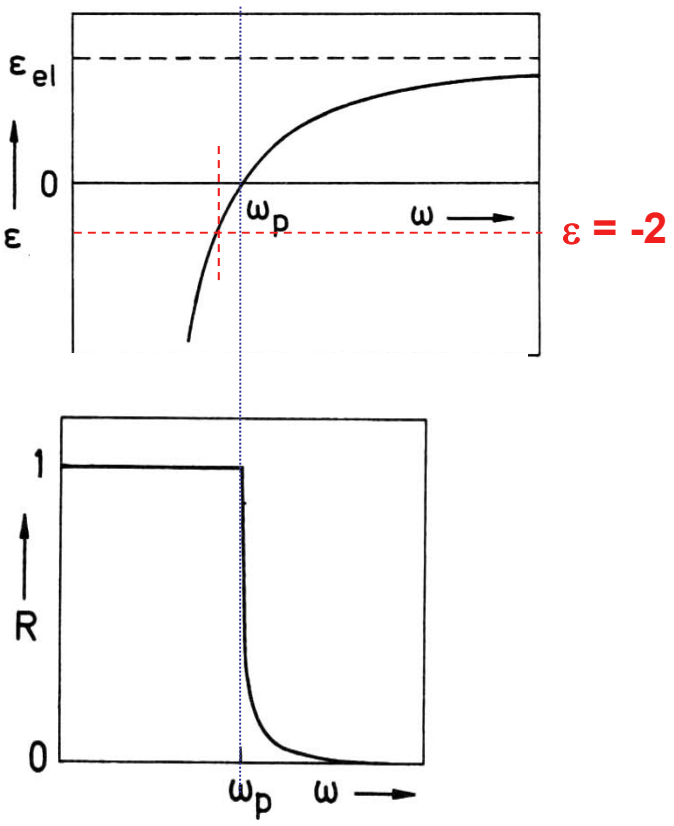

plasma frequency
(longitudinal oscillation)

Polar crystal
strong lattice vibrations (phonons)

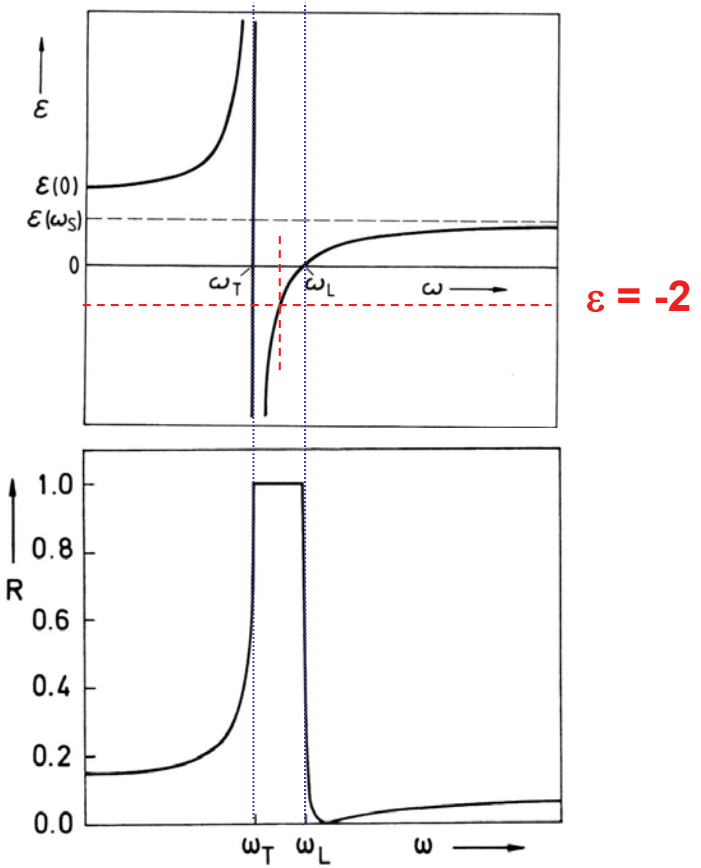

transversal optical
phonon frequency, TO

longitudinal optical
phonon frequency, LO

Plasmon vs. Phonon

Plasmon polaritons:	Phonon polaritons:
Light - electron coupling in • metals • semiconductors	Light - optical phonon coupling in polar crystals • SiC, SiO_2 • III-V, II-VI-semiconductors
typically visible *(metals)* typically IR and terahertz *(doped SC)*	mid-infrared to terahertz
resonant excitation of collective electron oscillation	resonant excitation of optical lattice vibrations

surface polariton resonances @ $\varepsilon \approx -1$

J. Aizpurua, Lecture given at SSOP Porquerolles, Sept. 2009

Optical cross sections of small spheres

Drude model

$$\varepsilon = 1 - \frac{\omega_p^2}{\omega^2 + 0.2i\omega}$$

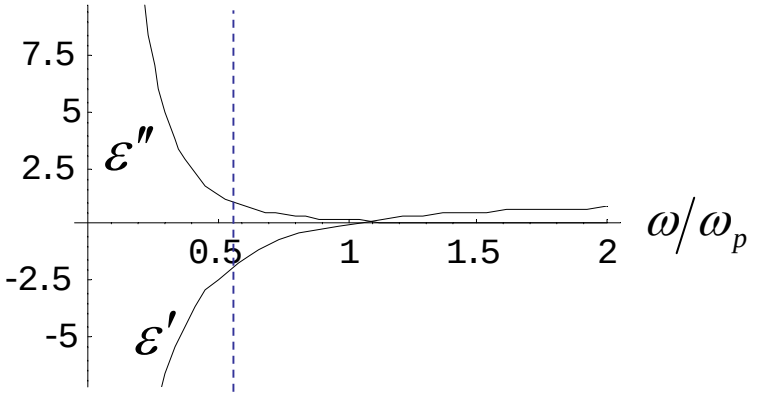

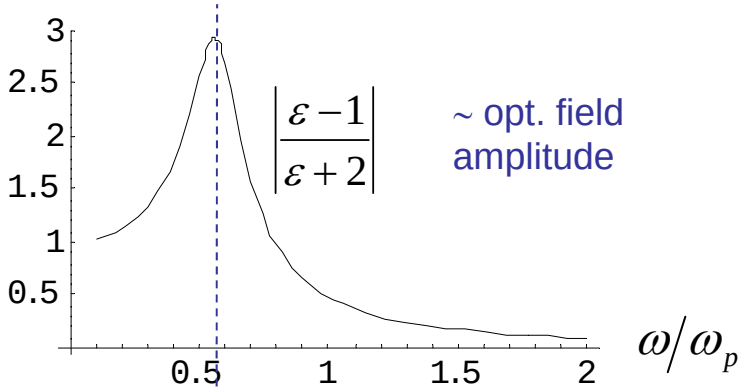

~ opt. field amplitude

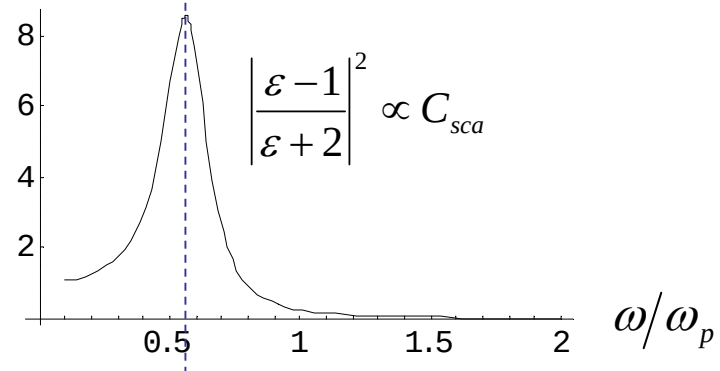

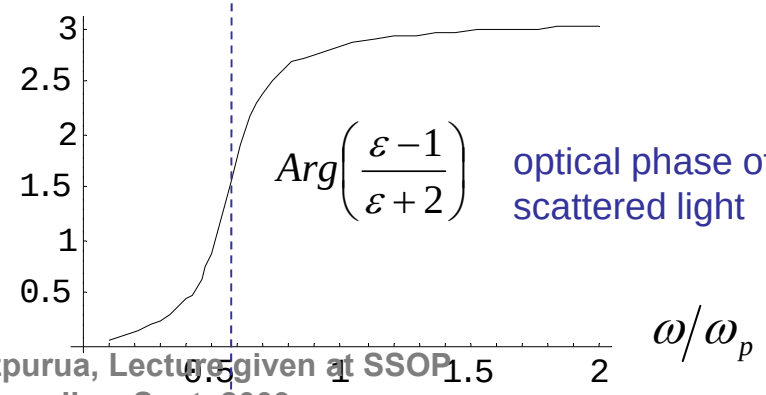

optical phase of scattered light

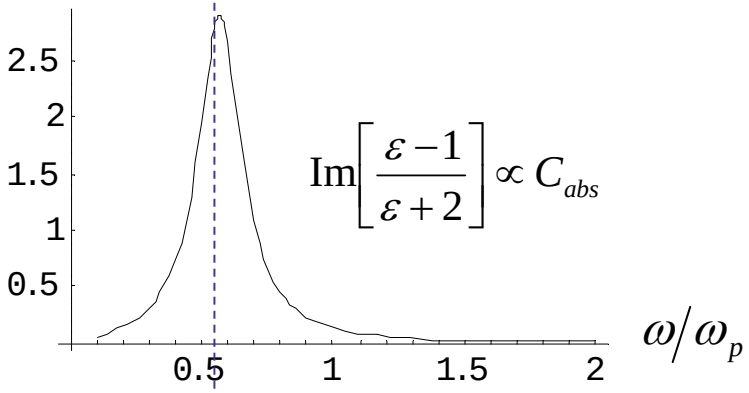

Small particle resonances

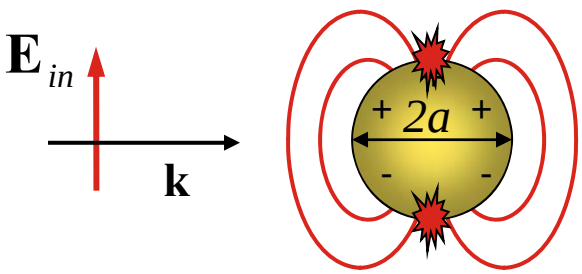

$E_0 =$ enhanced field at

$$E_0 = 2\frac{\varepsilon - \varepsilon_m}{\varepsilon + 2\varepsilon_m} E_{\text{in}}$$

$$\alpha = 4\pi a^3 \frac{\varepsilon - \varepsilon_m}{\varepsilon + 2\varepsilon_m}$$

polarizability:

resonance at $\varepsilon = -2\varepsilon_m$

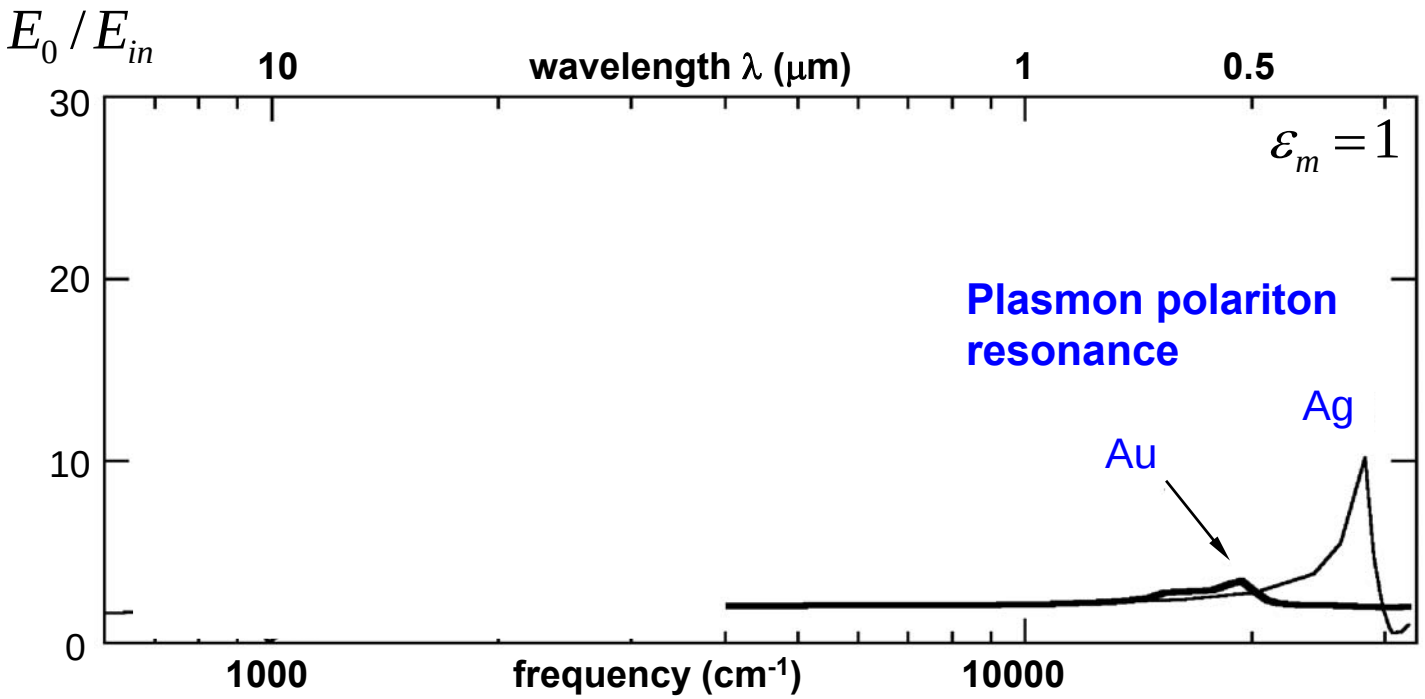

J. Aizpurua, Lecture given at SSOP Porquerolles, Sept. 2009

Nanotechnology with plasmonics: before the nanorevolution

Lycurgus Cup

(British Museum; 4th century AD)

Illumination: from outside **from inside**

(strong absorption at and below 520 nm)

Extinction vs. scattering

Ancient roman Lycurgus cup illuminated by a light source from behind. Light absorption by the embedded gold particles leads to a red color of the transmitted light whereas scattering at the particles yields a greenish color. From http://www.thebritishmuseum.ac.uk/ science/lycurguscup/sr-lycugus-p1.html.

J. Aizpurua, Lecture given at SSOP Porquerolles, Sept. 2009

Higher multipole resonances in quasistatic limit

In the quasistatic limit the Mie theory yields the resonance positions of the higher multipoles at

$$\varepsilon_L = -\varepsilon_{medium}\,\frac{l+1}{l} \quad \xrightarrow{\textbf{Drude}} \quad \omega_L = \omega_p \frac{1}{\sqrt{1+\frac{l+1}{l}\varepsilon_{medium}}}$$

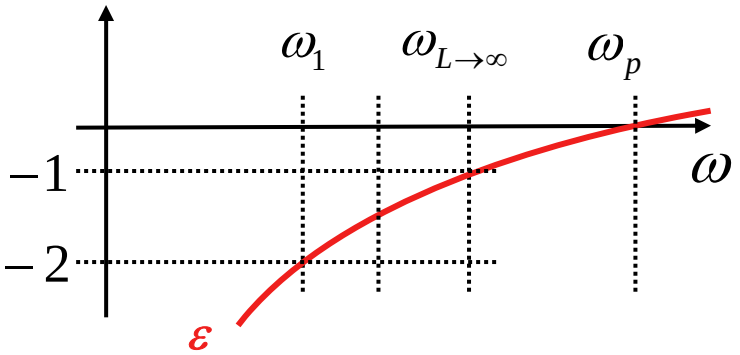

$\varepsilon_{medium} = 1$

However, higher multipoles in the quasistatic limit are negligible compared to the dipole contribution (*l*=1)

An alternative to excite high order modes in a sphere

EELS in nanoparticles

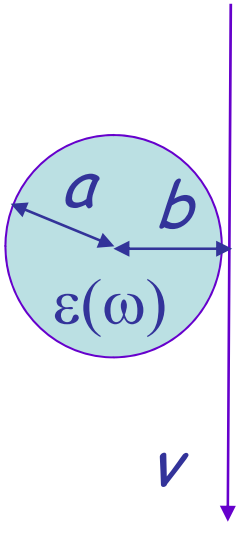

$$\alpha_l(\omega) = \frac{\varepsilon(\omega) - 1}{\varepsilon(\omega) + (l+1)/l} a^3$$

Ferrell and Echenique, PRL 55, 1526 (1985)

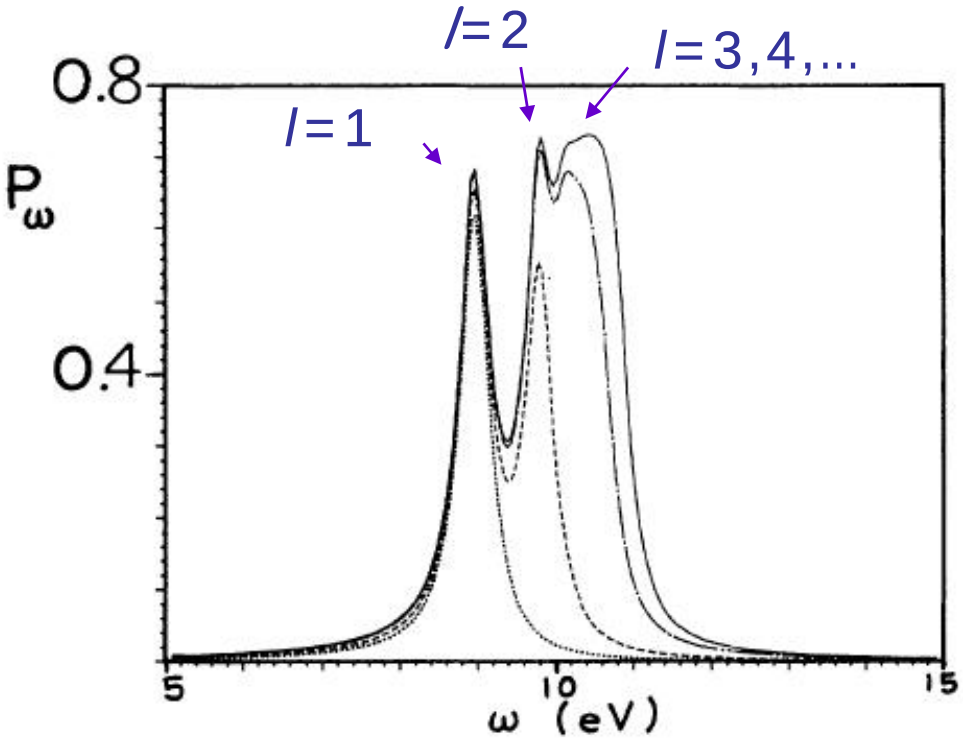

$$P_\omega(a,b,v) = \frac{4q^2}{\pi v^2 a^2} \sum_{l=0}^{\infty} \sum_{m=0}^{l} A_{lm} \left(\frac{\omega a}{v}\right)^{2l} K_m^2\left(\frac{\omega b}{v}\right) \mathrm{Im}\left[\alpha_l(\omega)\right]$$

Probability of losing energy hω for a 50-keV electron moving at grazing incidence on an aluminum sphere of radius a=10nm

J. Aizpurua, Lecture given at SSOP Porquerolles, Sept. 2009

Mie-theory

2.1.3 Exact Electrodynamic Calculation of Spherical Metal Clusters (Mie Theory)

Kreibig/Vollmer

The above discussion of the *quasi-static regime* serves as a first rough estimate which only holds for sufficiently small particles and needs to be extended considerably in order to account for larger particle sizes and particle-size distributions.

The general solution of the diffraction problem of a single sphere of arbitrary material within the frame of electrodynamics was first given by Mie in 1908 [2.19]. He applied Maxwell's equations with appropriate boundary conditions in spherical coordinates using multipole expansions of the incoming electric and magnetic fields. Input parameters were the particle size and the optical functions of the particle material and of the surrounding medium. His solution was based upon the determination of scalar electromagnetic potentials from which the various fields werde derived. In particular there are two sets of potentials Π, solving the wave equation

$$\Delta\Pi + |\boldsymbol{k}|^2\Pi = 0 \tag{2.15a}$$

in spherical coordinates: $\Pi^{\mathrm{inc}}_{\mathrm{e,m}}$ of the incident plane wave
$\Pi^{\mathrm{in}}_{\mathrm{e,m}}$ of the wave inside the cluster
$\Pi^{\mathrm{sca}}_{\mathrm{e,m}}$ of the outgoing scattered wave

The indices e and m indicate the sets of *electrical* and *magnetical* partial waves, respectively. The solutions can be separated in spherical coordinates

$$\Pi = R(r)\Theta(\theta)\Phi(\phi) \tag{2.15b}$$

and have the form

$$\Pi = \{\text{cylindrical fct.}\} \cdot \{\text{Legendre spherical fct.}\} \cdot \{\text{trigonometric fct.}\} \tag{2.15c}$$

The relevant parameter in all formulas is the size parameter $x = |\boldsymbol{k}|R$ which distinguishes the regime of geometrical optics ($x \gg 1$) from the one important for clusters ($x \ll 1$) (a compressed description is given in [2.9]).

Mie-theory is an electrodynamic theory for optical properties of spherical particles. The solution is divided into two parts: the elctromagnetic one which is treated from first principles (Maxwell equations) and the material problem with is solved by using phenomenological dielectric functions taken from experiments or model calculations

See also Bohren/Huffman

Mie theory - results

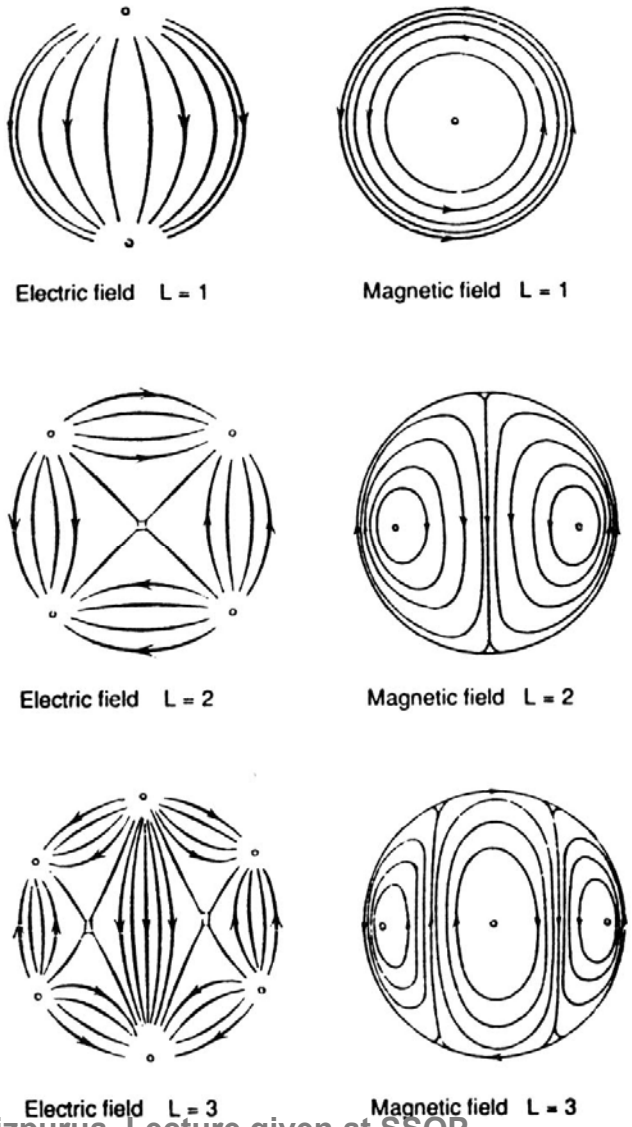

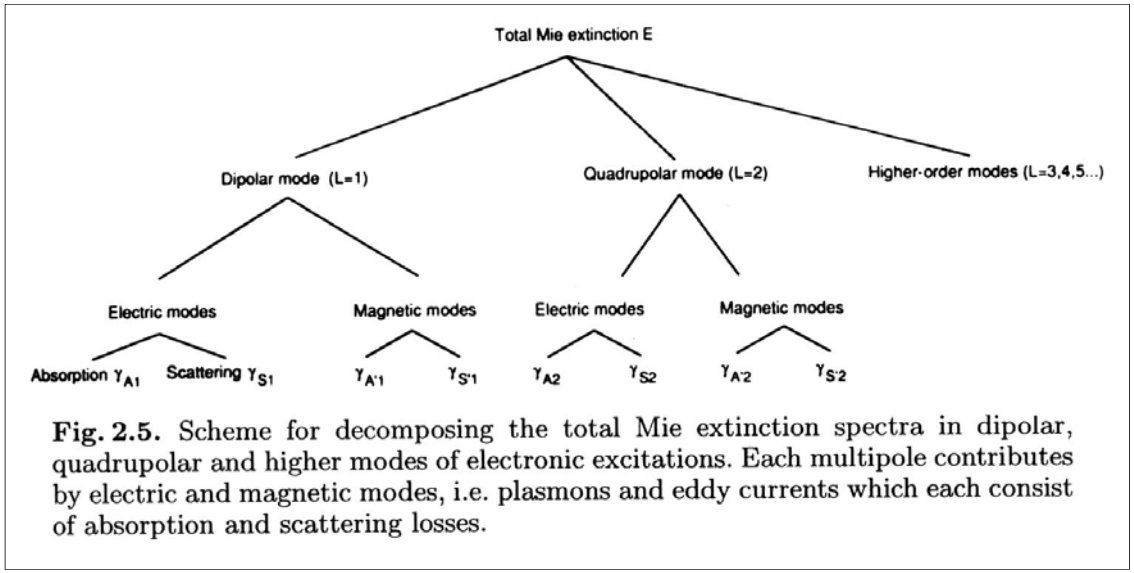

Fig. 2.5. Scheme for decomposing the total Mie extinction spectra in dipolar, quadrupolar and higher modes of electronic excitations. Each multipole contributes by electric and magnetic modes, i.e. plasmons and eddy currents which each consist of absorption and scattering losses.

Fig. 2.6. Electric and magnetic fields far away from the clusters, of the $L = 1$, 2, and 3 electric partial wave, i.e. the electric dipole, quadrupole, and octupole mode. The same field distributions hold for the magnetic partial waves, if electric and magnetic fields are interchanged (after [2.19]).

Fig. 2.6 shows farfield distribution at the surface of a large sphere centered at the small cluster

Kreibig/Vollmer

J. Aizpurua, Lecture given at SSOP Porquerolles, Sept. 2009

Scattering characteristics (far-field)

Small particle

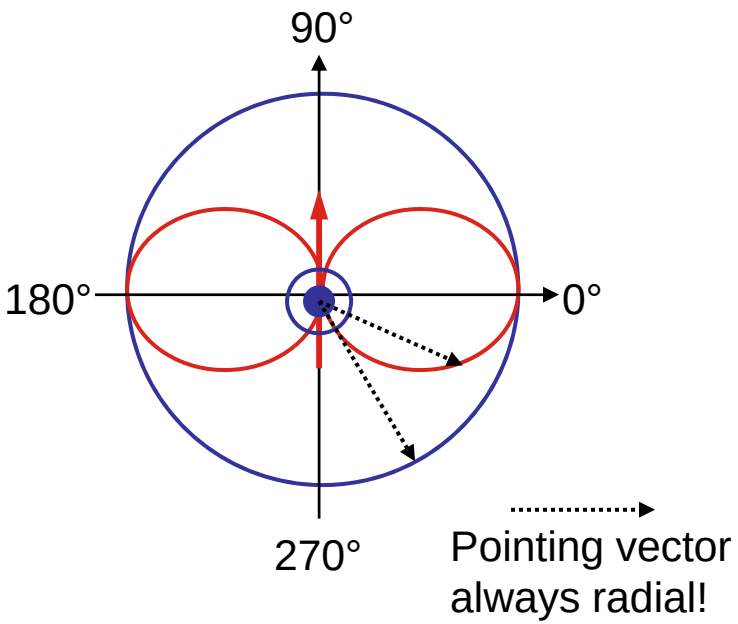

Large particle (Mie calculation)

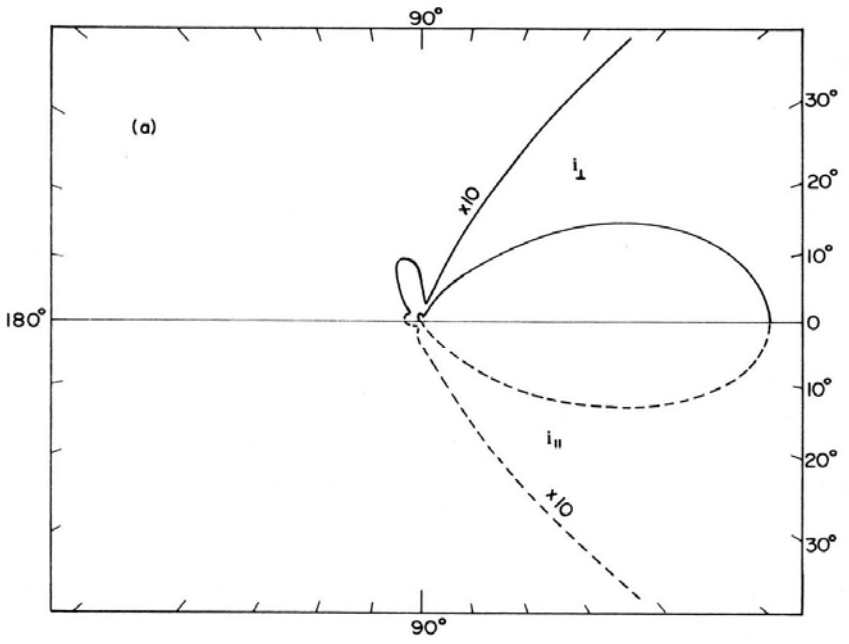

Figure 4.9 Scattering by a sphere with $x = 3$ and $m = 1.33 + i10^{-8}$.

→ **Strong forward scattering**

Spherical plasmons:
Mie modes derivaded from Maxwell's equations

$$\omega_l = \sqrt{\frac{l}{2l+1}}\,\omega_p$$

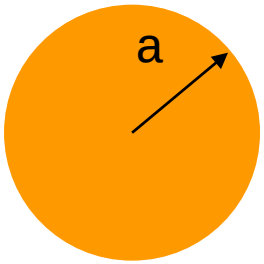

$$\varepsilon = 1 - \frac{\omega_p^2}{\omega^2}$$

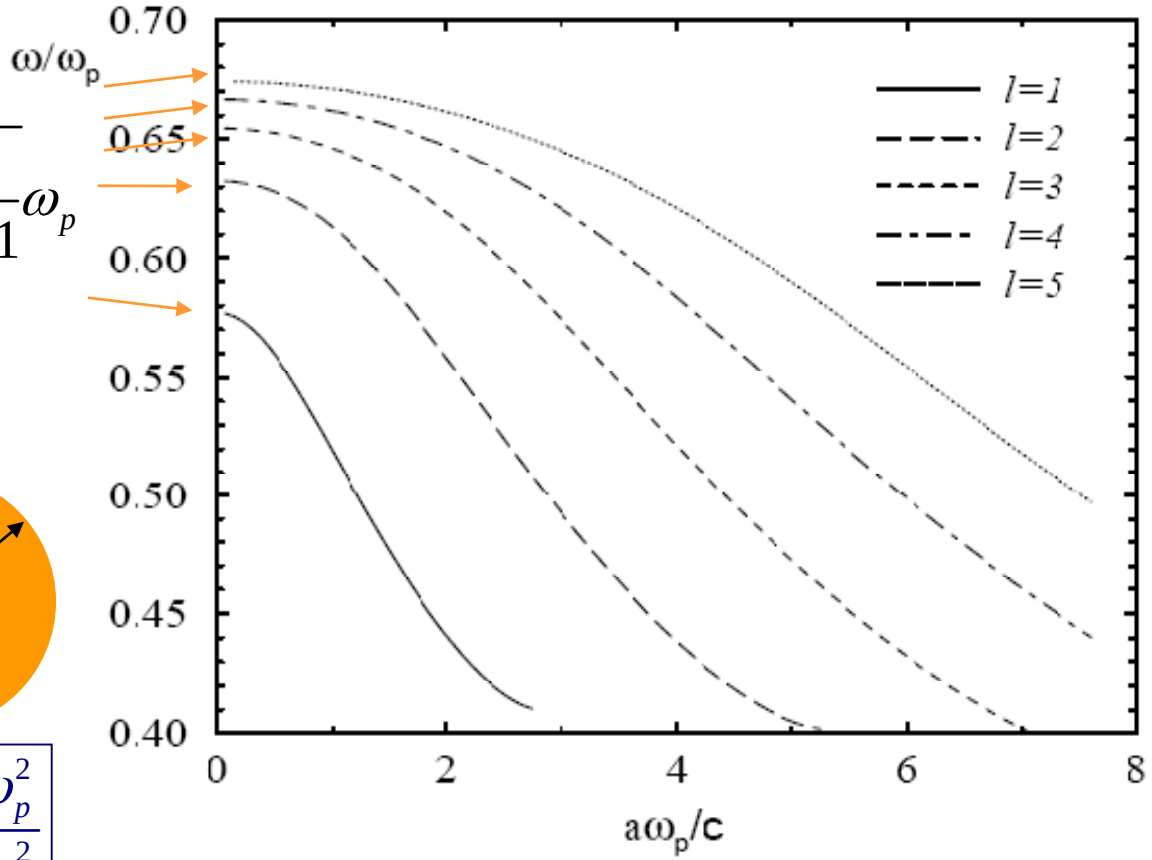

Drude-like metal

Effect of finite size on the resonant frequency

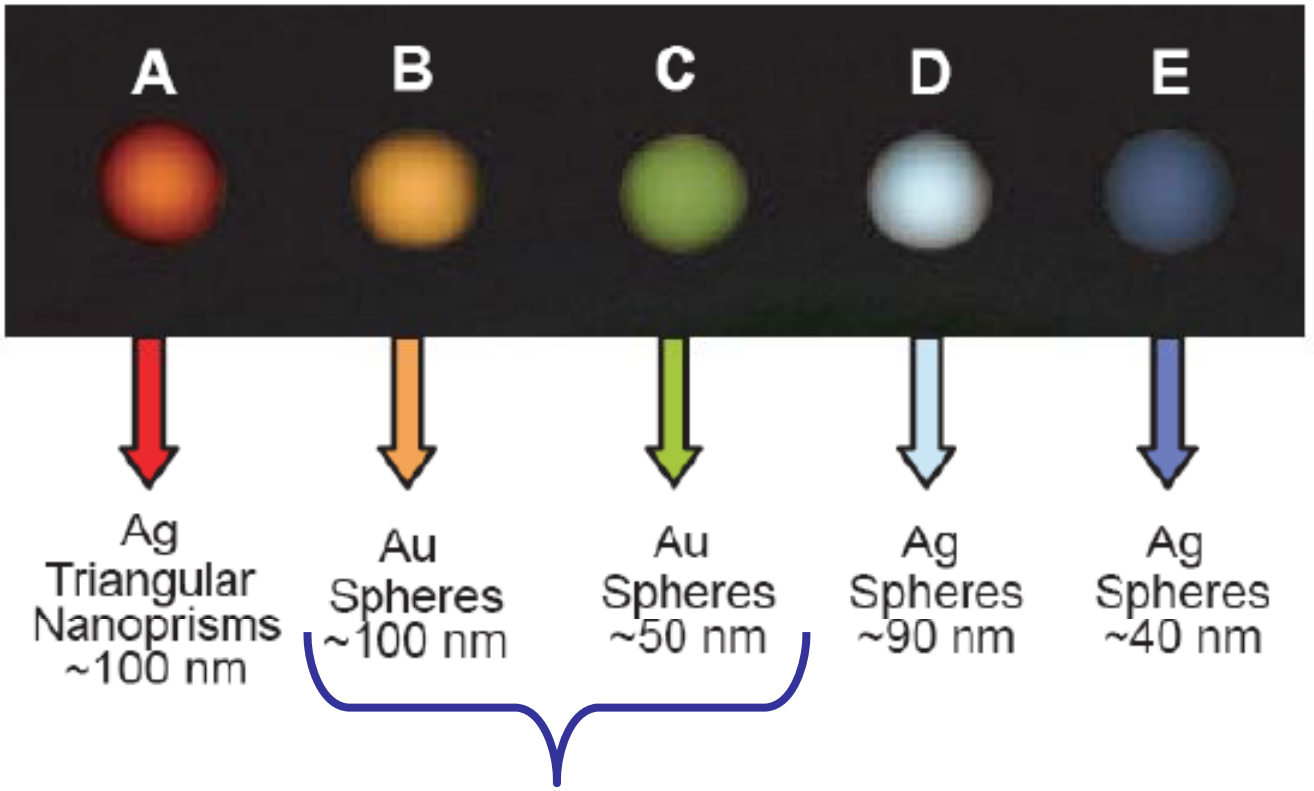

same shape, different size
redshift due to higher multipoles

Jin et. al., Science 294, 1901 (2001)

Shape: Polarizability of small ellipsoids

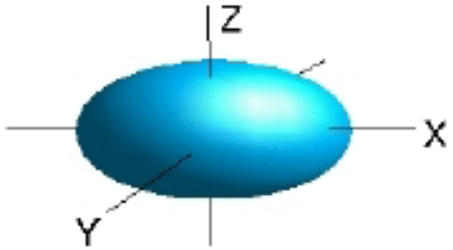

quasistatic approximation:

$$\alpha_{xyz} = \frac{4}{3}\pi abc \frac{\varepsilon - \varepsilon_m}{\varepsilon_m + L_{xyz}\left(\varepsilon - \varepsilon_m\right)}$$

geometrical factors

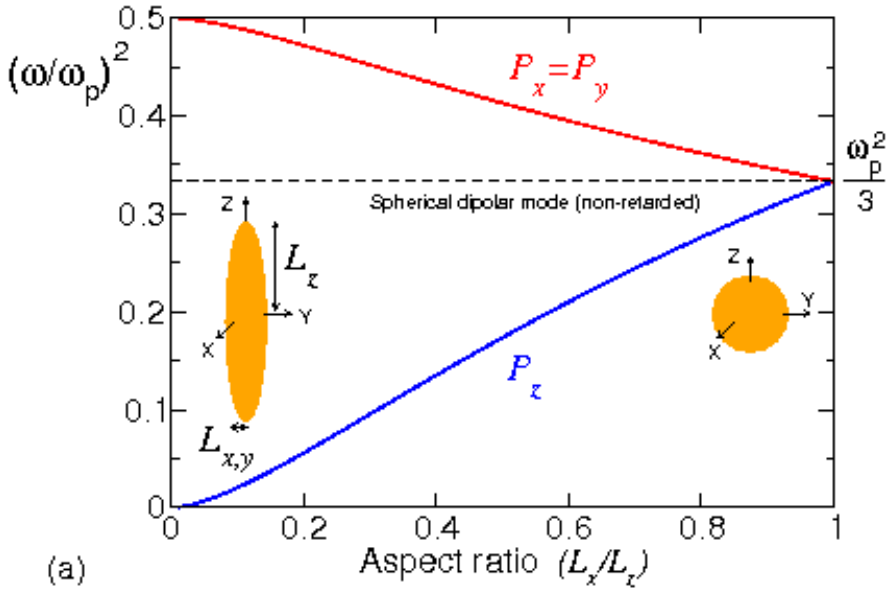

sphere: $L_x = L_y = L_z = \frac{1}{3}$

generally: $L_x \neq L_y \neq L_z$

$\longrightarrow$ 3 resonances at $\varepsilon = \varepsilon_m\left(1 - \frac{1}{L_{xyz}}\right)$

Silver ellipsoid illuminated by a plane wave

size shifts dipole resonance for
E_0 || long axis

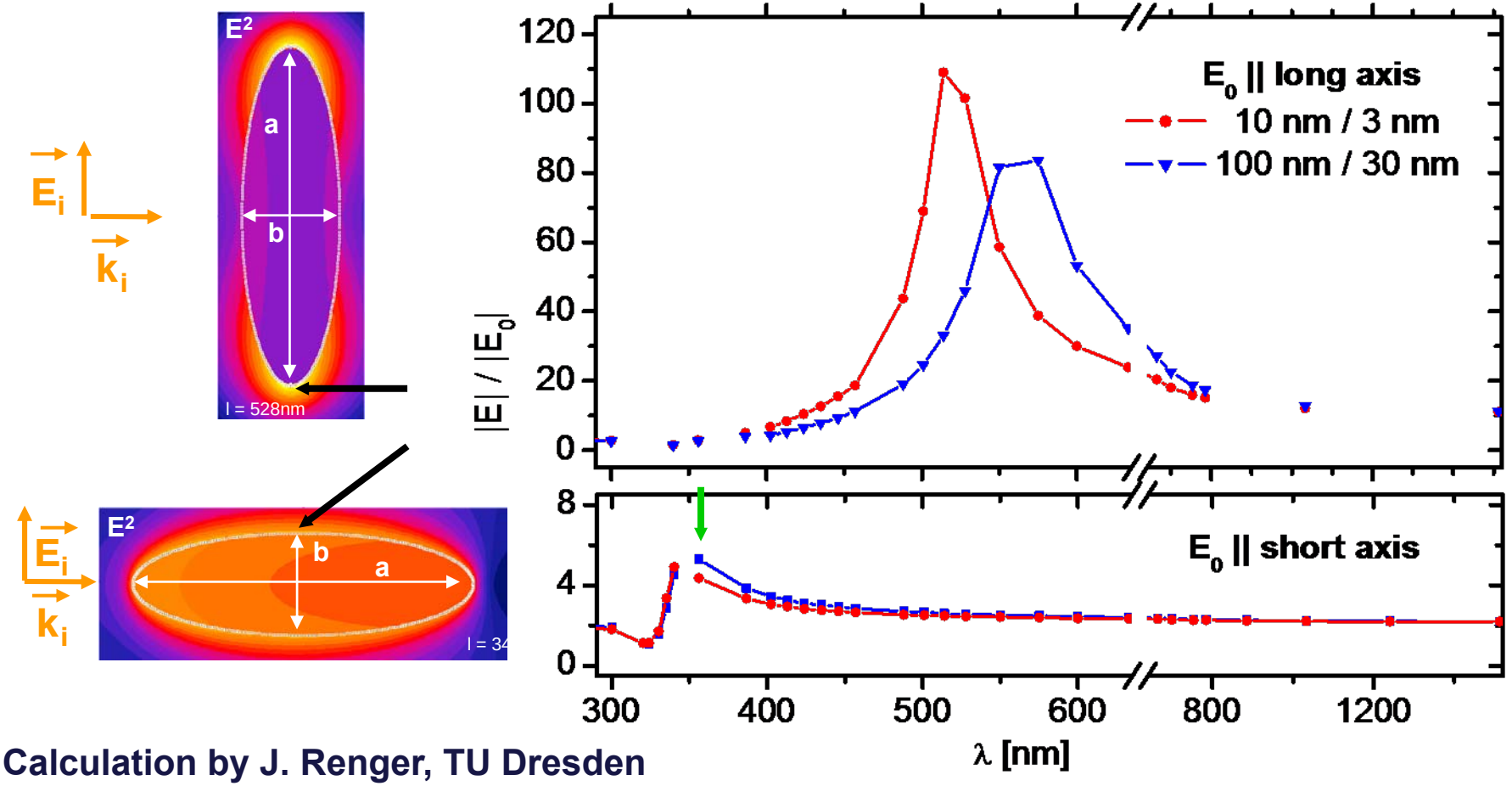

Calculation by J. Renger, TU Dresden

J. Aizpurua, Lecture given at SSOP Porquerolles, Sept. 2009

Plasmon resonances:dependence on the geometry

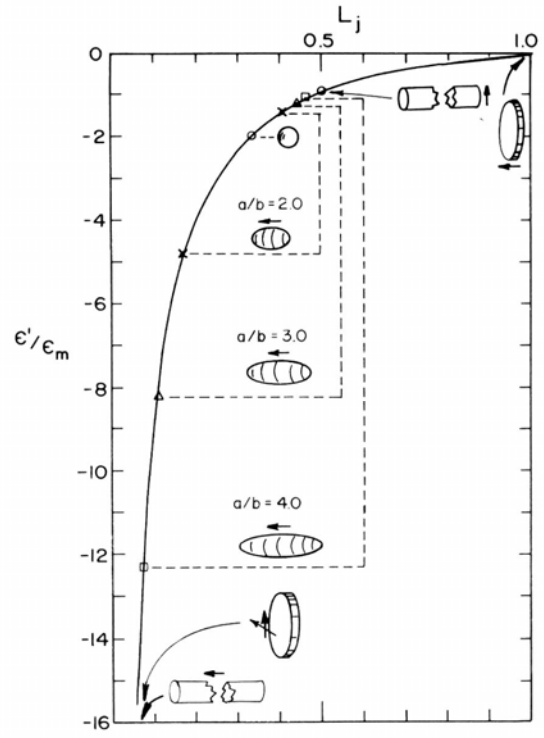

Figure 12.5 Effect of shape on the position of the lowest-order surface mode of small spheroids. Arrows next to the various shapes show the direction of the electric field.

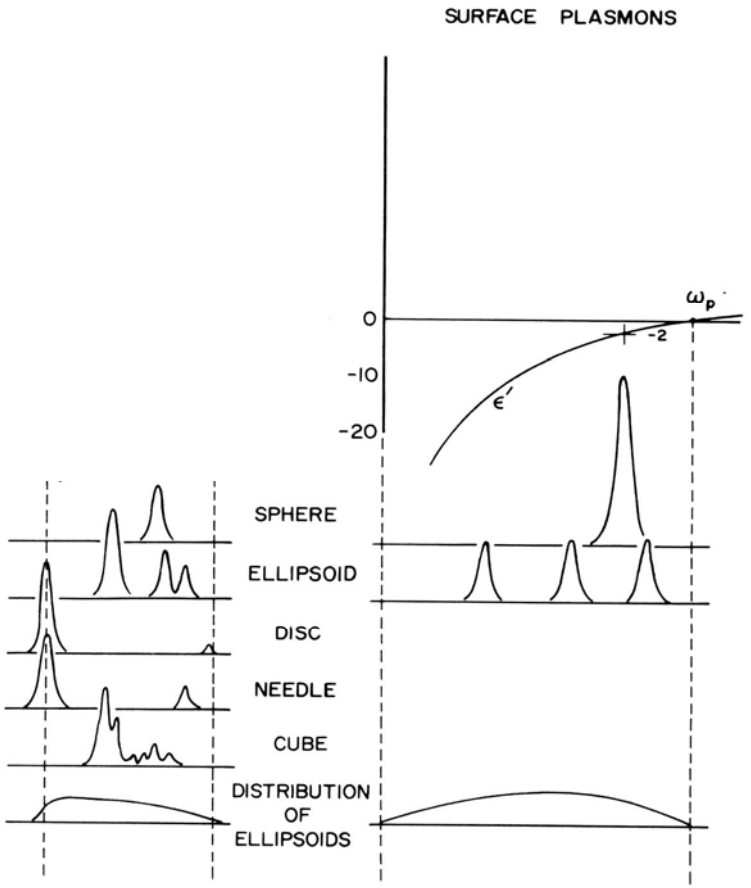

Figure 12.11 Surface mode frequencies for insulating and metallic particles of various shapes.

More complex geometries

Control over the plasmon frequencies by playing with particle shapes and coupling

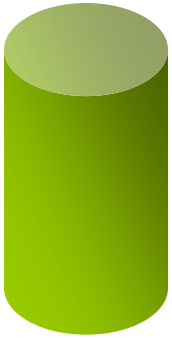

Nanorods, nanoshells, nanorings, dimers,.....

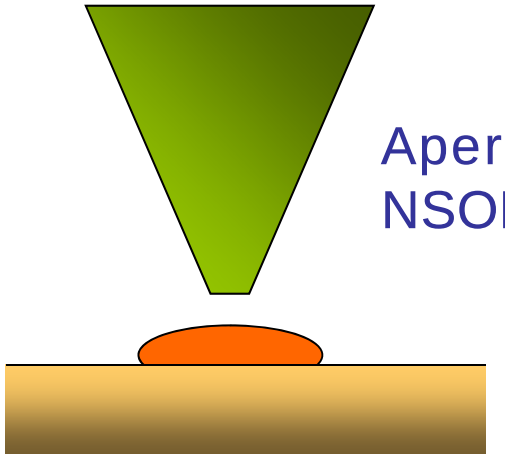

Aperture less NSOM

Coupled systems

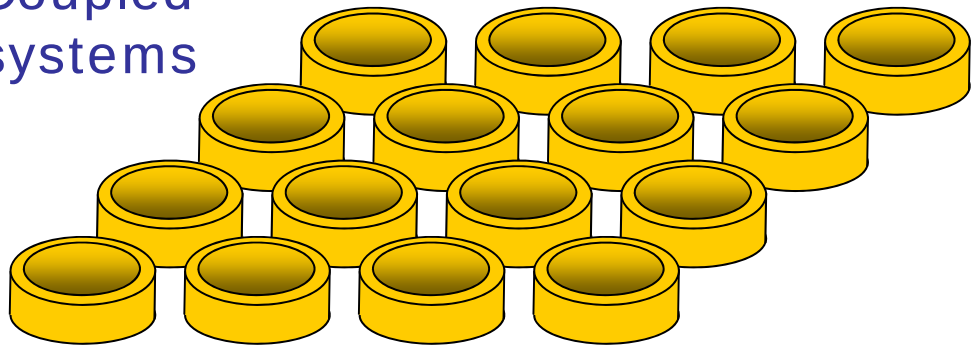

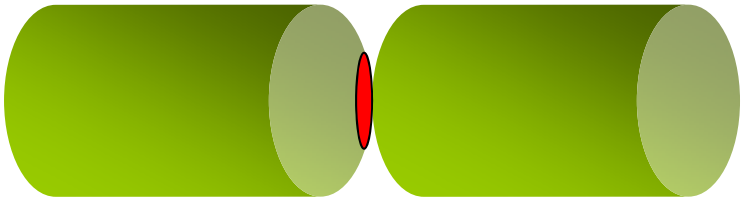

Nanometrology, sensing, spectroscopy

Boundary Element Method

$$\mathbf{E}(\mathbf{r}) = i\frac{\omega}{c}\mathbf{A}(\mathbf{r}) - \nabla\phi(\mathbf{r})$$

$$\mathbf{A}(\mathbf{r}) = \mathbf{A}^{\text{ext}}(\mathbf{r}) + \int_{S_j} d\mathbf{s}\, G_j(\mathbf{r}-\mathbf{s})\, \mathbf{h}_j(\mathbf{s})$$

$$\phi(\mathbf{r}) = \phi^{\text{ext}}(\mathbf{r}) + \int_{S_j} d\mathbf{s}\, G_j(\mathbf{r}-\mathbf{s})\, \sigma_j(\mathbf{s})$$

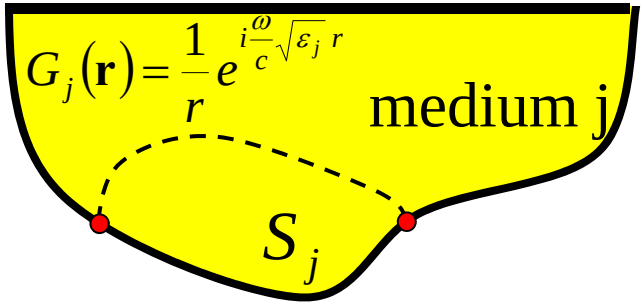

The boundary conditions lead to a set of surface integral equations with the interface currents $\mathbf{h}_j$ and charges σ_j as variables. For example, the continuity of ϕ leads to

$$\int_{S_j} d\mathbf{s}' \left[G_1(\mathbf{s}-\mathbf{s}')\, \sigma_1(\mathbf{s}') - G_2(\mathbf{s}-\mathbf{s}')\, \sigma_2(\mathbf{s}') \right] = \phi_2^{\text{ext}}(\mathbf{s}) - \phi_1^{\text{ext}}(\mathbf{s}),$$

(1 and 2 refer to the interface sides). The surface integrals are now discretized using *N* representative points $\mathbf{s}_i$. This leads to a system of 8*N* linear equations with $\mathbf{h}_1(\mathbf{s}_i)$, $\mathbf{h}_2(\mathbf{s}_i)$, $\sigma_1(\mathbf{s}_i)$, and $\sigma_2(\mathbf{s}_i)$ as unknowns.

García de Abajo and Aizpurua, PRB **56**, 15873 (1997) García de Abajo and Howie, PRB **65**, 115418 (2002)

Optical properties of metallic nanorings

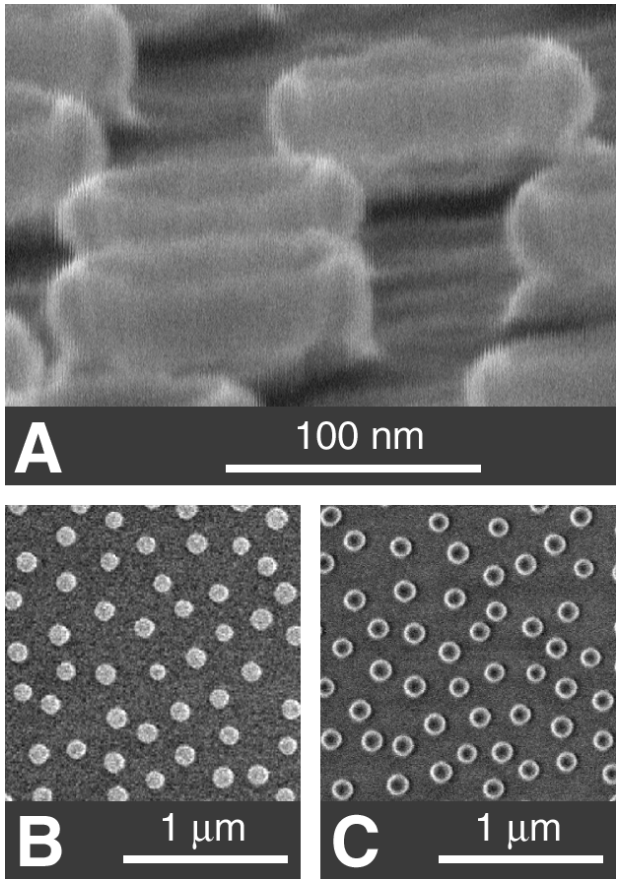

Disk

Nanoring

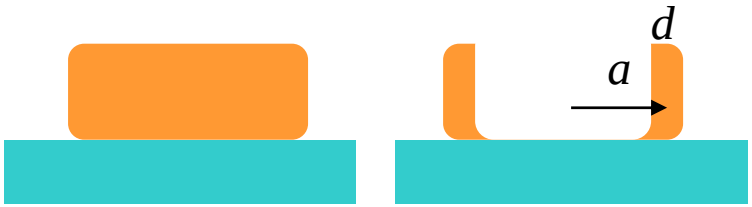

d/a smaller -> red shift

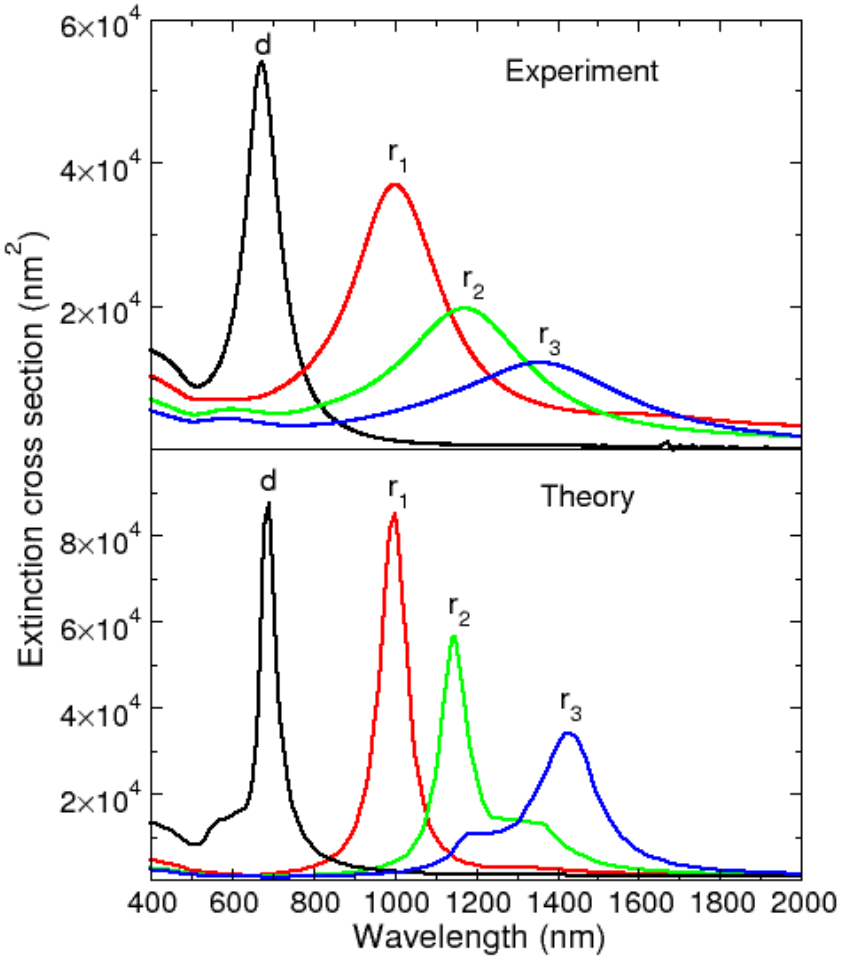

Aizpurua *et al*. Phys. Rev. Lett. **90**, 057401 (2003)

Optical properties of metallic nanoshells

Mode tunning thanks to the aspect ratio

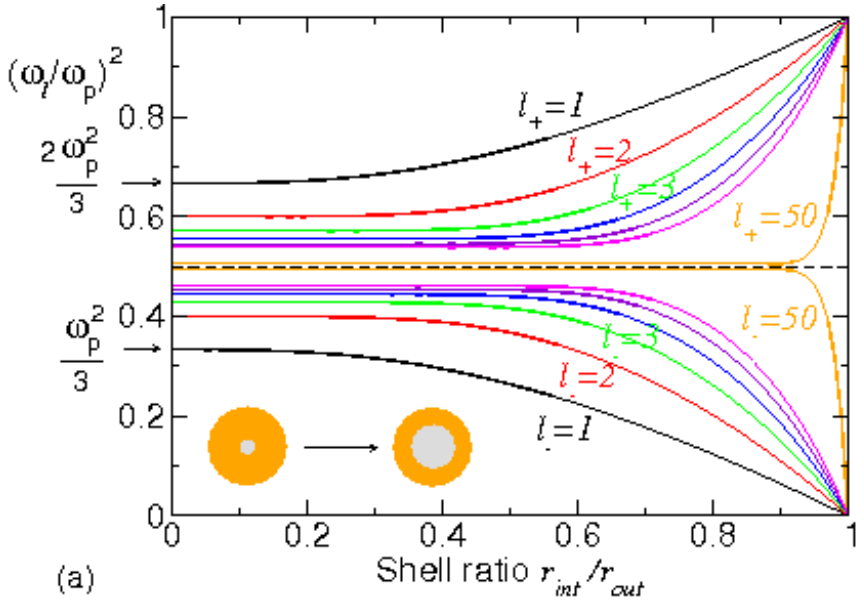

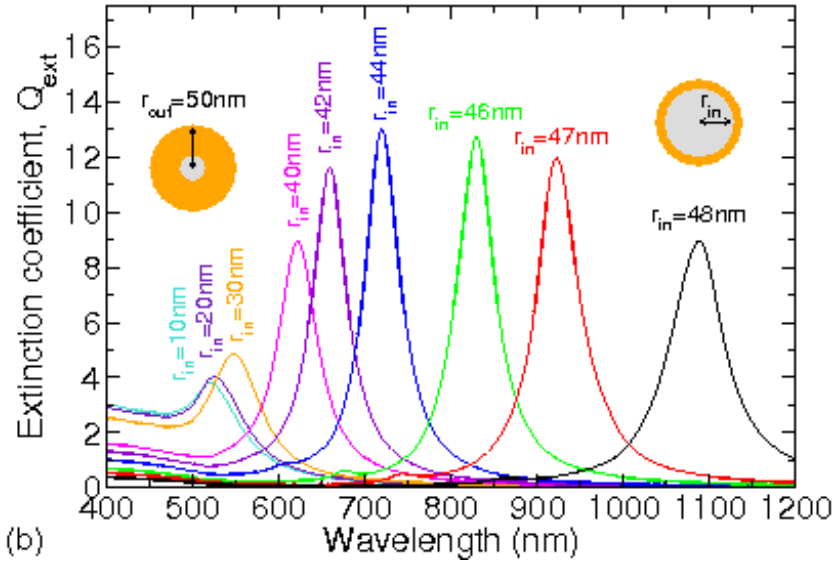

J. Aizpurua, Lecture given at SSOP Porquerolles, Sept. 2009

Modes in a nanoring. The twisted slab

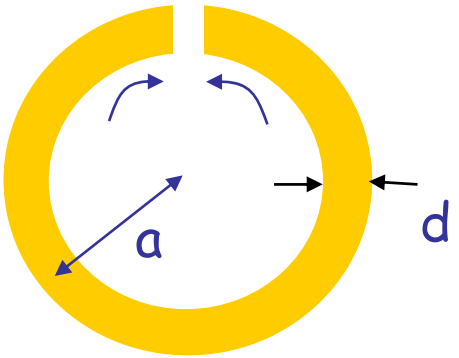

$$\omega_{\pm} = \omega_s (1 \pm e^{-kd})^{1/2}$$

$$kd = n\frac{2\pi}{L}d = n\frac{d}{a}$$

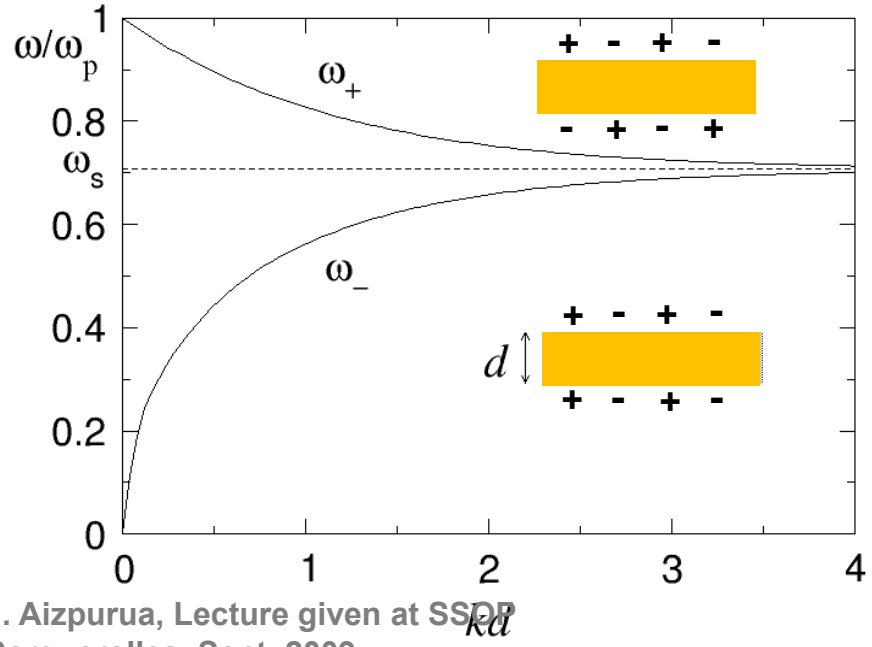

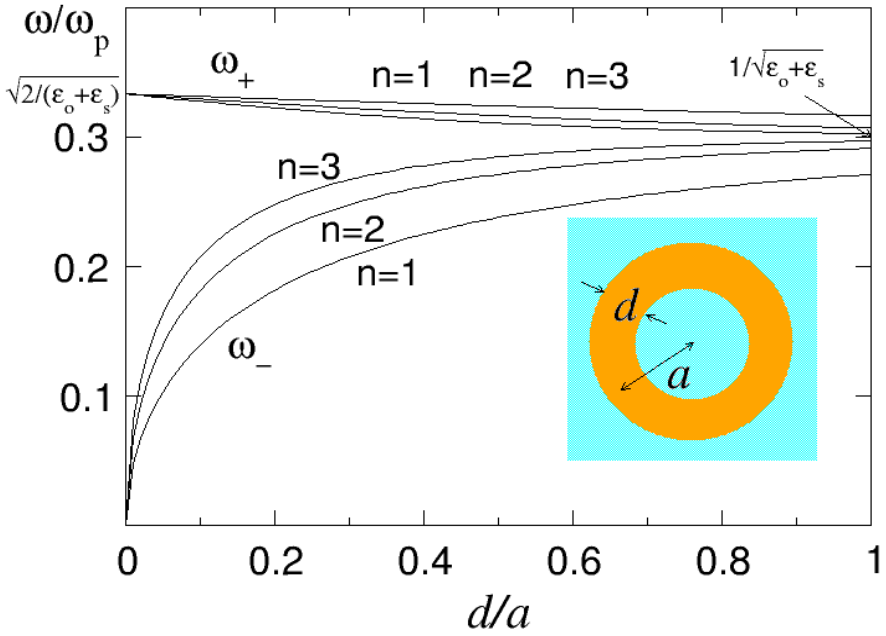

Field-enhancement in a nanoring

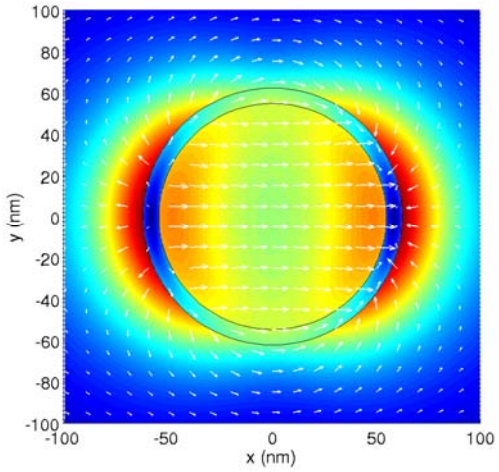

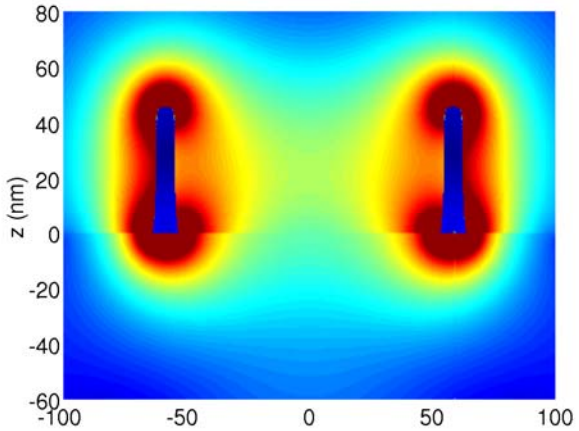

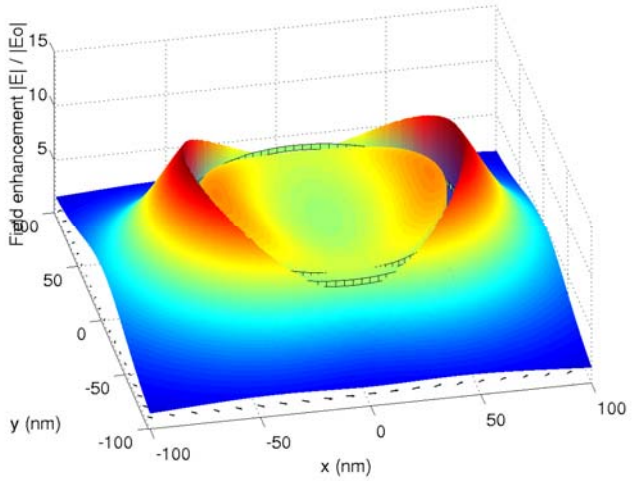

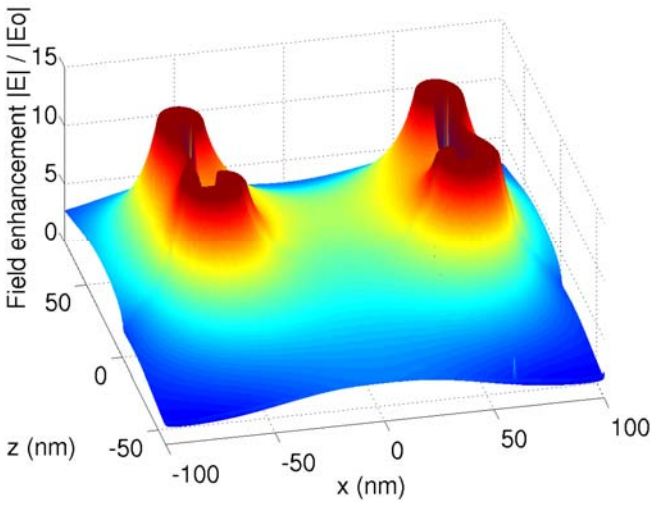

J. Aizpurua, Lecture given at SSOP Porquerolles, Sept. 2009

Different types of radio antennas

λ/4 antenna

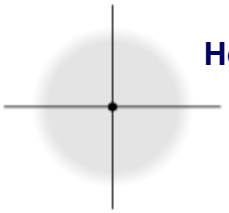

Horizontal radiation pattern

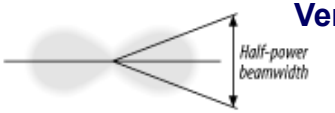

Vertical radiation pattern

λ/2 Dipole

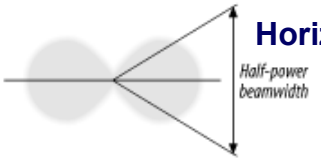

Horizontal radiation pattern

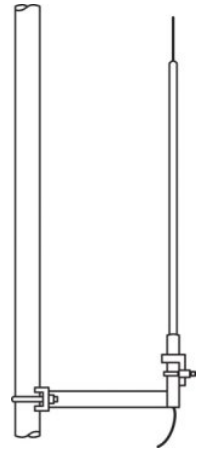

Omni-directional antenna often used at master station sites

Yagi

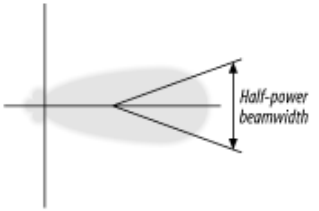

Parabolic

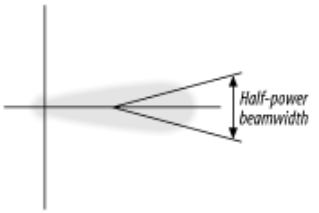

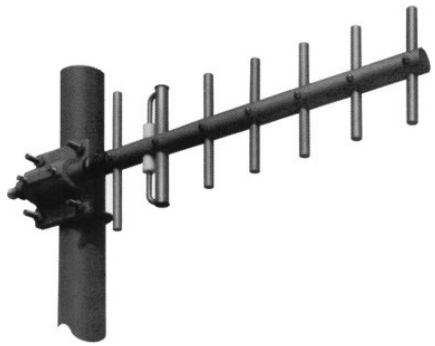

Directional Yagi antenna Commonly used at remote field sites

λ/2 nanoantenna

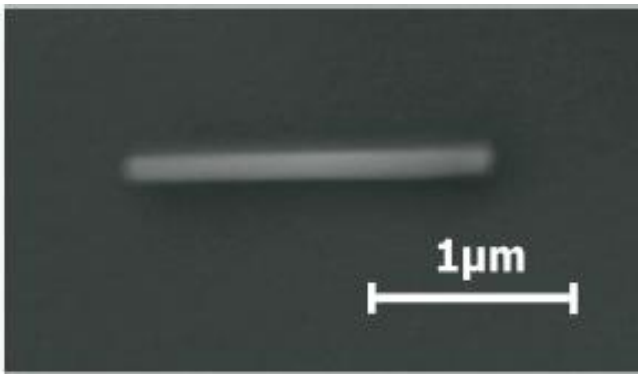

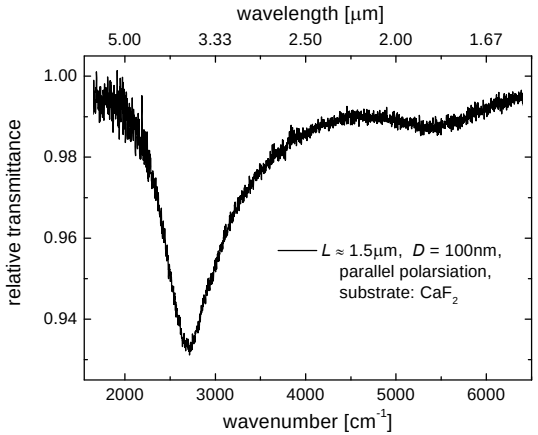

Neubrech *et al.*,
App. Phys. Lett. 89, 253104 (2006)

λ/4 optical antenna

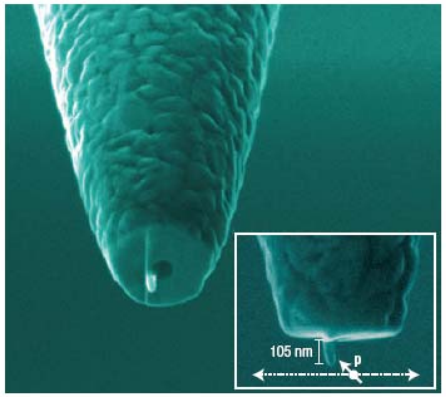

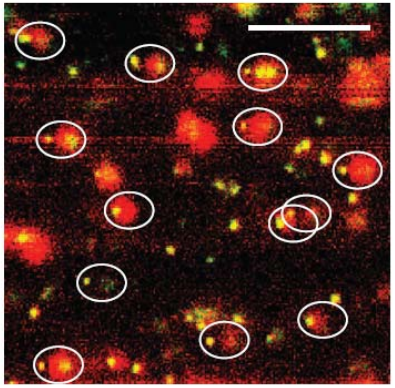

Taminiau *et al.*,
Nature Photonics 2, 234 (2008)

Different types of radio antennas

Vertical

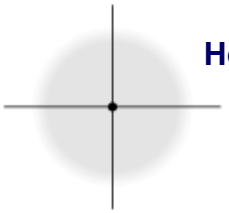

Horizontal radiation pattern

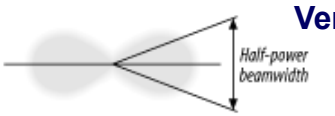

Vertical radiation pattern

Dipole

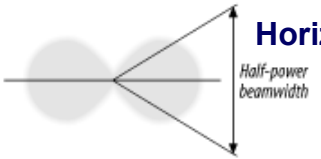

Horizontal radiation pattern

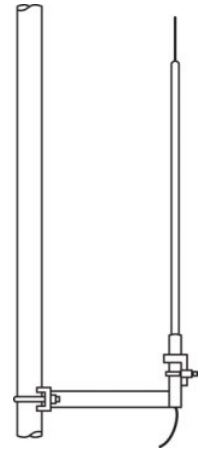

Omni-directional antenna
often used at master station sites

Yagi

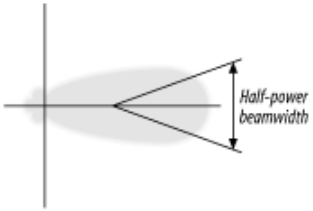

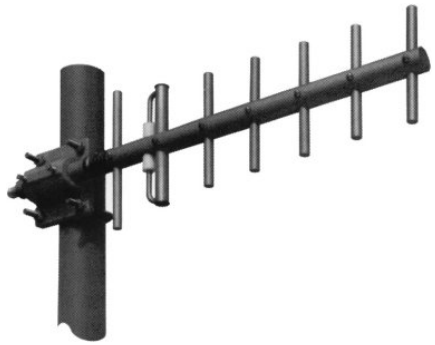

Directional Yagi antenna
Commonly used at remote field sites

Parabolic

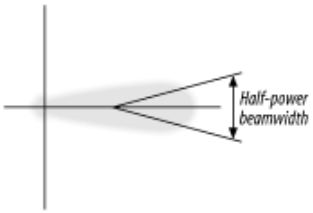

Yagi-Uda antenna

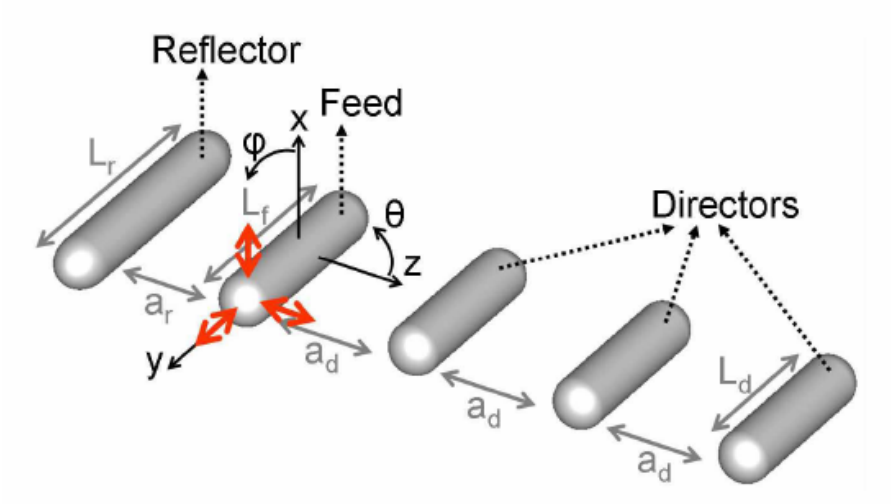

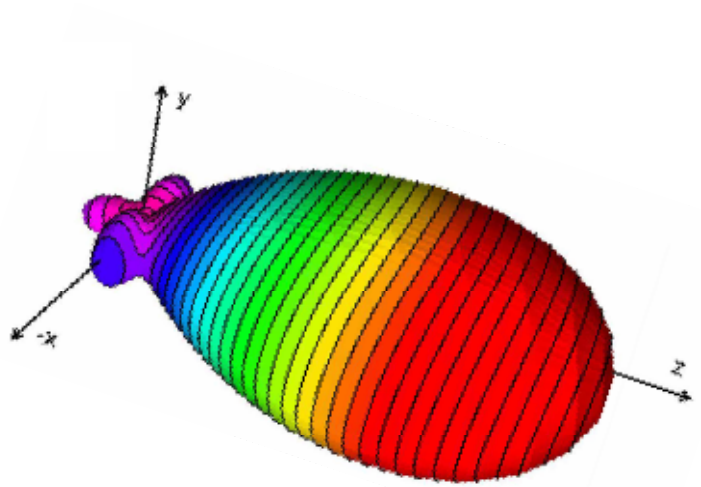

Taminiau *et al.*,
Optics Express 14, 10858 (2008)

Different types of radio antennas

Vertical

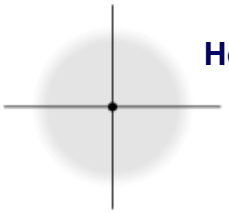

Horizontal radiation pattern

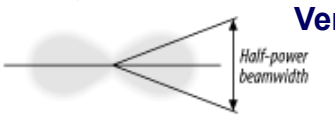

Vertical radiation pattern

Dipole

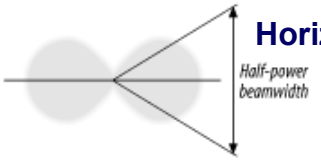

Horizontal radiation pattern

Yagi

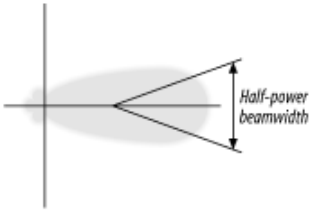

Parabolic

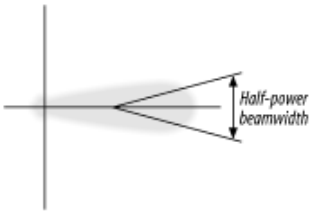

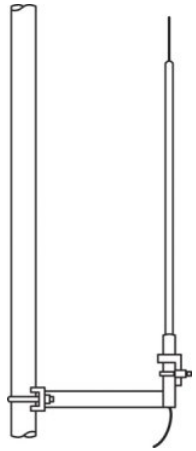

Omni-directional antenna
often used at master station sites

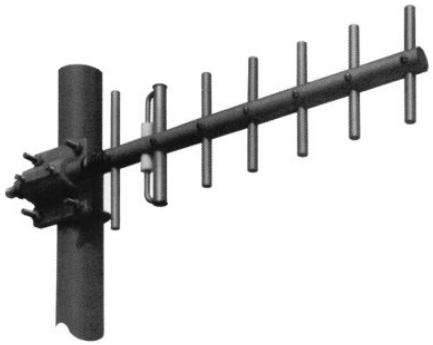

Directional Yagi antenna
Commonly used at remote field sites

Parabolic-like optical nanoantennas

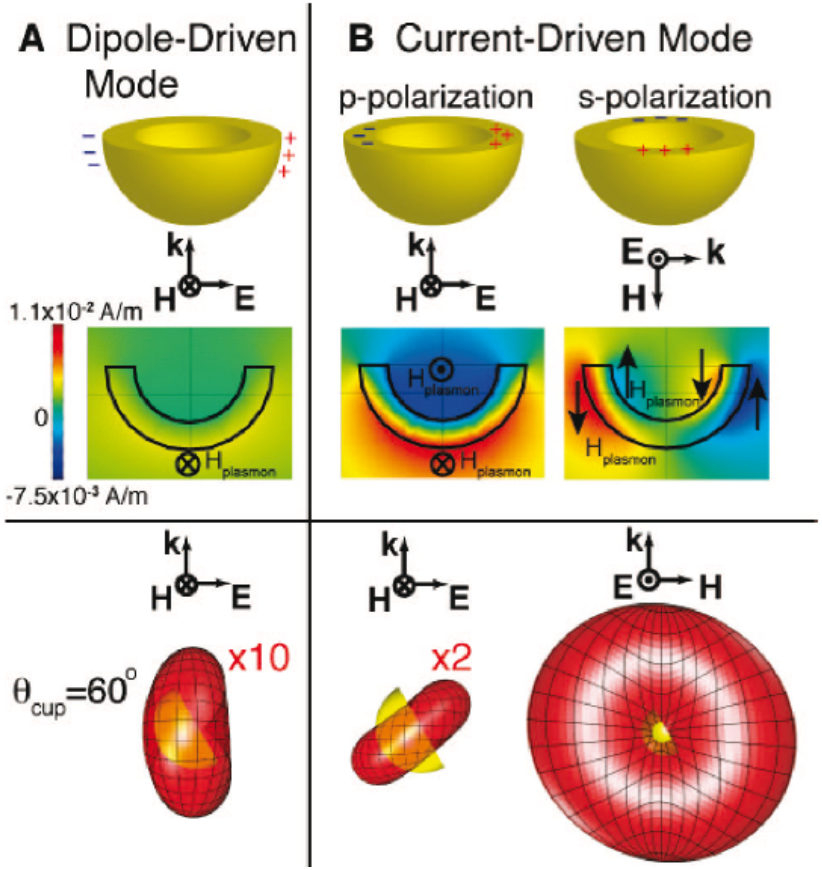

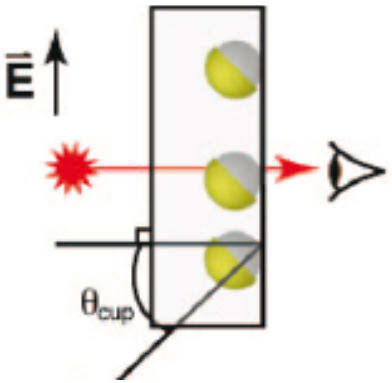

N. Mirin and N. Halas, Nano Letters 9, 1255 (2009)

Resonant Optical Antennas

P. Mühlschlegel,[1] H.-J. Eisler,[1] O. J. F. Martin,[2] B. Hecht,[1*]
D. W. Pohl[1]

SCIENCE VOL 308 10 JUNE 2005

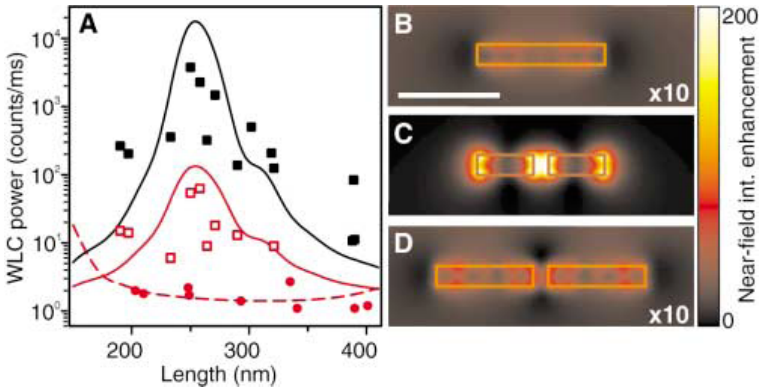

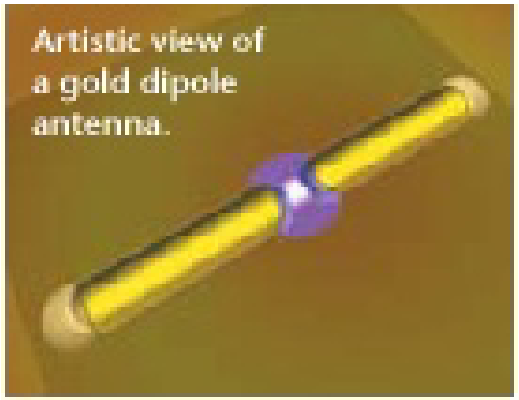

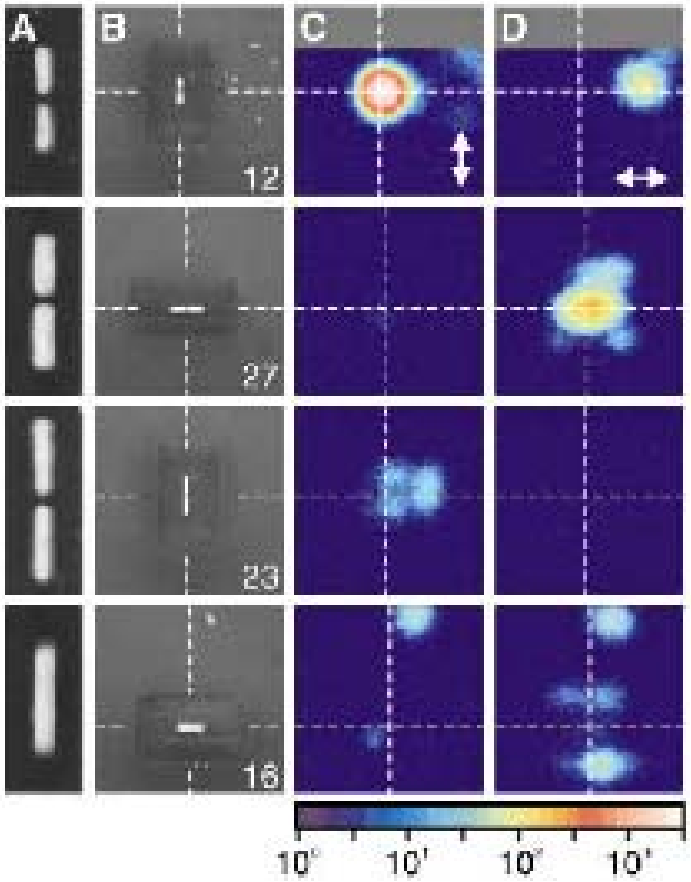

λ/4 optical antenna

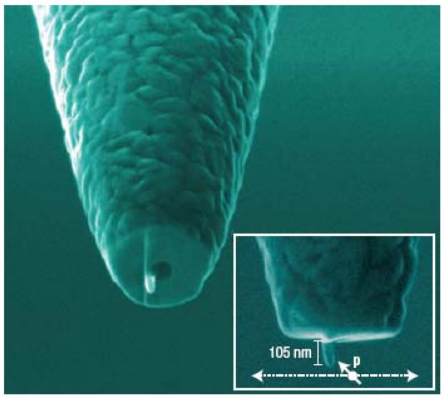

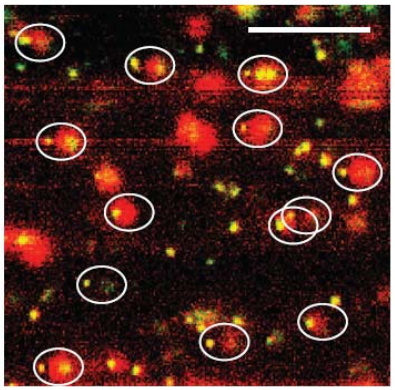

Taminiau *et al.*,
Nature Photonics 2, 234 (2008)

Bowtie antennas

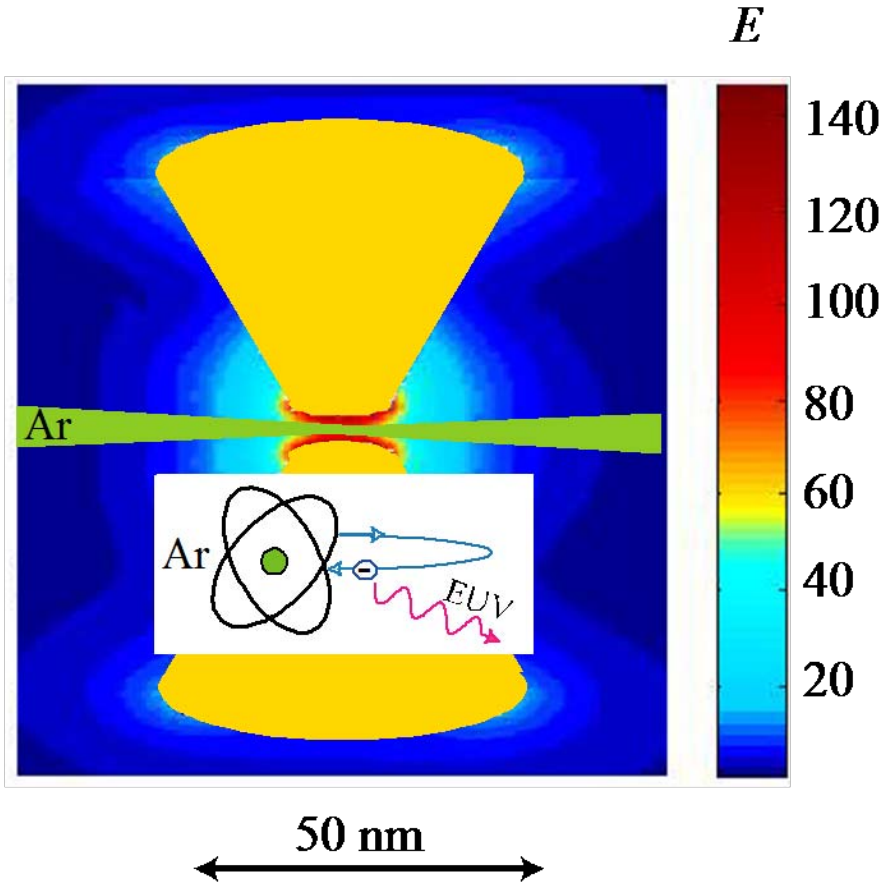

Nature 453, 731 (2008)

Fundamentals of metallic nano–optical components (optical response)

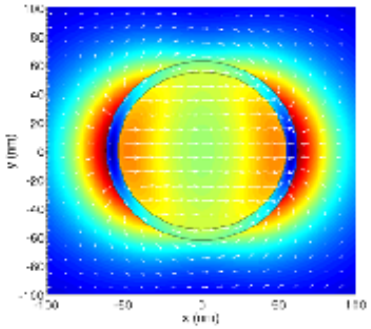

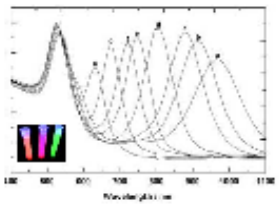

Plasmon–enhanced spectroscopies and microscopies (SERS, SEIRA, s–SNOM)

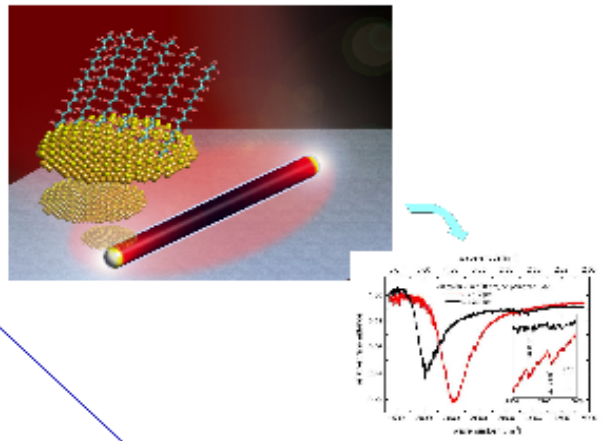

Biomedical applications

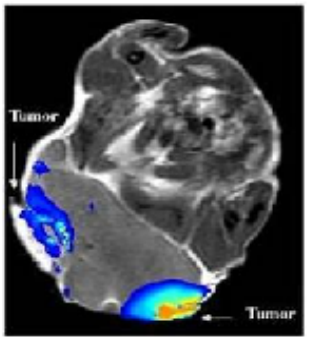

Optical guides, interconnects in opto–electronic devices

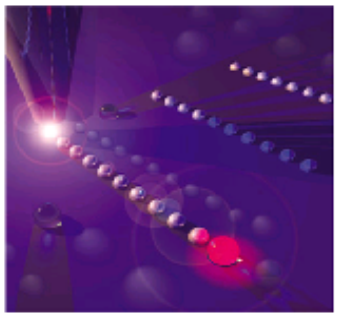

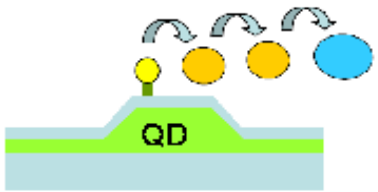

Sensing and biolabeling

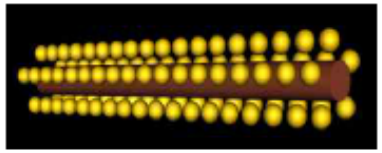

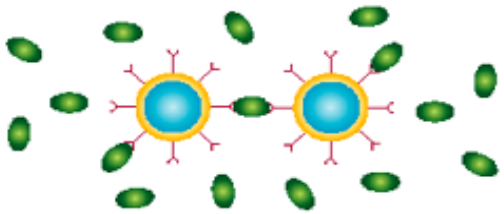

Outline

- Basics: Plasmonics

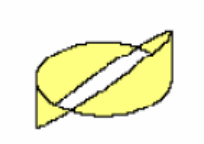

- Optical antennas for SERS
  (Surface-Enhanced Raman Scattering)

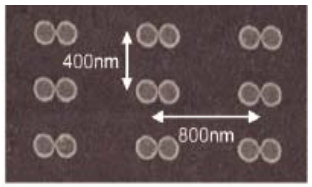

- ½ λ dipole Infrared antennas for SEIRA

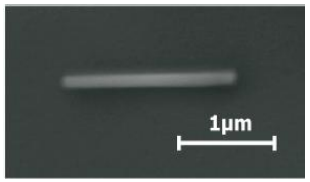

- Substrate-Enhanced Infrared
  Near-Field Microscopy

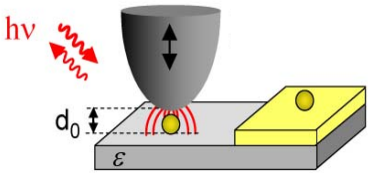

- THz Near-field Nanoscopy

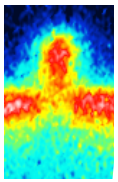

Surface-Enhanced Raman Scattering (SERS)

Resonant antennas for enhanced signal of molecular vibrations

Concept

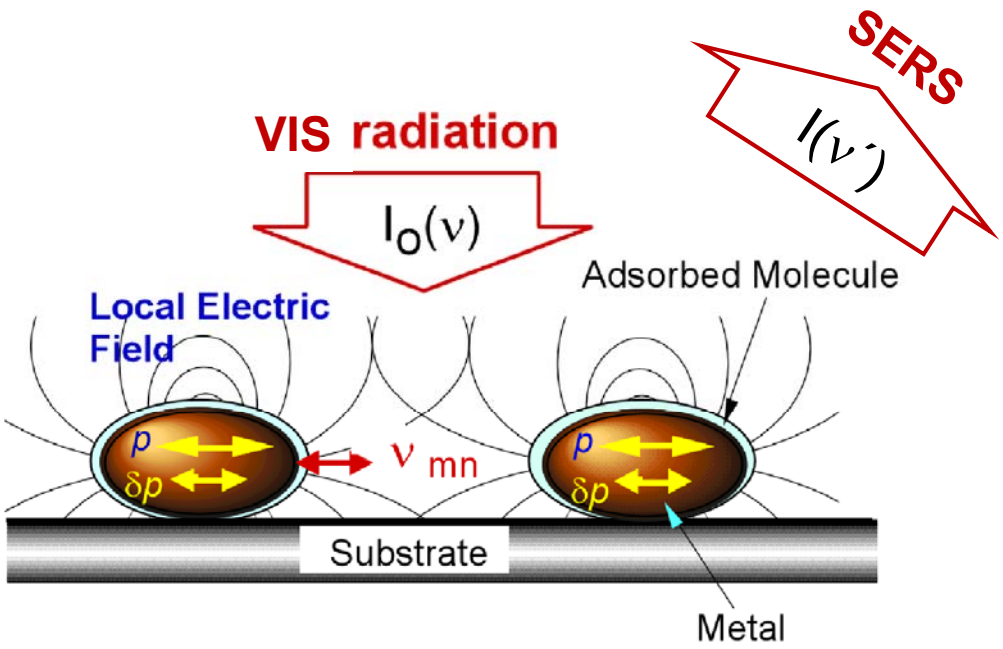

Molecular fingerprints

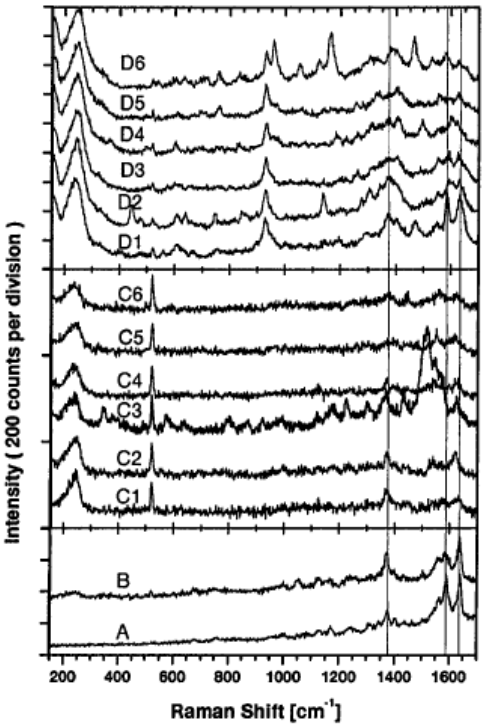

Identif s
for selec ies

J. Aizpurua, Lecture given at SSOP Porquerolles, Sept. 2009

Surface Enhanced Raman Scattering, SERS

Electromagnetic effect

$$M_i^{EM} = \left|E^L(\omega_I)/E^I(\omega_I)\right|^2 \cdot \left|E^L(\omega_I-\omega_v)/E^I(\omega_I-\omega_v)\right|^2$$

If $\omega_v << \omega_I$

$$M_i^{EM} = \left|E^L(\omega_I)/E^I(\omega_I)\right|^4$$

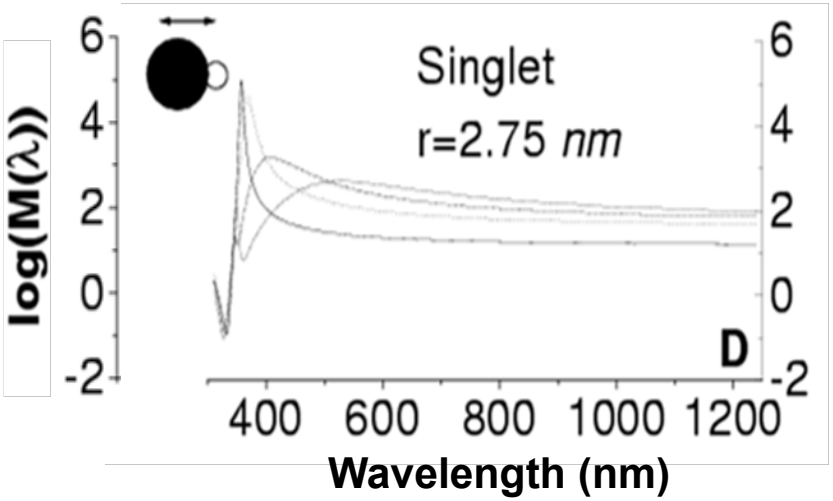

H. Xu, J. Aizpurua, M. Käll and P. Apell, Phys. Rev. E. **62**, 4318 (2000)

Near-field coupling – simple systems

Sphere - plane

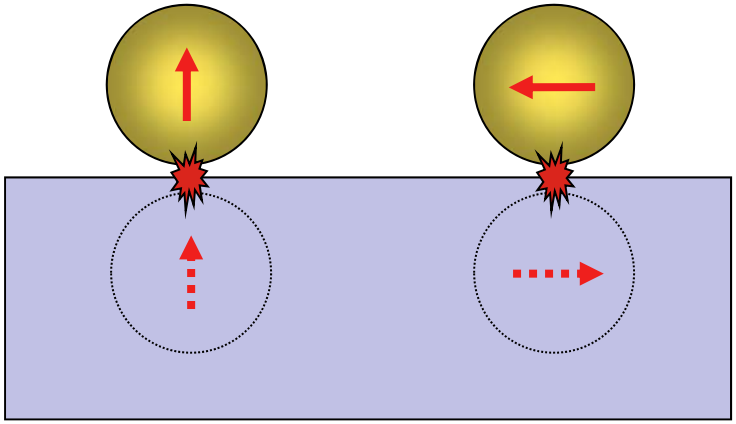

dipole – mirror dipole near-field interaction

Sphere - sphere

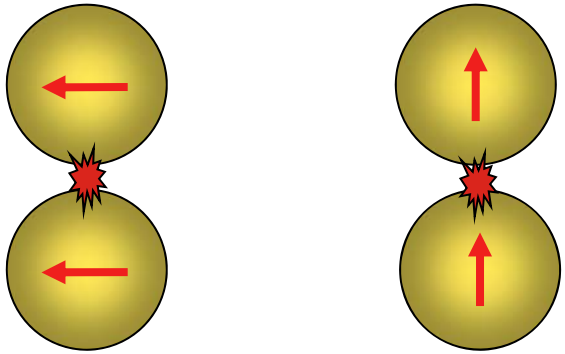

dipole – dipole near-field interaction

→ High field enhancement in the gap due to resonant near-field coupling

→
- local light sources
- enhanced Raman signals (detection of single molecule Raman signals)
- nonlinear effects

Dipolar sphere-sphere near-field interaction

Polarizability of spheres: $\alpha_i = 4\pi a_i^{\,3} \dfrac{\varepsilon_i - 1}{\varepsilon_i + 2}$

Scattered field:

$$E_{sca} \propto \alpha_{eff} E_{in}$$

Effective polarizability of interacting dipoles (dipole approximation):

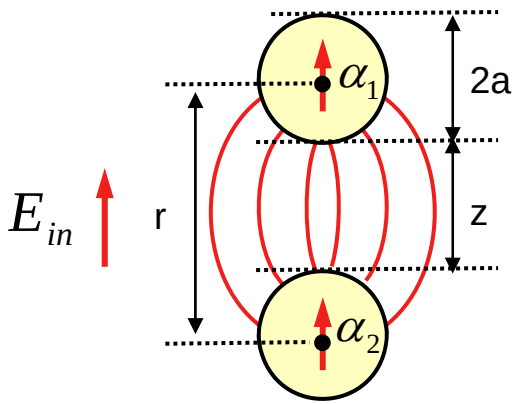

$$\alpha_{eff} = \frac{\alpha_1 + \alpha_2 + \dfrac{\alpha_1 \alpha_2}{\pi r^3}}{1 - \dfrac{\alpha_1 \alpha_2}{4\pi^2 r^6}}$$

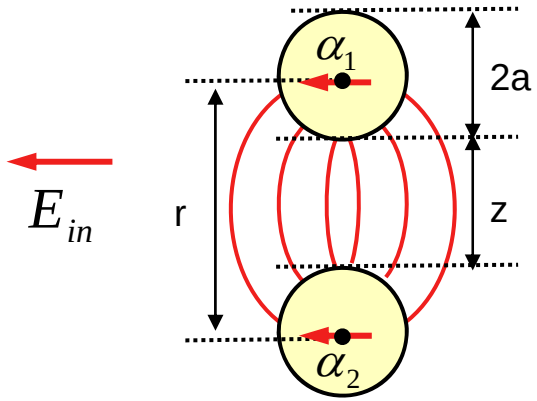

$$\alpha_{eff} = \frac{\alpha_1 + \alpha_2 - \dfrac{\alpha_1 \alpha_2}{2\pi r^3}}{1 - \dfrac{\alpha_1 \alpha_2}{16\pi^2 r^6}}$$

Resonance shift effects – two resonant spheres

2 metal spheres: $\varepsilon_1 = \varepsilon_2 = 1 - \dfrac{\omega_p^2}{\omega^2 + i\gamma\omega}$

(drude term)

$\gamma = 0.2$

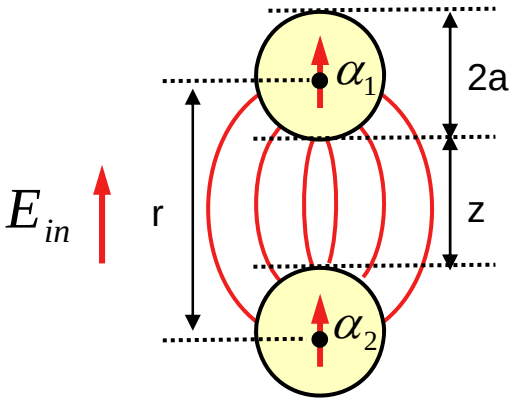

$$\alpha_{eff} = \frac{\alpha_1 + \alpha_2 + \dfrac{\alpha_1\alpha_2}{\pi r^3}}{1 - \dfrac{\alpha_1\alpha_2}{4\pi^2 r^6}}$$

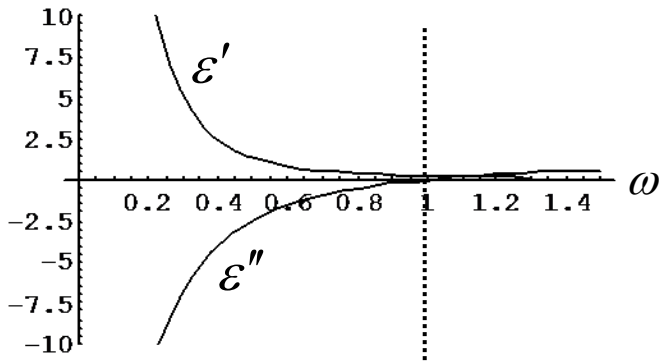

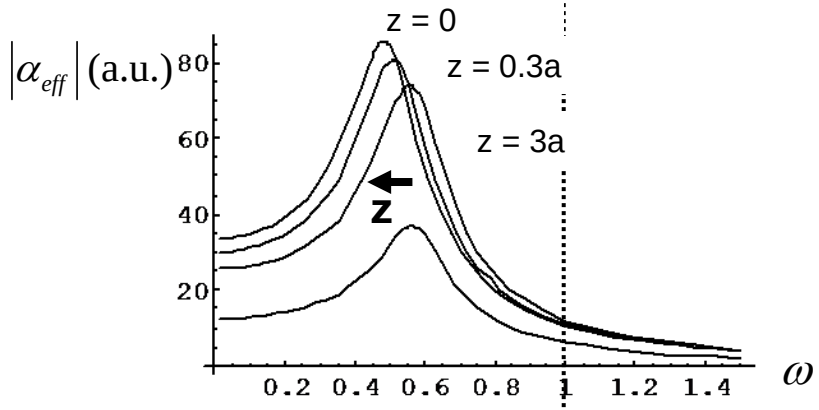

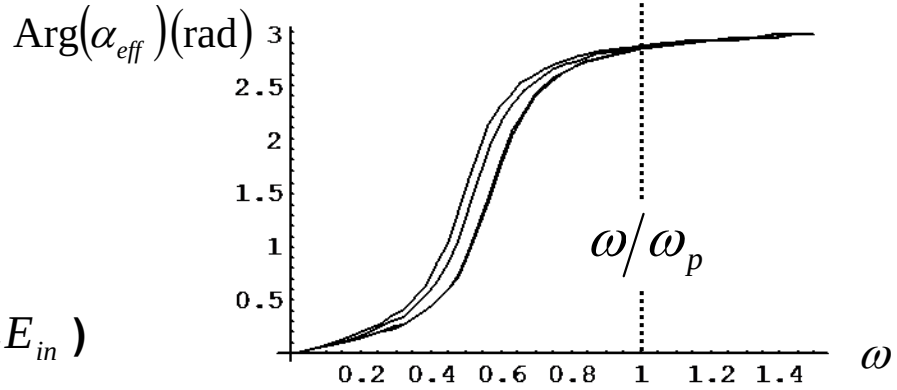

→ dipolar approximation predicts

- **resonance shifts**
- **field enhancement** ($E_{sca} \propto \alpha_{eff} E_{in}$)

Dimers assisting in spectroscopy: SERS

Xu et al. Phys Rev. Lett. (1999)

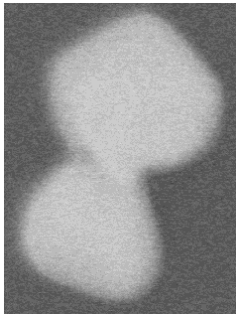

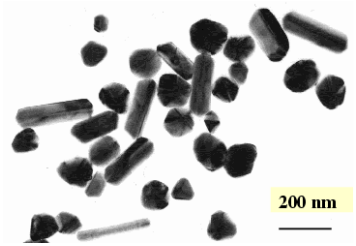

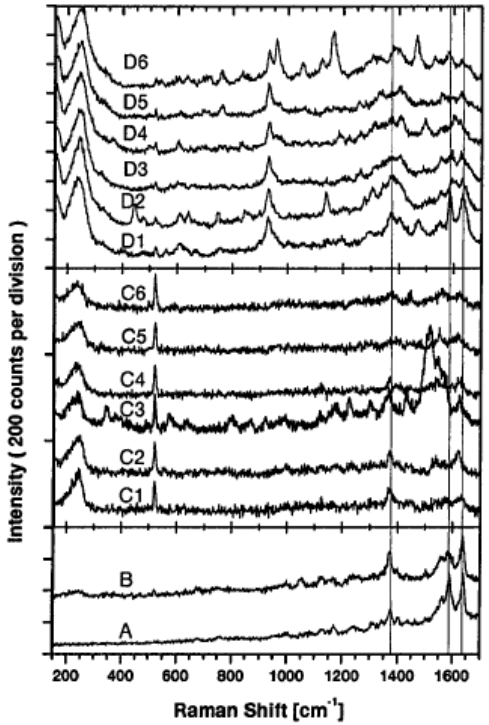

Xu, Aizpurua, Käll and Apell, Phys. Rev. E. **62**, 4318 (2000)

Hot sites

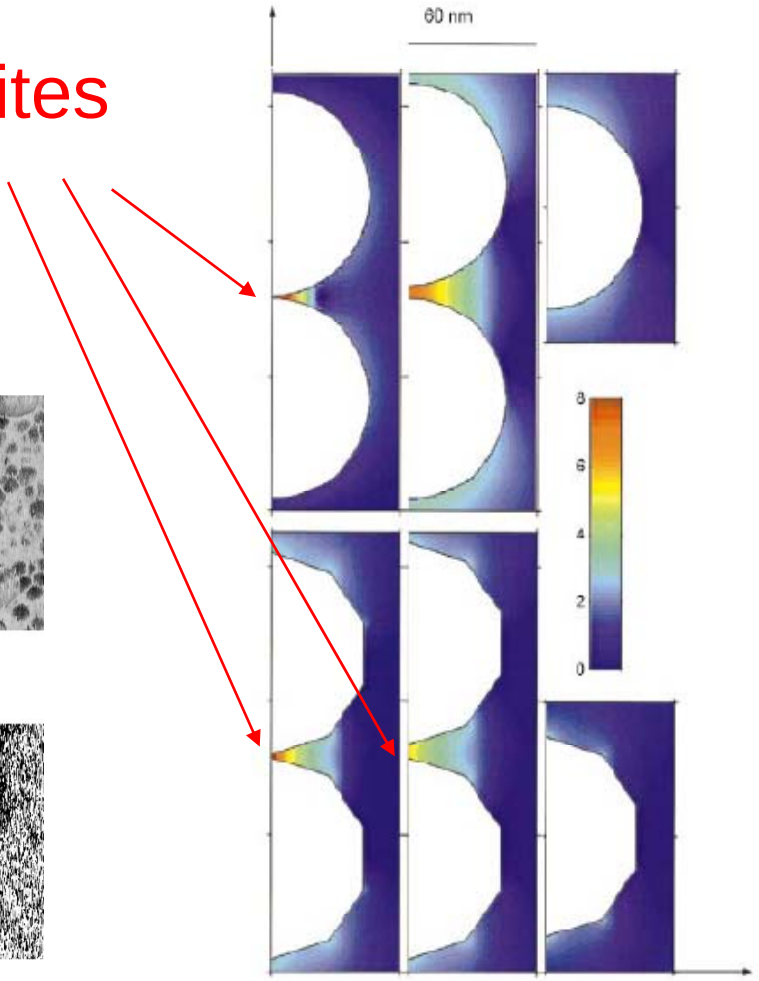

topography

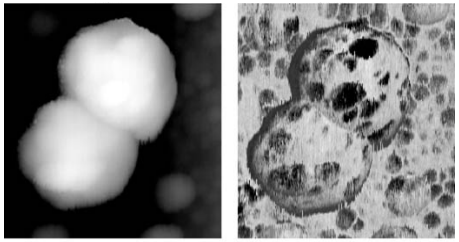

amplitude 400nmx400nm phase

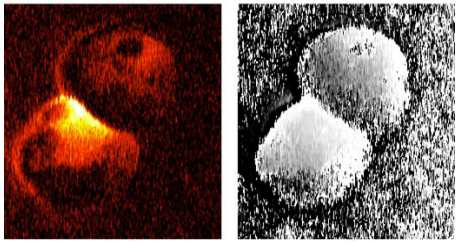

Image obtained by R. Hillenbrand, (Max Planck, Munich)

Two near-field interacting gold discs I

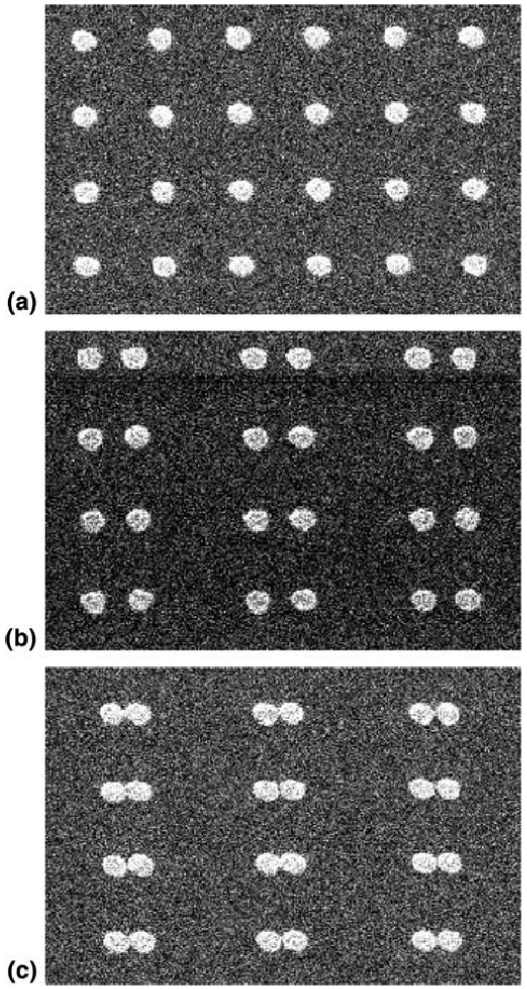

Fig. 1. SEM images of particle pair samples with varying interparticle distance (center-to-center) of (a) 450 nm, (b) 300 nm and (c) 150 nm. The particle diameter is 150 nm, the particle height is 17 nm.

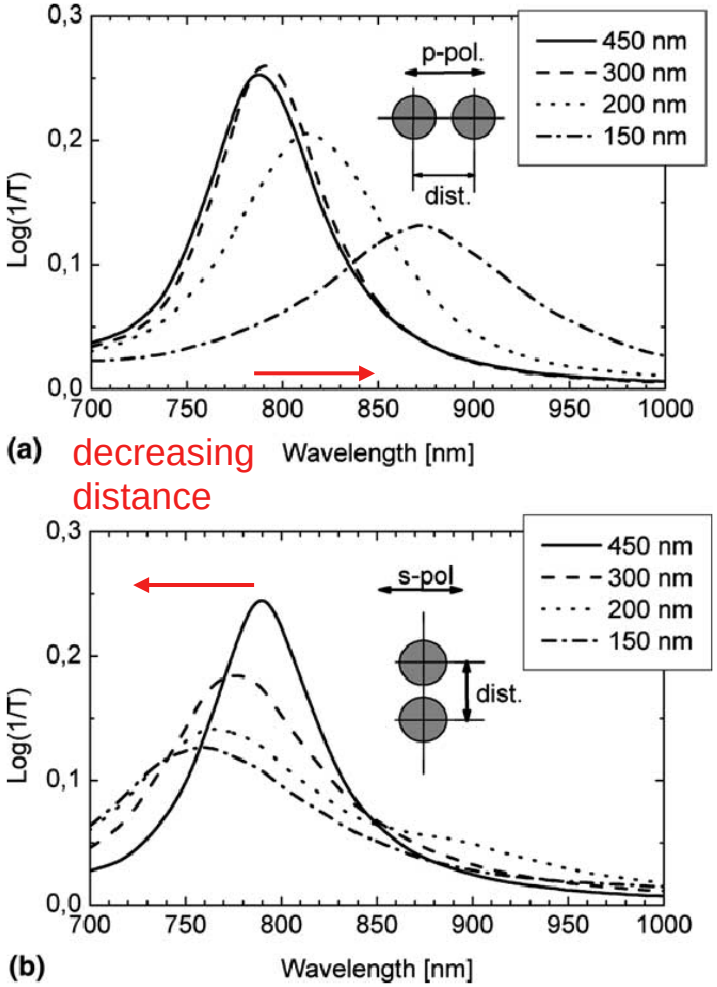

Fig. 2. Extinction (=log(1/Transmission)) spectra of a 2D array of the Au nanoparticle pairs with the interparticle center-to-center distances as the parameter. The orthogonal particle separation is kept constant, as can be seen in Fig. 1. The polarization direction of the exciting light is (a) parallel to the long particle pair axis and (b) orthogonal to it.

W. Rechenberger et.al., Opt. Commun. **220,** 137 (2003)

J. Aizpurua, Lecture given at SSOP Porquerolles, Sept. 2009

Field-enhancement: geometrical squeezing

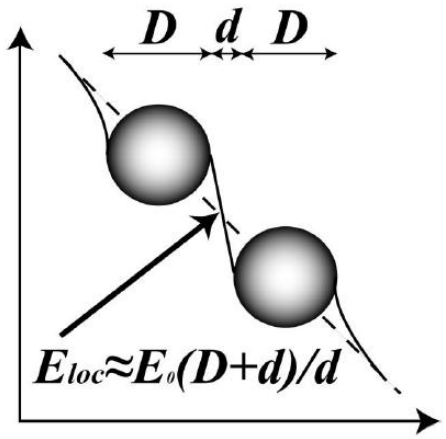

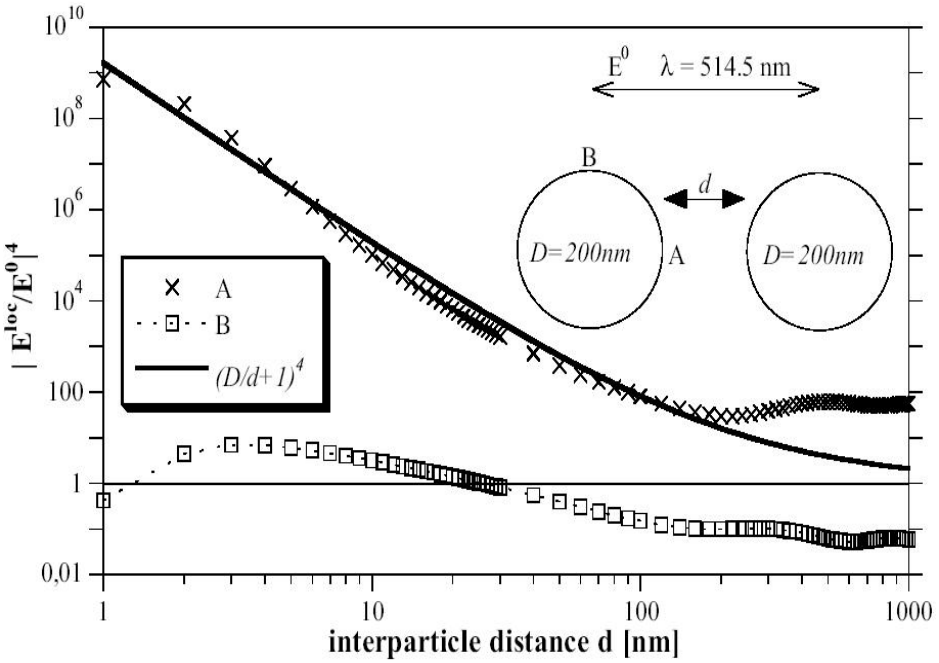

$$E_{loc} = E_0 (D+d)/d$$

$$M = (\frac{D}{d}+1)^4$$

Dimers assisting in spectroscopy: SERS

$$M_i^{EM} = \left| E^L(\omega_I) / E^I(\omega_I) \right|^4$$

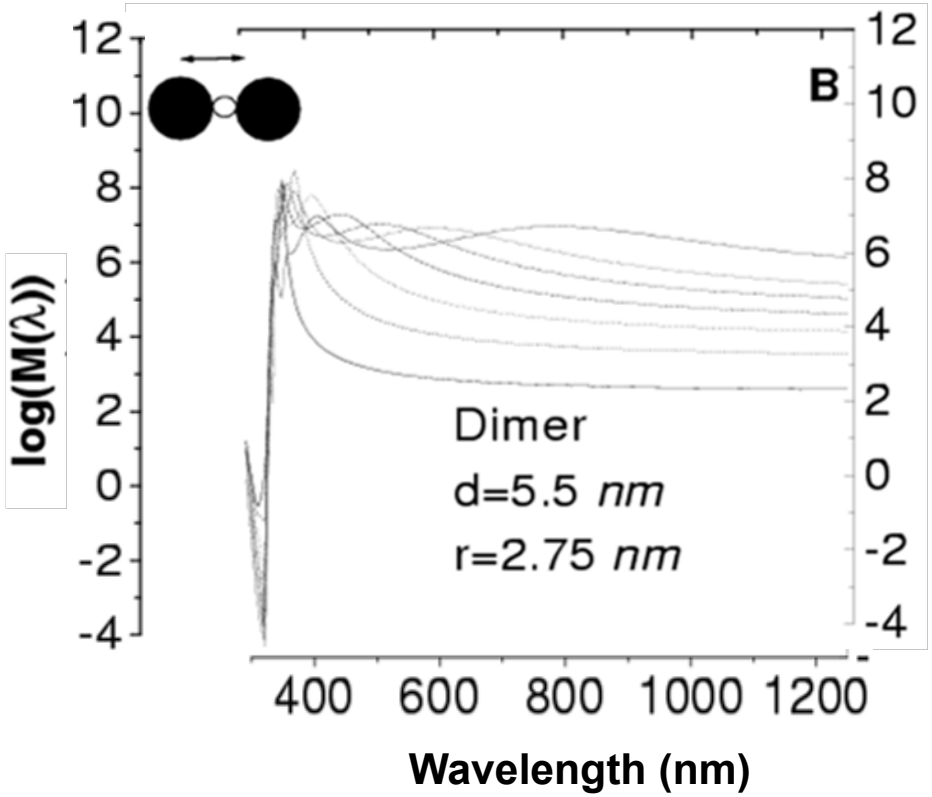

H. Xu, J. Aizpurua, M. Käll and P. Apell, Phys. Rev. E. **62**, 4318 (2000)

Plasmon hybridization

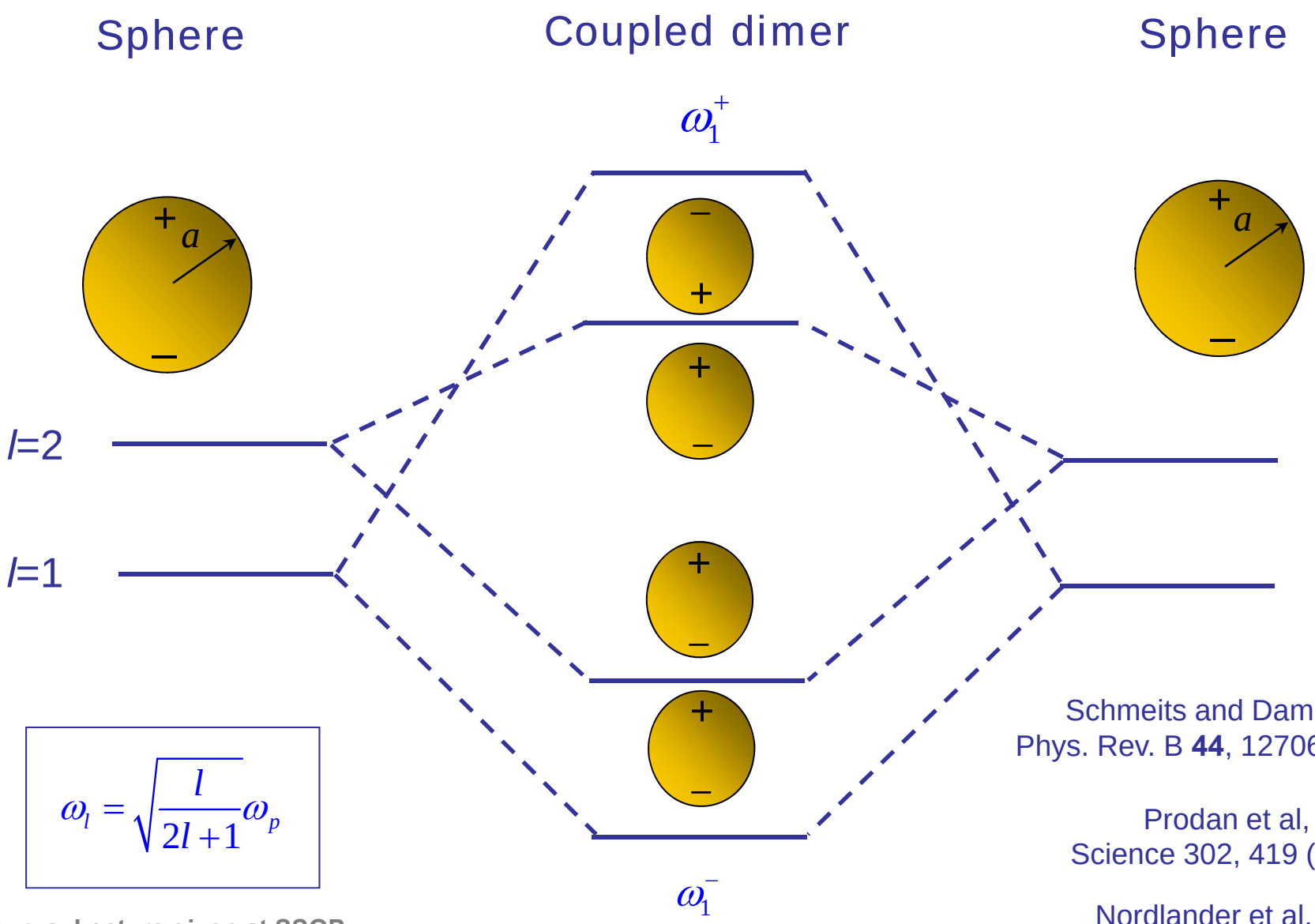

$$\omega_l = \sqrt{\frac{l}{2l+1}}\omega_p$$

Schmeits and Dambly,
Phys. Rev. B **44**, 12706 (1991)

Prodan et al,
Science 302, 419 (2003)

Nordlander et al,
Nanoletters **4**, 899 (2004)

Coupled modes in a metallic dimer

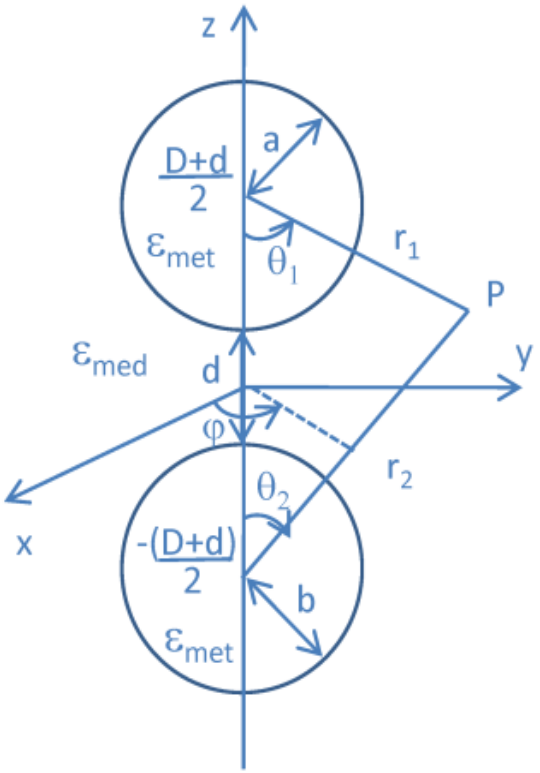

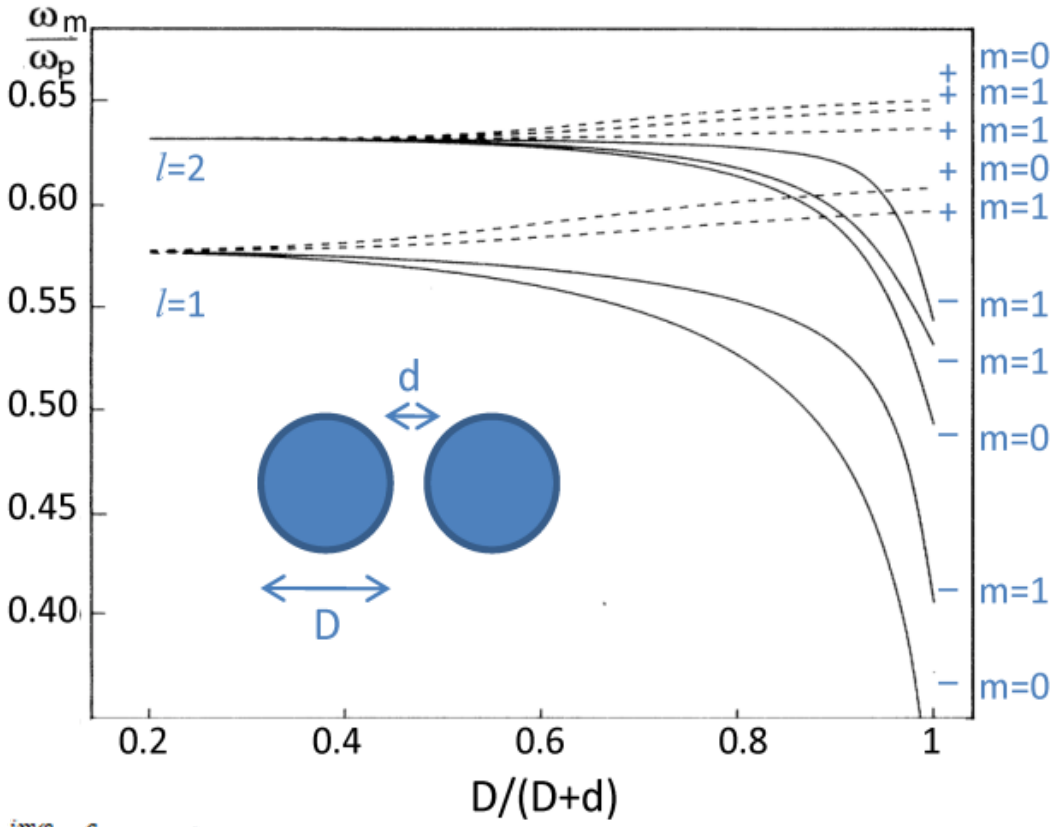

$$\Psi^{(1)}(r,\theta,\varphi) = \sum_{l=0}^{\infty}\sum_{m=-l}^{m=+l}\left(\frac{r_1}{a}\right)^l A_{lm}\,Y_{lm}(\theta_1,\varphi)\,e^{im\varphi} \quad for\ r_1 < a,$$

$$\Psi^{(2)}(r,\theta,\varphi) = \sum_{l=0}^{\infty}\sum_{m=-l}^{m=+l}\left(\frac{r_2}{b}\right)^l D_{lm}\,Y_{lm}(\theta_2,\varphi)\,e^{im\varphi} \quad for\ r_2 < b,$$

$$\Psi^{(3)}(r,\theta,\varphi) = \sum_{l=0}^{\infty}\sum_{m=-l}^{m=+l}\left[\left(\frac{a}{r_1}\right)^{l+1} B_{lm}\,Y_{lm}(\theta_1,\varphi) + \left(\frac{b}{r_2}\right)^{l+1} C_{lm}\,Y_{lm}(\theta_2,\varphi)\right]e^{im\varphi}$$

$$\left(\frac{\omega_{m=0;l=1}}{\omega_p}\right)^2_{\pm} = \frac{\left(1 \pm 2\left(\frac{D/2}{D+d}\right)^3\right)}{3}$$

J. Aizpurua, Lecture given at SSOP Porquerolles, Sept. 2009

Schmeits and Dambly, Phys. Rev. B **44**, 12706 (1991)

Nanoparticles in the touching limit

Map of the resonances

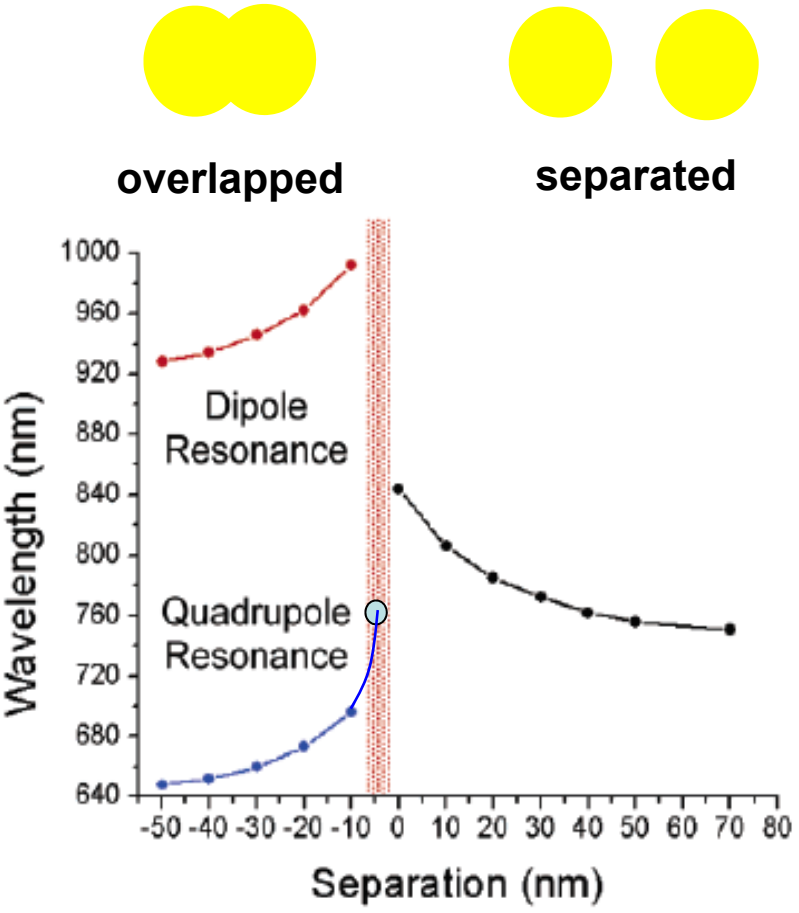

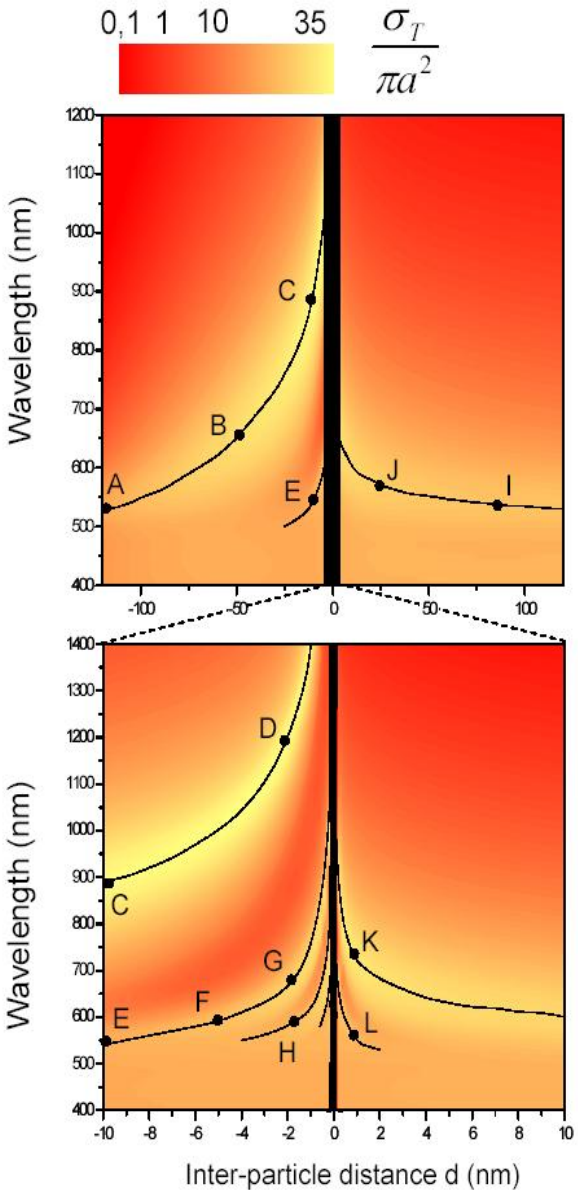

I. Romero, *et al*. Optics Express 14, 9988 (2006)

Charge density modes

Low frequency modes of non-touching and touching dimers are distinctly different

NOT TOUCHING

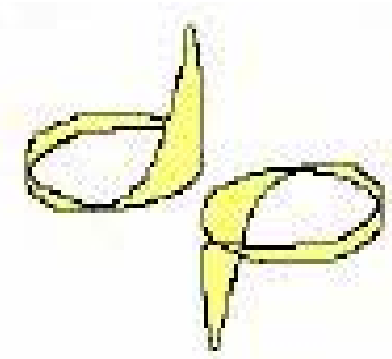

Neutral charge in each particle

TOUCHING

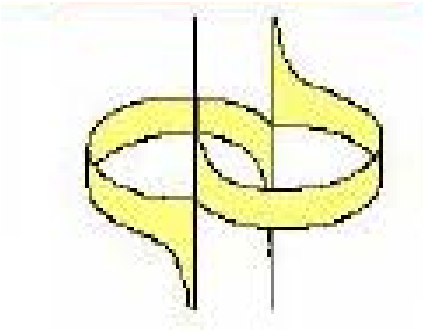

Net electrical charge in each half of the dimer

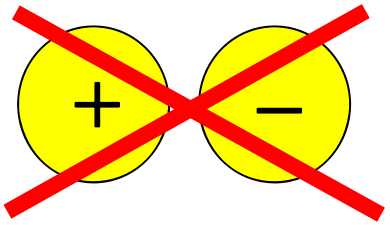

Unphysical mode

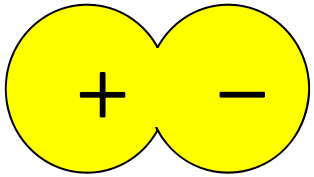

1st physical mode

1st physical mode

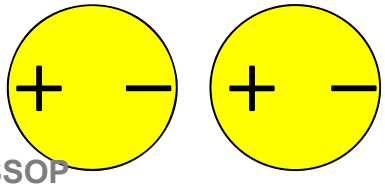

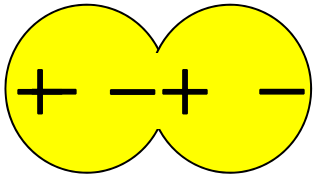

2nd physical mode

Close Encounters between Two Nanoshells

J. Britt Lassiter,[†,||] Javier Aizpurua,[⊥] Luis I. Hernandez,[||] Daniel W. Brandl,[†,||] Isabel Romero,[⊥] Surbhi Lal,[‡,||] Jason H. Hafner,[†,§,||] Peter Nordlander,[†,‡,||] and Naomi J. Halas*[,†,‡,§,||]

NANO LETTERS

2008
Vol. 8, No. 4
1212-1218

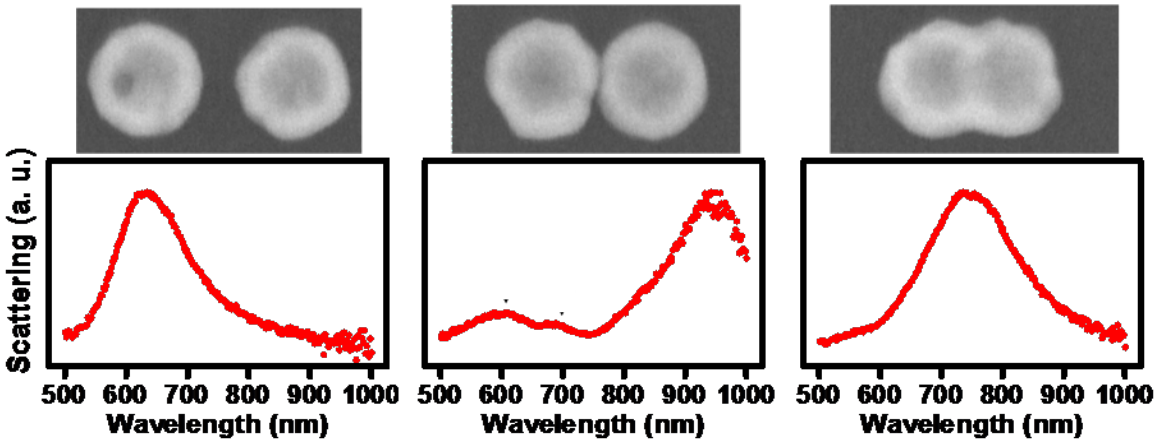

Slightly close: Slight shift

Close proximity: red shift

Overlapped: Blue-shift

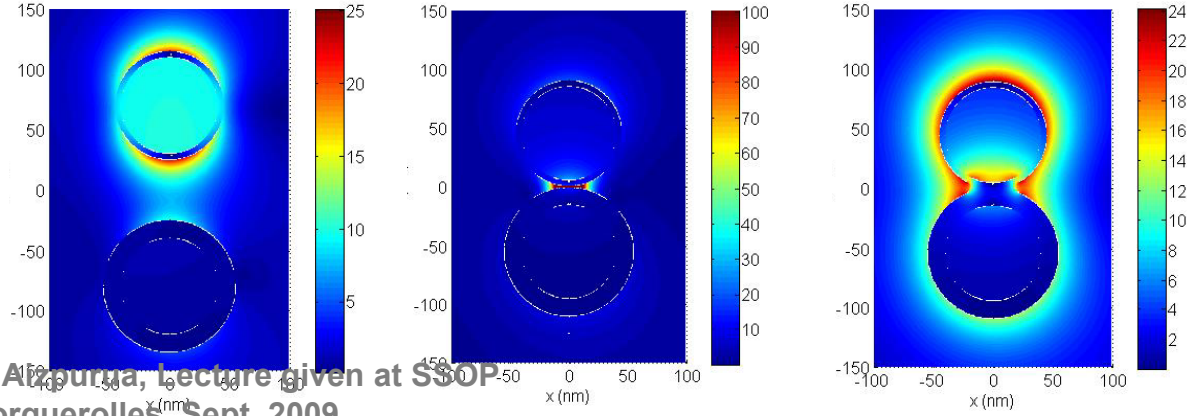

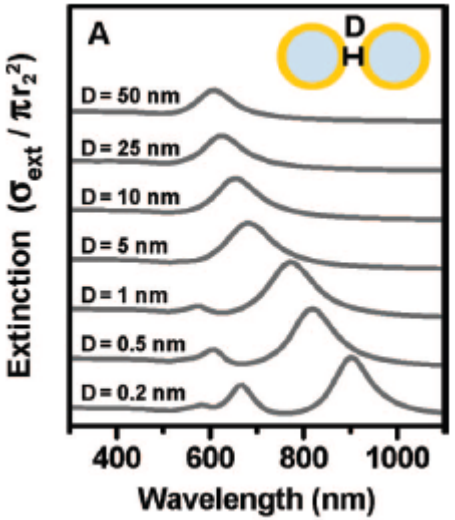

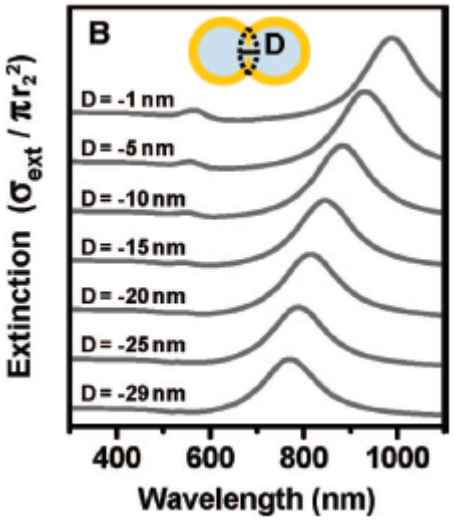

J. Aizpurua, Lecture given at SSOP Porquerolles, Sept. 2009

Outline

- Basics: Plasmonics

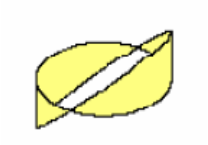

- Optical antennas for SERS

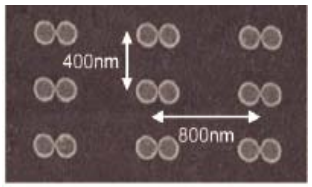

- Infrared antennas for SEIRA
  (Surface-Enhanced IR Absorption)

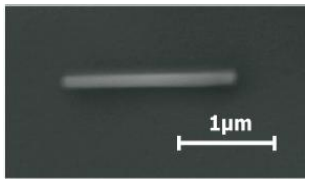

- Substrate-Enhanced Infrared Near-Field Microscopy

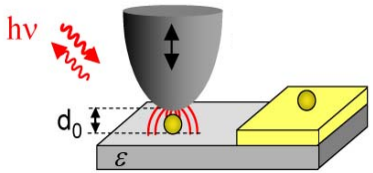

- THz Near-field Nanoscopy

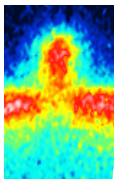

Surface-enhanced IR absorption (SEIRA)

Resonant antennas for enhanced signal of molecular vibrations

Concept

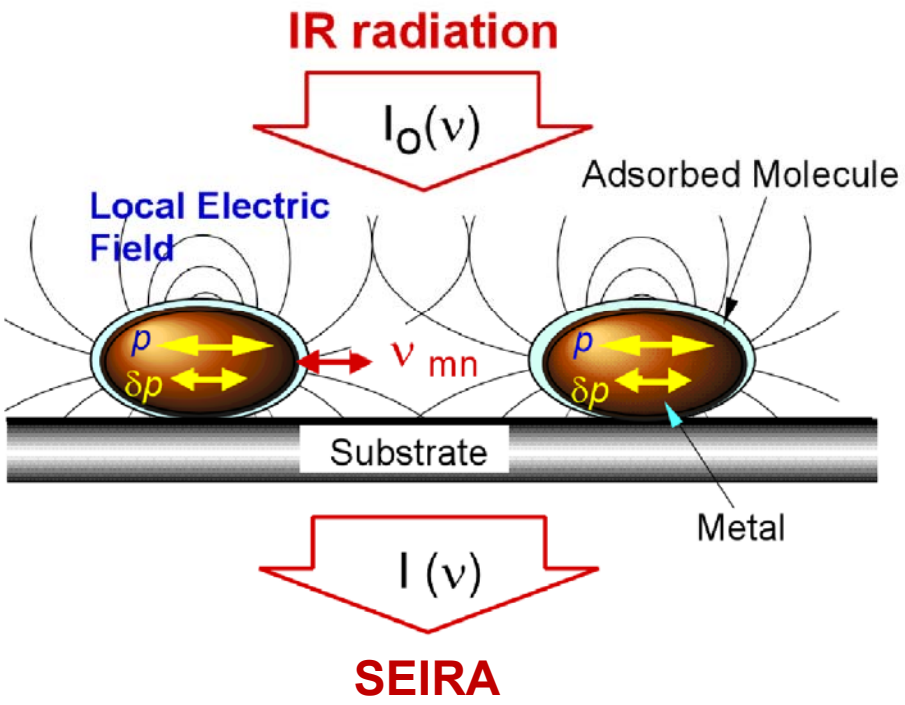

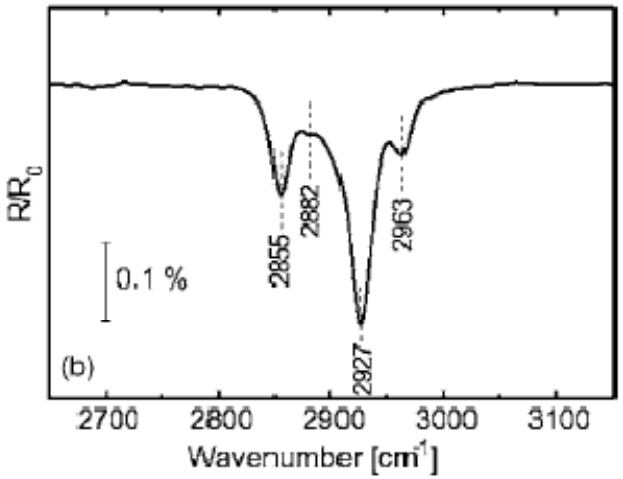

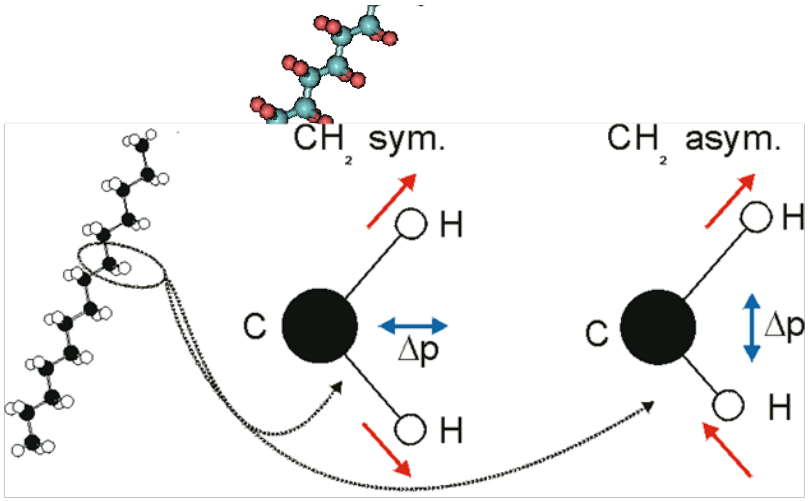

J. Aizpurua, Lecture given at SSOP Porquerolles, Sept. 2009

Nanoshell arrays: Substrates for infrared spectroscopy

Metallic nanoparticle arrays for SERS and SEIRA

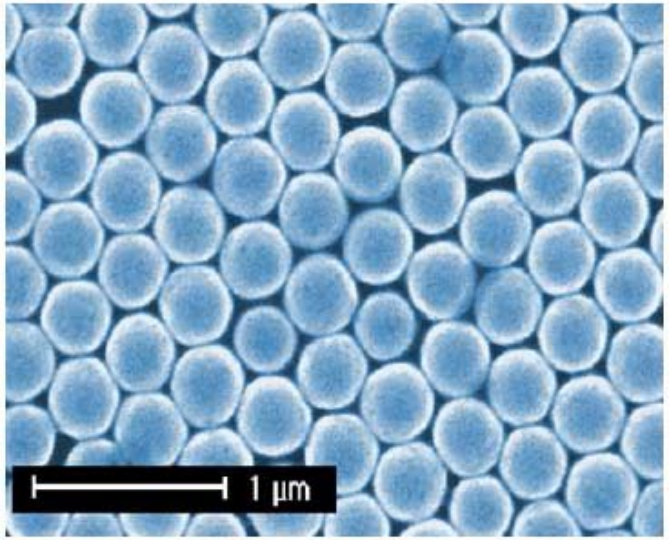

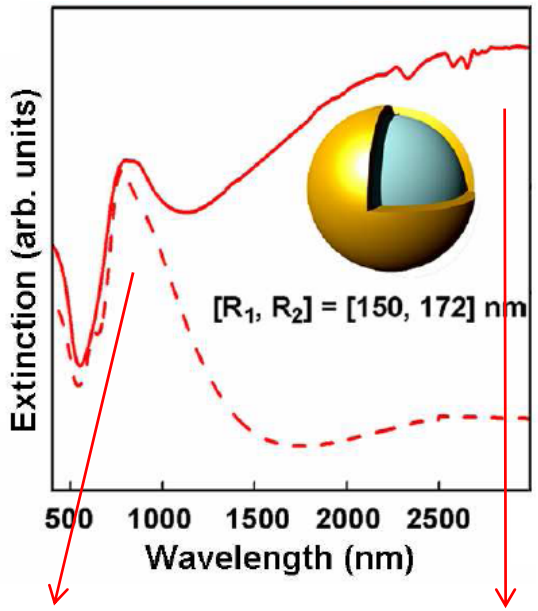

VISIBLE
Max = 12.9

INFRARED
Max = 19.1

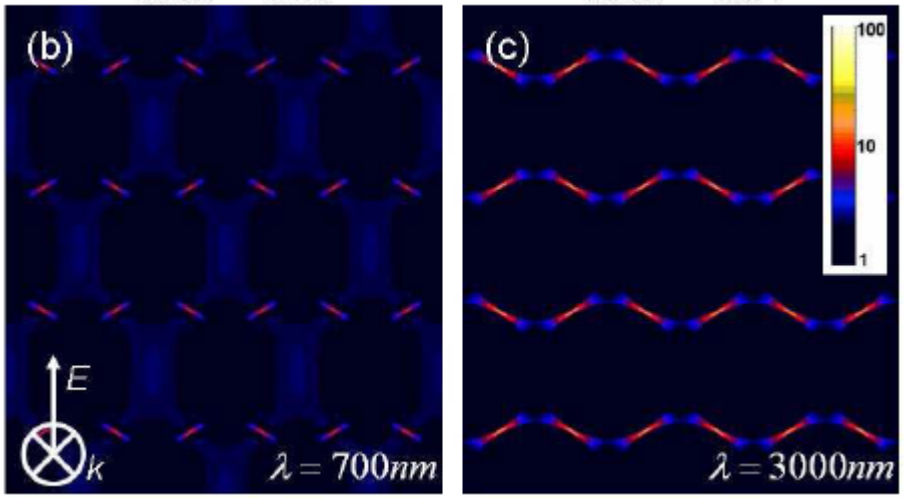

Kundu et al. Angew. Chem. (2007)
Halas group, Rice Univ.

Fei et al. ACS Nano. 2, 707 (2008)
In collaboration with P. Nordlander's group

Metallic Nanoparticle Arrays: A Common Substrate for Both Surface-Enhanced Raman Scattering and Surface-Enhanced Infrared Absorption

Fei Le,[†] Daniel W. Brandl,[†] Yaroslav A. Urzhumov,[‡] Hui Wang,[§] Janardan Kundu,[§] Naomi J. Halas,[§,⊥] Javier Aizpurua,[∥] and Peter Nordlander[†,⊥,*]

ACSNANO

2, 707 (2008)

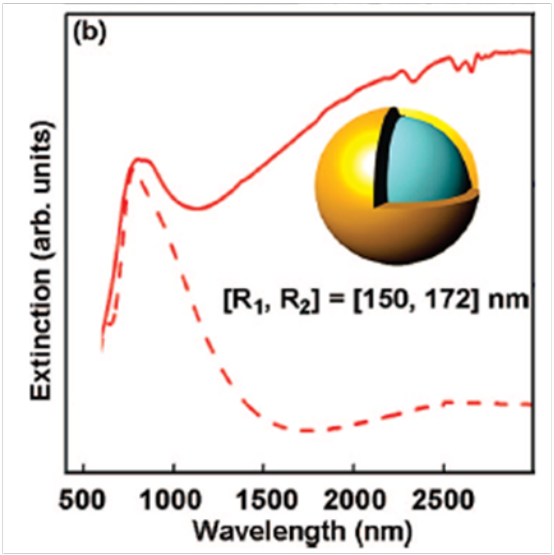

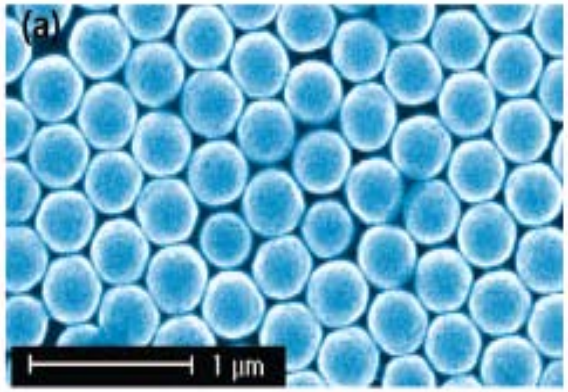

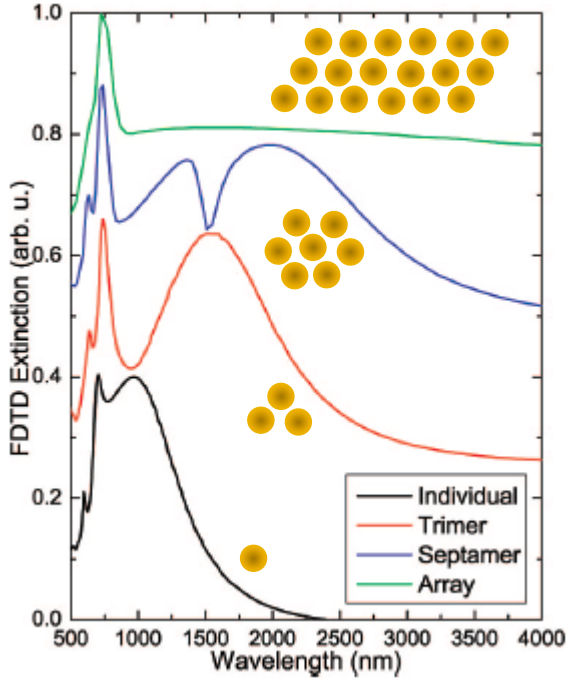

J. Aizpurua, Lecture given at SSOP Porquerolles, Sept. 2009

Surface-enhanced IR absorption (SEIRA)

Resonant antennas for enhanced signal of molecular vibrations

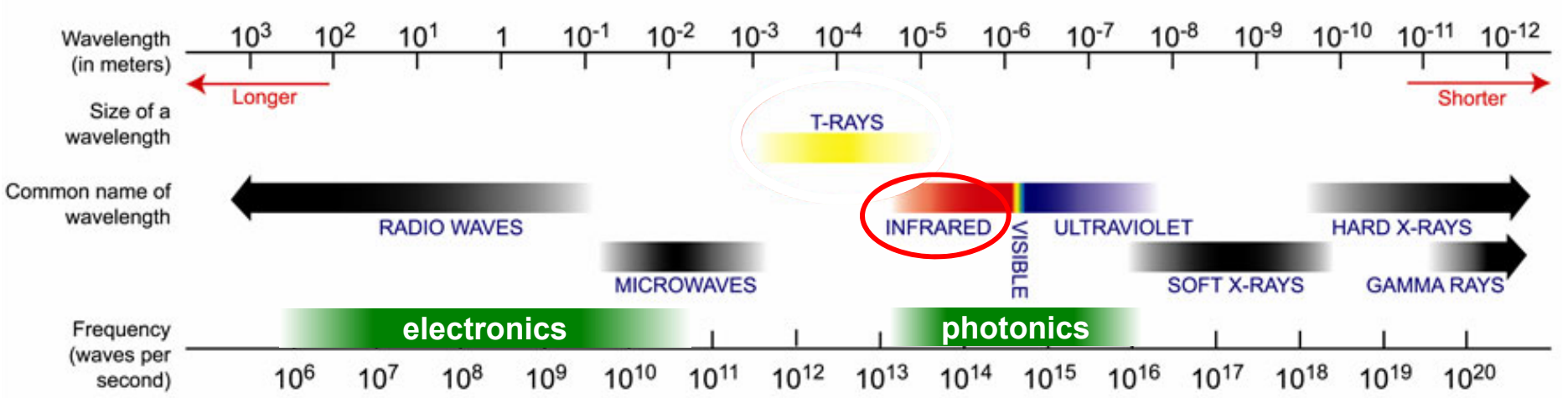

J. Aizpurua, Lecture given at SSOP Porquerolles, Sept. 2009

Single antenna for infrared resonant spectroscopy

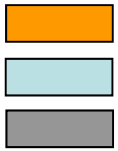

Resonant structure
Layer to be investigated
Non-resonant structure

Resonant triangles (coated)

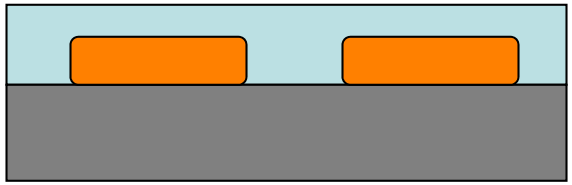

T.R. Jensen et al., J. Phys. Chem B**, 104**, 10549 (2000)

Nanoshell arrays

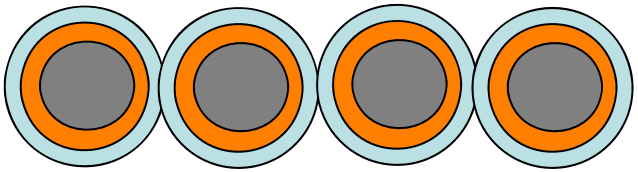

H. Wang et al., Angew. Chem. **46**, 9040 (2007)

Resonant particle

(coated) (embedded)

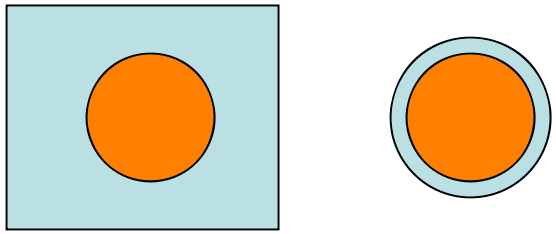

M.S. Anderson, App. Phys. Lett. **83**, 2964 (2003)

Resonant rod (coated)

F. Neubrech et al.,
Phys. Rev. Lett. **101**, 157403 (2008)

Basics of nanorods

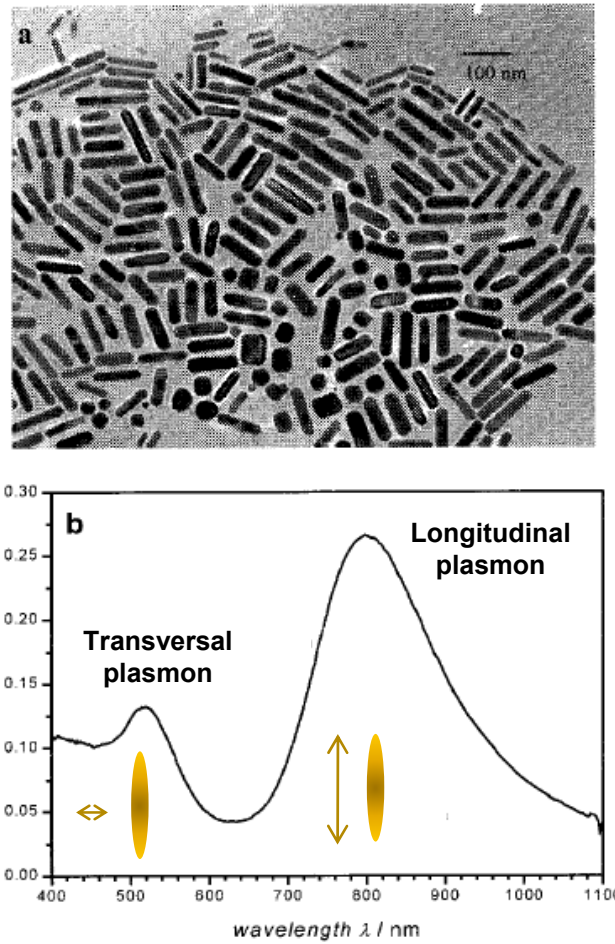

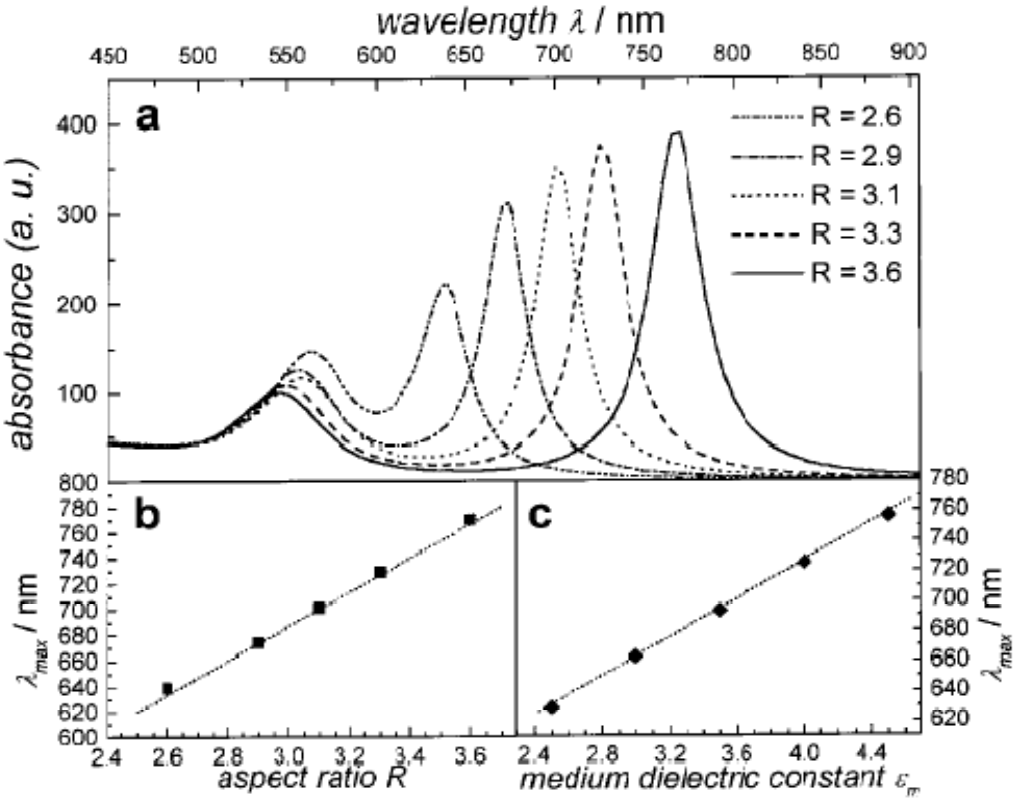

L=λ/m ?

S. Link and M.A. El-Sayed. J. Phys. Chem. B 103,8410 (1999).

Calculation of gold antenna modes

Antenna modes:

D=80nm,L=200nm; ratio=2.5

Dipole response:

L α $\lambda/2$

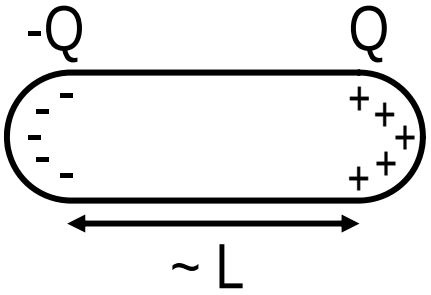

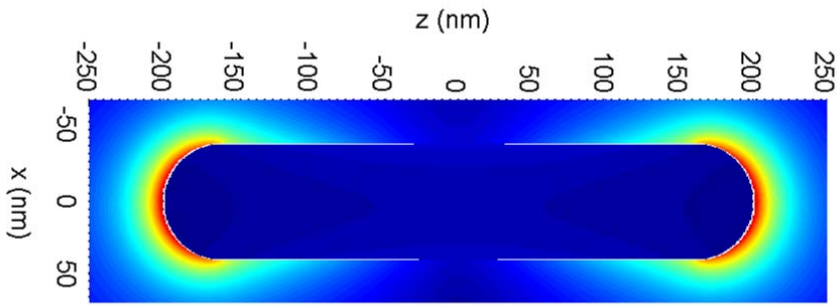

Aizpurua et al. Physical Review B 71, 235420 (2005)

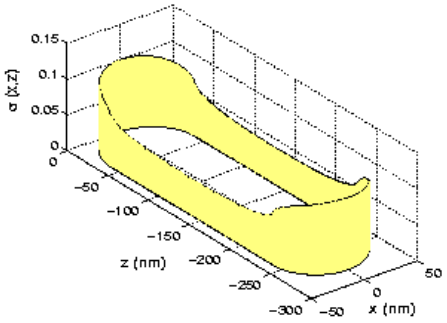

0: λ=8814 nm

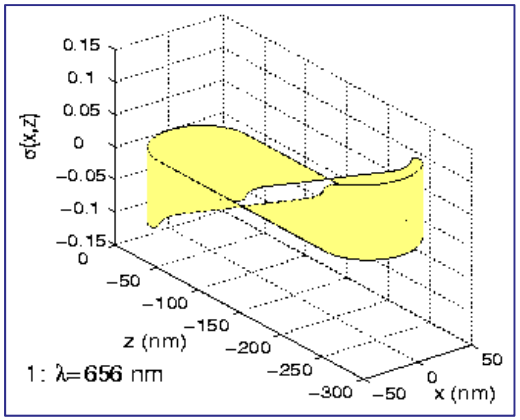

1: λ=656 nm

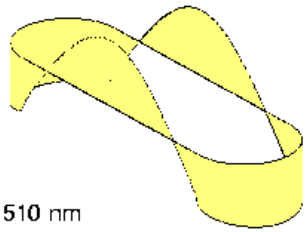

2: λ=510 nm

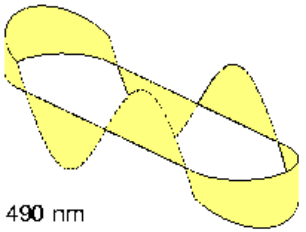

3:λ= 490 nm

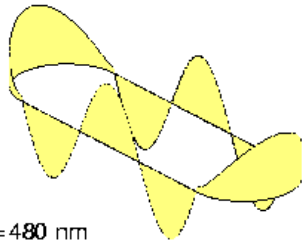

4: λ=480 nm

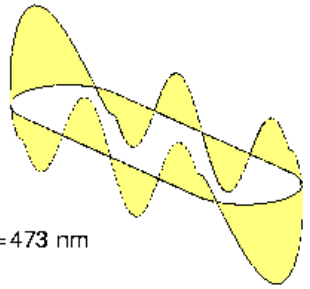

5: λ=473 nm

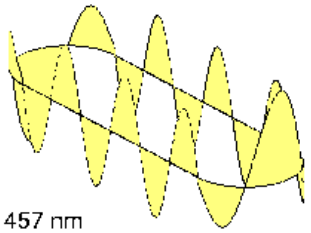

9:λ=457 nm

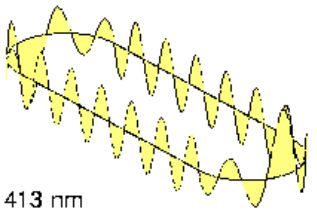

19: λ= 413 nm

Metallic nanorod as a λ/2 optical antenna

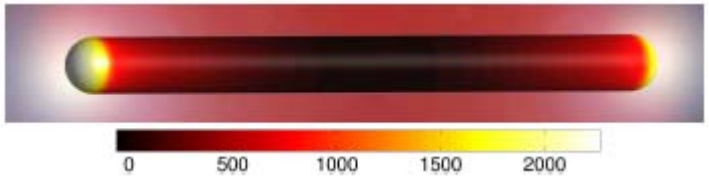

Mapping the plasmon resonances of metallic nanoantennas

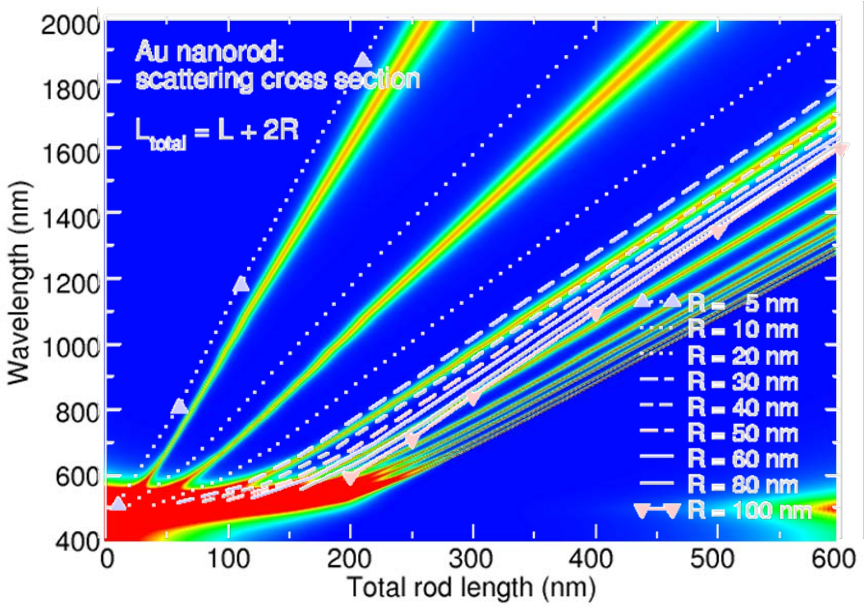

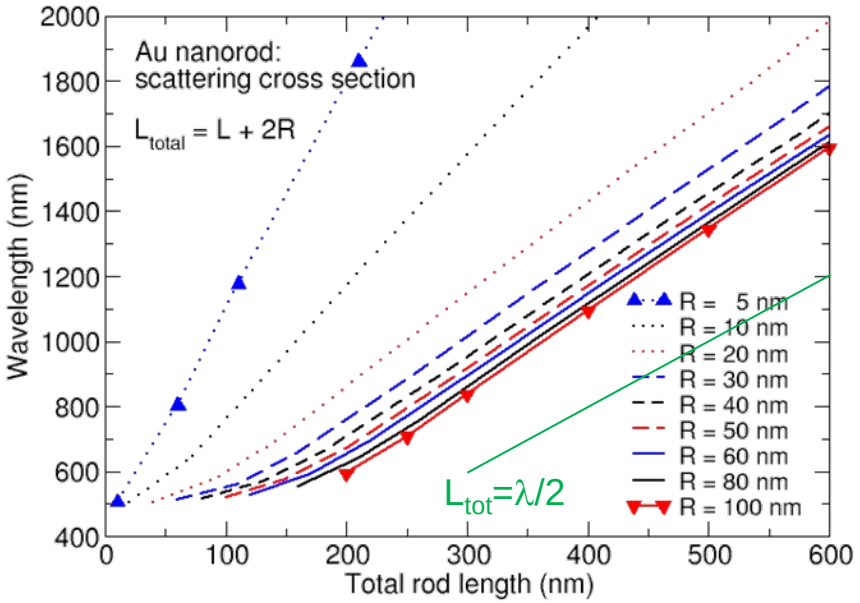

$$(q^2 - \varepsilon k^2)^{1/2}\, I_0((q^2 - \varepsilon k^2)^{1/2} R) K_1((q^2 - k^2)^{1/2} R) + \varepsilon\, (q^2 - k^2)^{1/2}\, I_1((q^2 - \varepsilon k^2)^{1/2} R) K_0((q^2 - k^2)^{1/2} R) = 0$$

$$q = \pi / L_{tot}$$

J. Aizpurua, Lecture given at SSOP Porquerolles, Sept. 2009

G.W. Bryant, F.J. García de Abajo and J. Aizpurua, Nano Lett. **8**, 631 (2008)

Optical nanoantenna resonant at λ=3.41μm with L=1.31μm and D=100nm

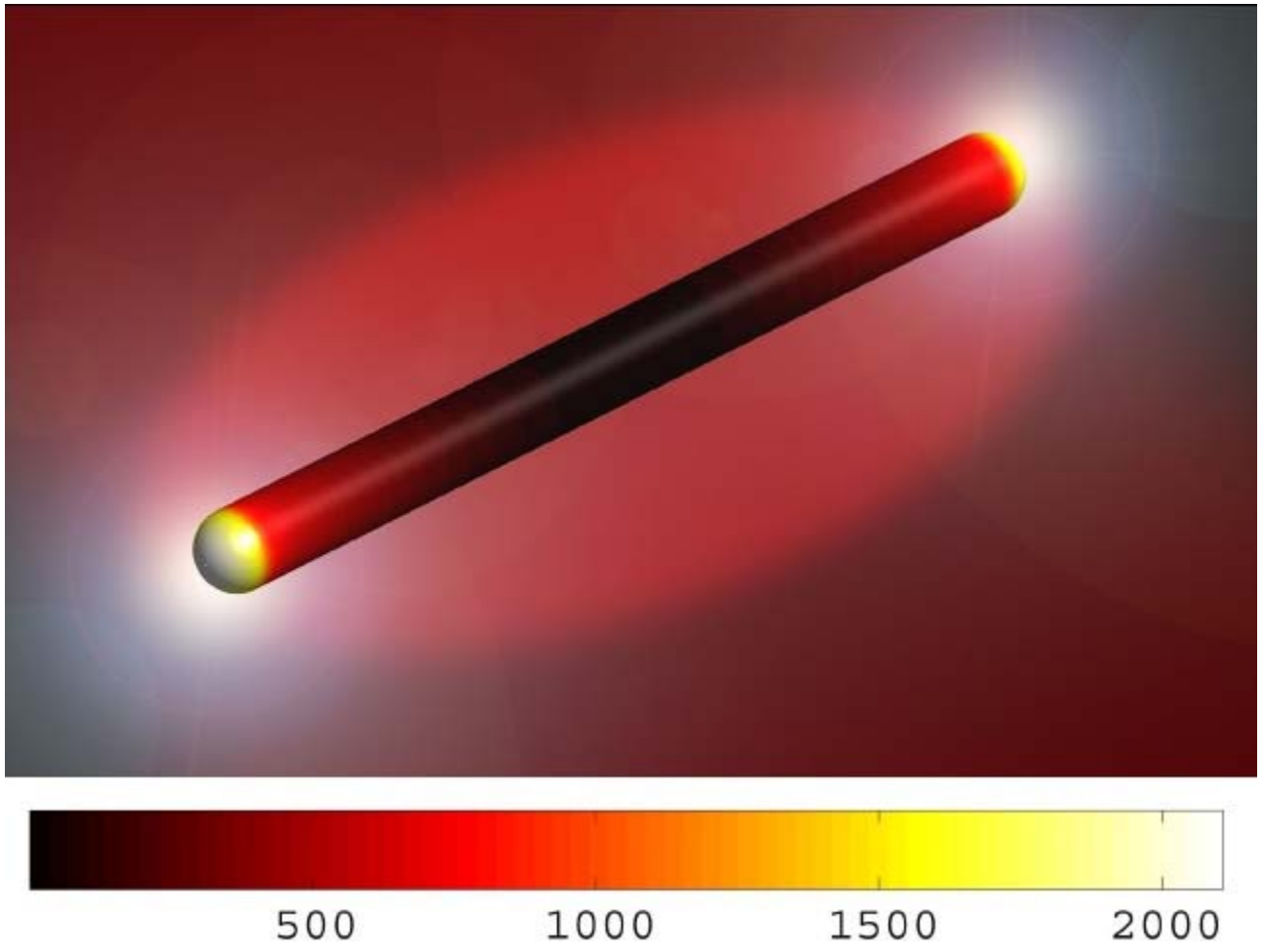

J. Aizpurua, Lecture given at SSOP Porquerolles, Sept. 2009

Finding the right nanowire resonance for IR spectroscopy

Experiments by Prof. A. Pucci's group (Heidelberg, Germany)

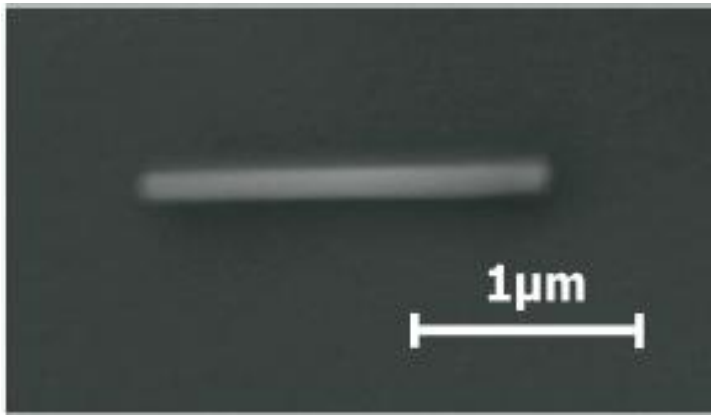

Gold nanowire (L=1.5μm and D=100nm, on a silicon wafer)

SEM image: perfect cylindrical shape

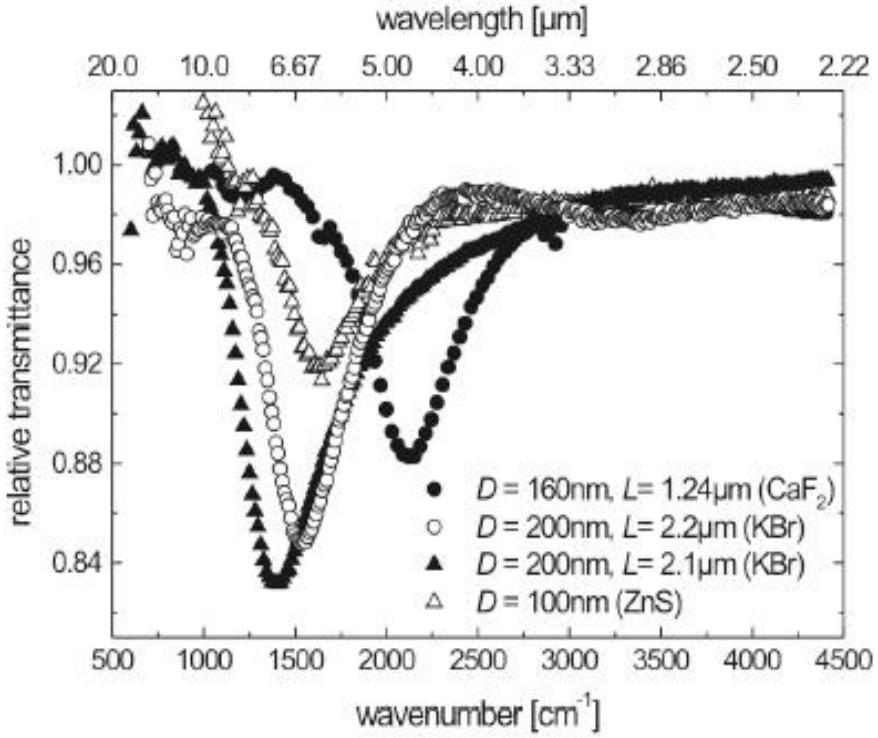

Relative IR transmittance spectra
Electric field along the long wire axis

F. Neubrech et al. Appl. Phys. Lett. 89, 253104 (2006)

Near-field mapping of IR nanoantennas

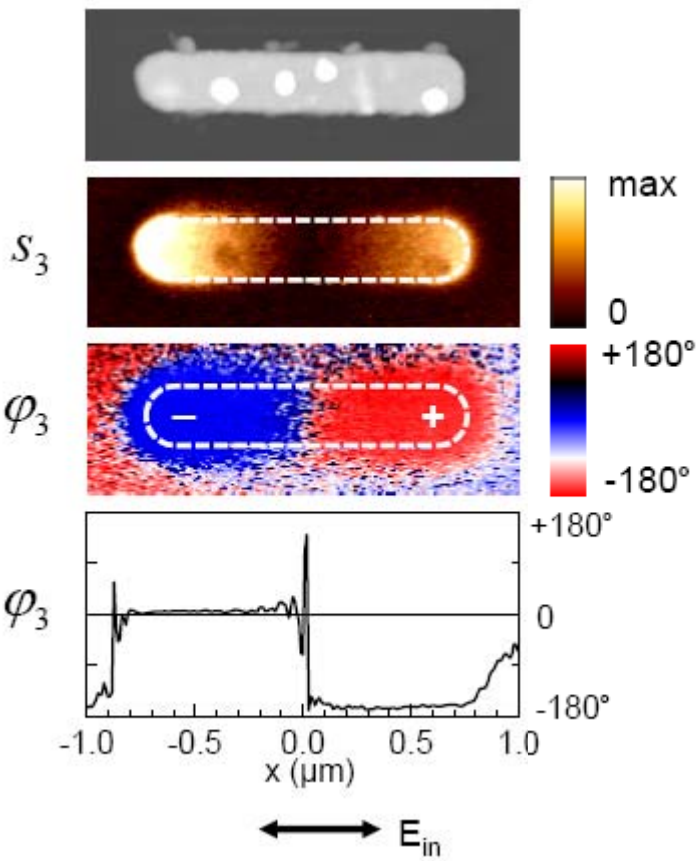

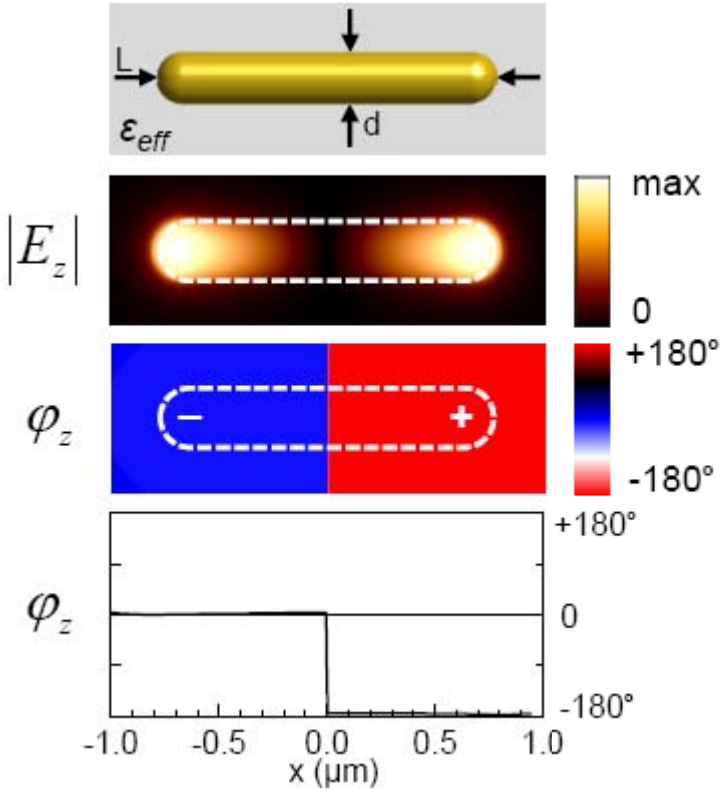

Experiment by Martin Schnell,
R. Hillenbrand's group

Calculation by A. Garcia-Etxarri,
San Sebastian

(M. Schnell, Nat. Phot. 3, 287 (2009))

λ/2 antenna enhanced IR spectroscopy

Relative IR transmitance of ODT molecules on a gold nanowire

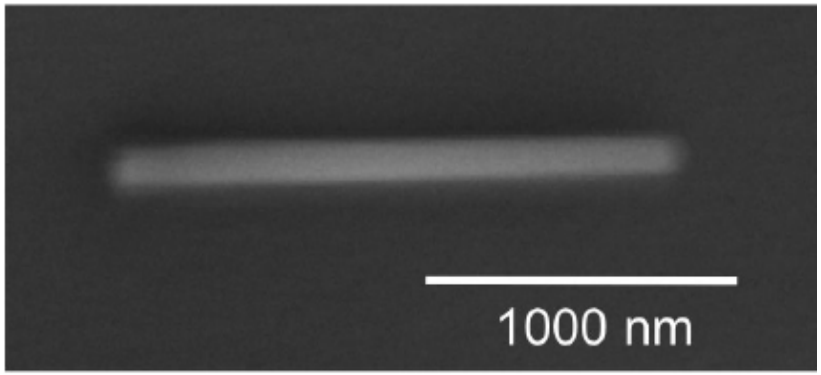

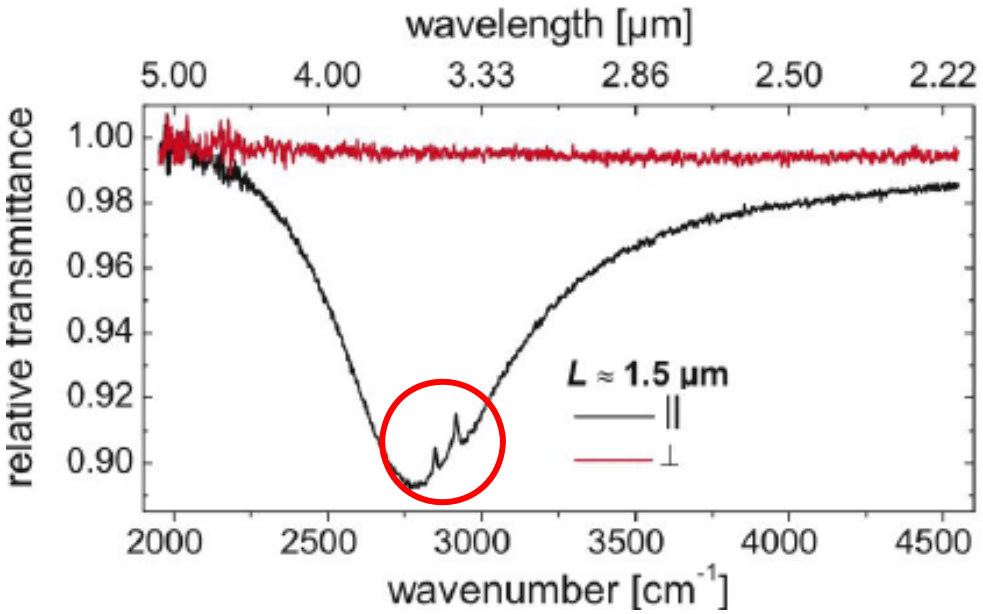

J. Aizpurua, Lecture given at SSOP Porquerolles, Sept. 2009

F. Neubrech et al. Phys. Rev. Lett. **101**, 157403 (2008)

Outline

- Basics: Plasmonics

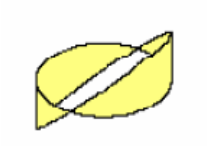

- Optical antennas for SERS

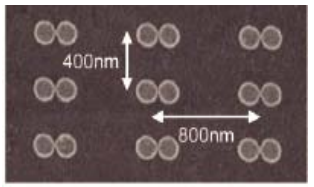

- ½ λ dipole Infrared antennas for SEIRA

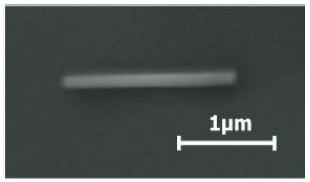

- Substrate-Enhanced Infrared Near-Field Microscopy

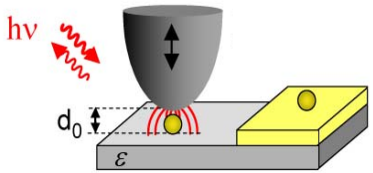

- THz Near-field Nanoscopy

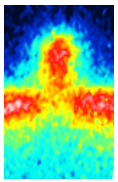

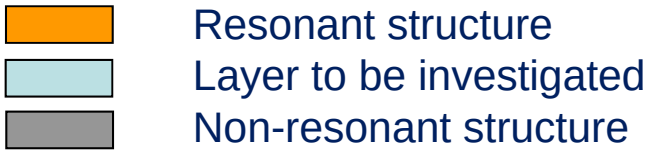

Resonant triangles (coated)

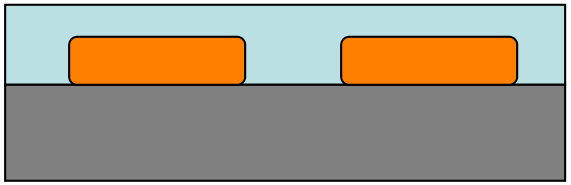

T.R. Jensen et al., J. Phys. Chem B**, 104**, 10549 (2000)

Resonant particle

(coated) (embedded)

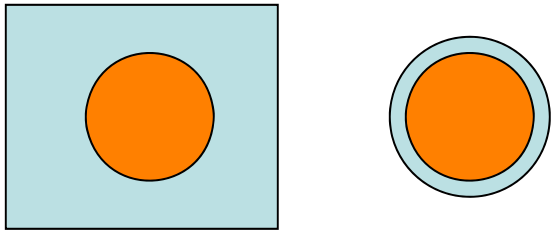

M.S. Anderson, App. Phys. Lett. **83**, 2964 (2003)

Nanoshell arrays

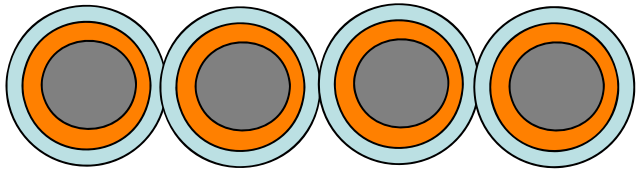

H. Wang et al., Angew. Chem. **46**, 9040 (2007)

Resonant rod (coated)

F. Neubrech et al., APL **89**, 253104 (2006)

Near-field IR spectroscopy

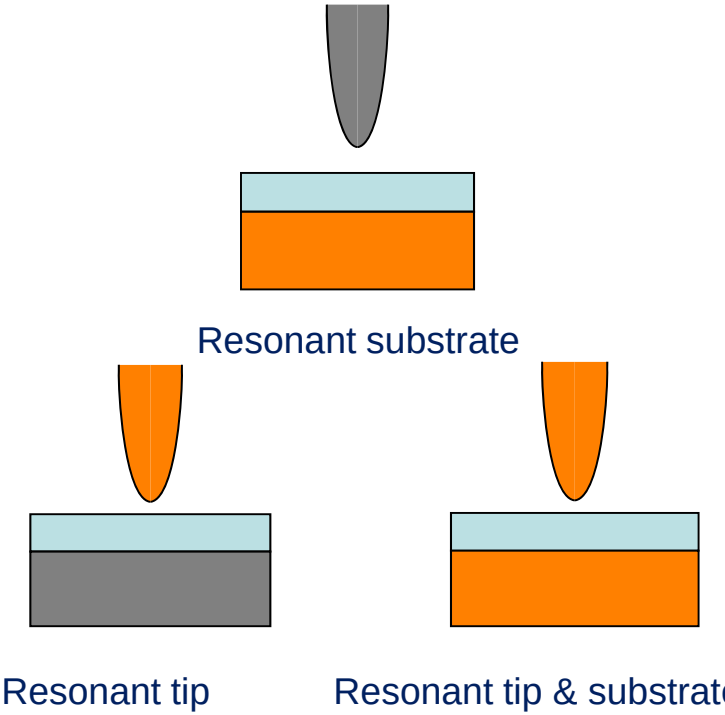

J. Aizpurua et al., Optics Exp **16**, 1529 (2008)

Scattering–type Near Field Optical Microscopy
Rainer Hillenbrand

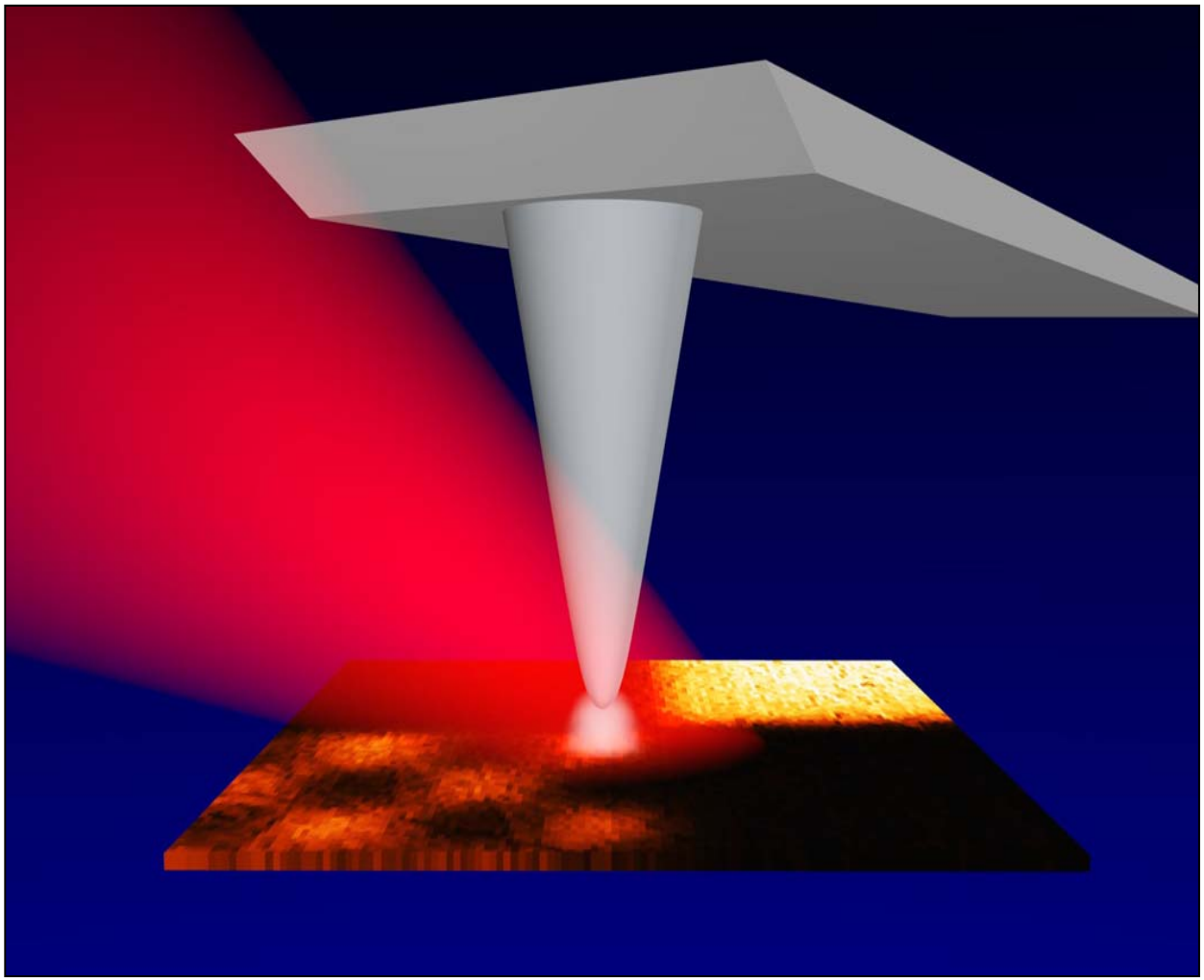

Localization of plasmons by a probe

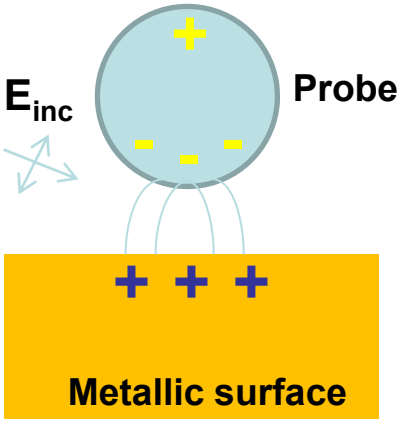

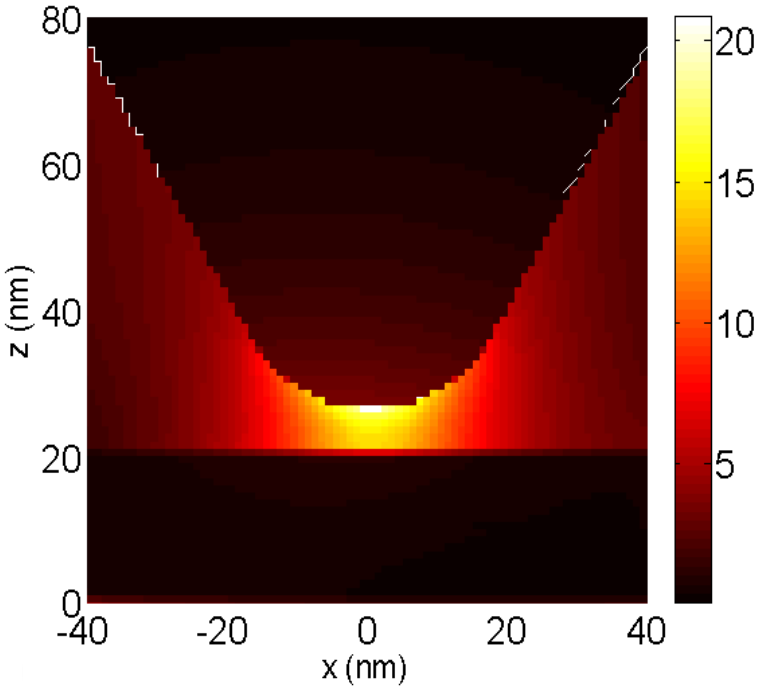

J. Aizpurua, Lecture given at SSOP Porquerolles, Sept. 2009

Dipolar sphere-plane near-field interaction

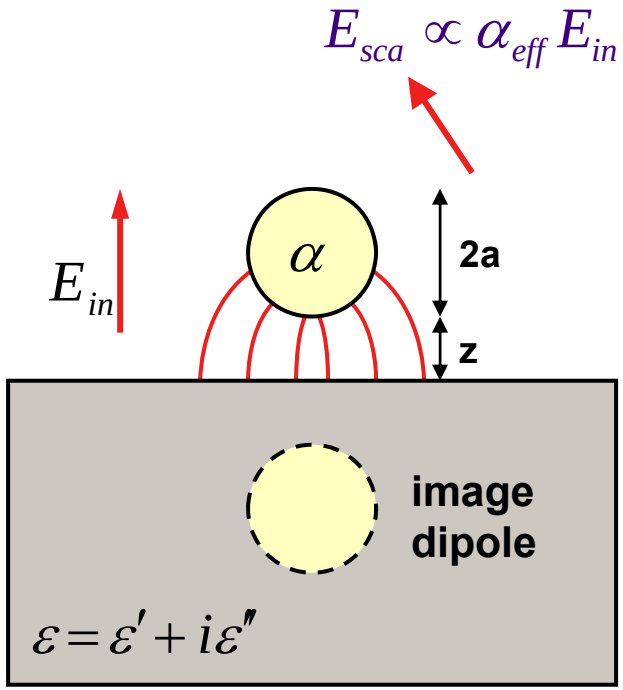

Polarizability of the tip

$$\alpha = 4\pi a^3 \frac{\varepsilon - 1}{\varepsilon + 2}$$

Effective polarizability of interacting dipoles

$$\alpha_{eff} = \frac{\alpha(1+\beta)}{1 - \frac{\alpha\beta}{16\pi(z+a)^3}} \quad \text{with} \quad \beta = \frac{\varepsilon - 1}{\varepsilon + 1}$$

→ **near-field interaction modifies amplitude and phase of Esca**

→ **resonance through a) sphere** $\varepsilon_p = -2$

b) plane $\varepsilon = -1$

No multipoles included in this description

s-SNOM contrast of SiC/Au

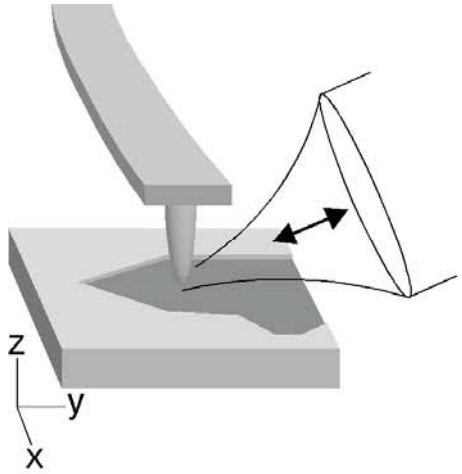

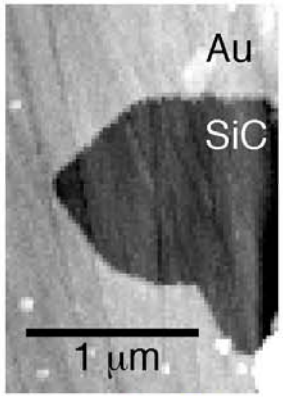

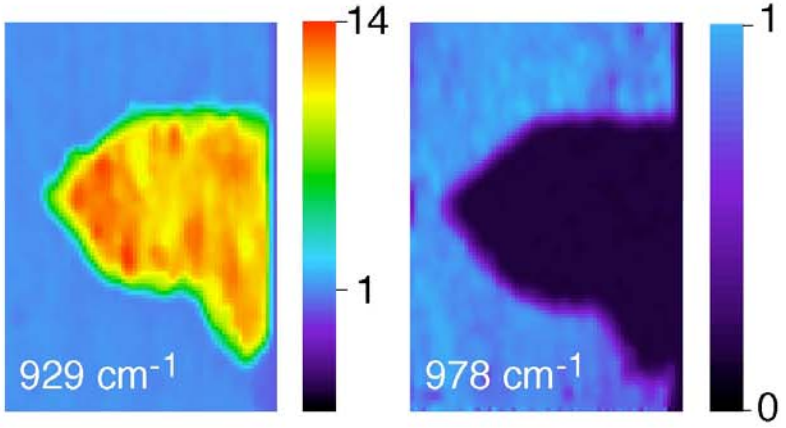

phonon-enhanced near-field interaction → **identification of materials at nanoscopic spatial resolution**

- strong signals
- high spectral sharpness
- optical fingerprint

< λ / 100 !

R. Hillenbrand, T. Taubner, F. Keilmann, Nature **418**, 159-162 (2002)

Can we do the same in a simple optical antenna?

Mapping the fields of a metal-nanoparticle

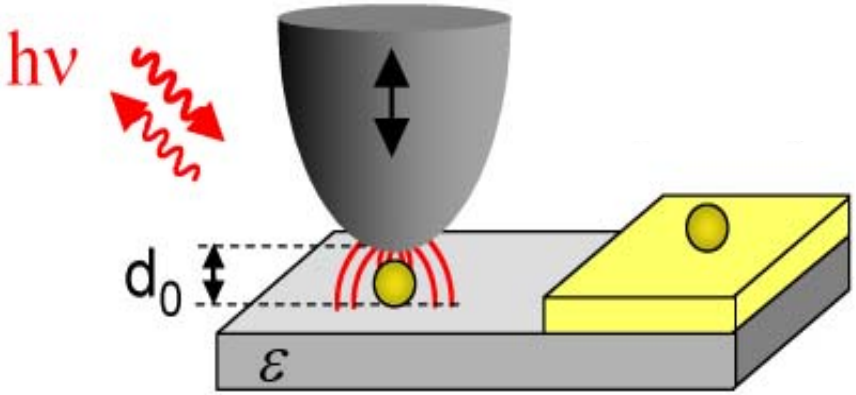

Absorption

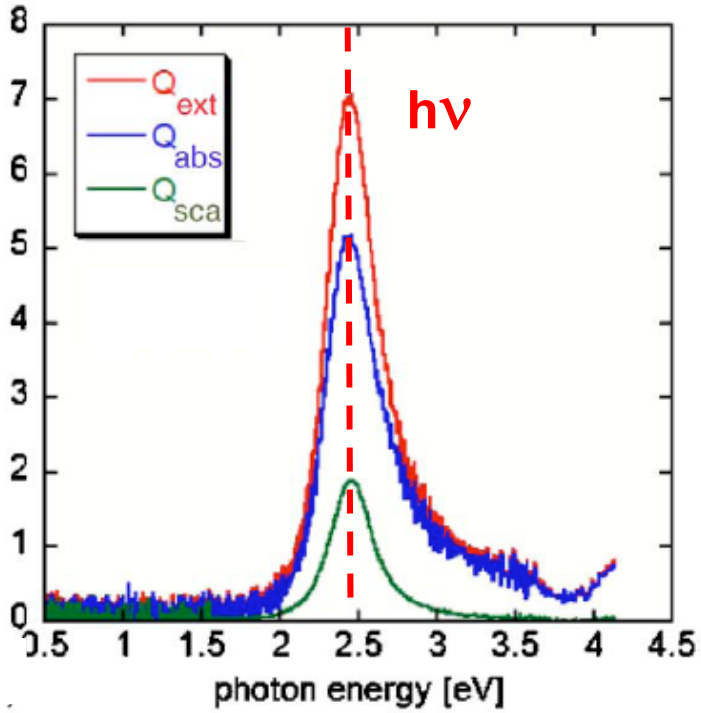

Imaging nanoparticles in the IR

Label-free high-resolution optical imaging of nanoparticles

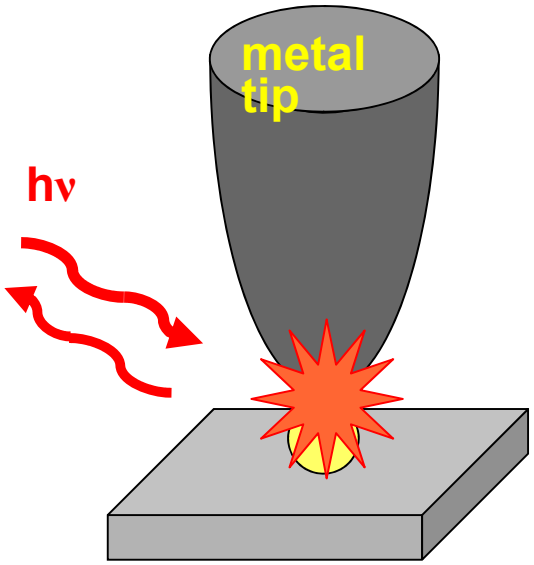

Probing - tip based chemicaly specific methods

IR	**Raman**
$C_{sca} \sim d^6/\lambda^4$	$C_{sca} \sim$
10^{-28} cm^2	10^{-30} cm^2
(1 nm particle @ mid-IR)	(typical molecule)

extremely small scattering cross-sections !

Solution → **field enhancement in an antenna cavity!**

J. Aizpurua, Lecture given at SSOP Porquerolles, Sept. 2009

Substrate-enhanced IR microscopy

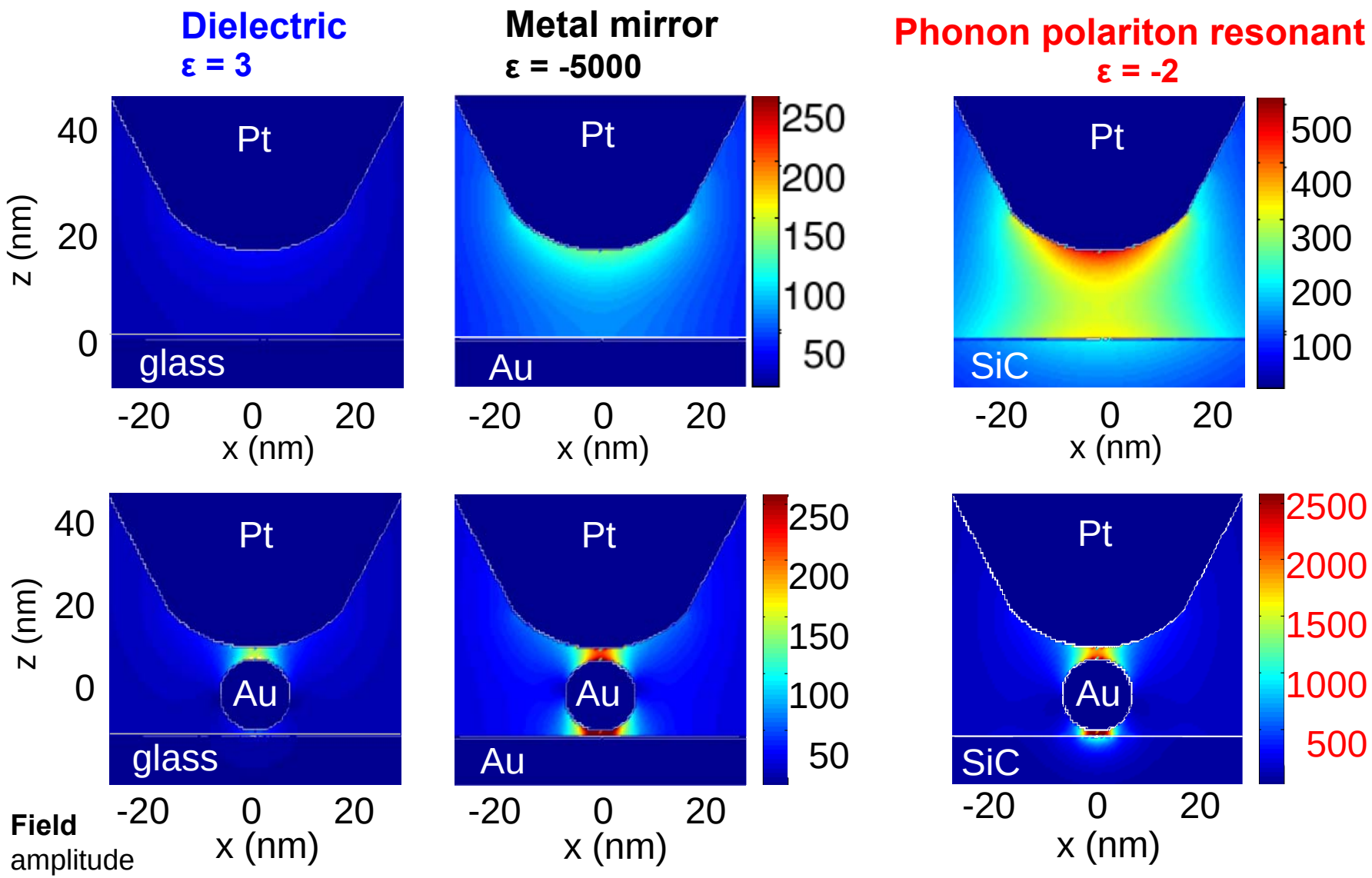

J. Aizpurua, Lecture given at SSOP Porquerolles, Sept. 2009

Cvitkovic et al., Phys. Rev. Lett. **97**, 060801 (2006)

Outline

- Basics: Plasmonics

- Optical antennas for SERS

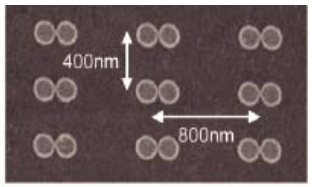

- Infrared antennas for SEIRA

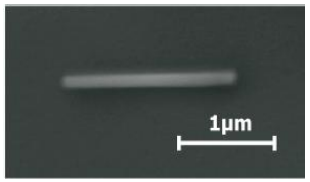

- Substrate-Enhanced Infrared Near-Field Microscopy

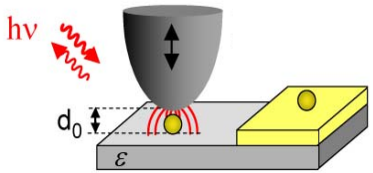

- THz Near-field Nanoscopy

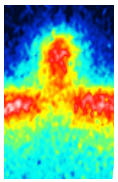

Terahertz radiation (THz, T-RAYS)

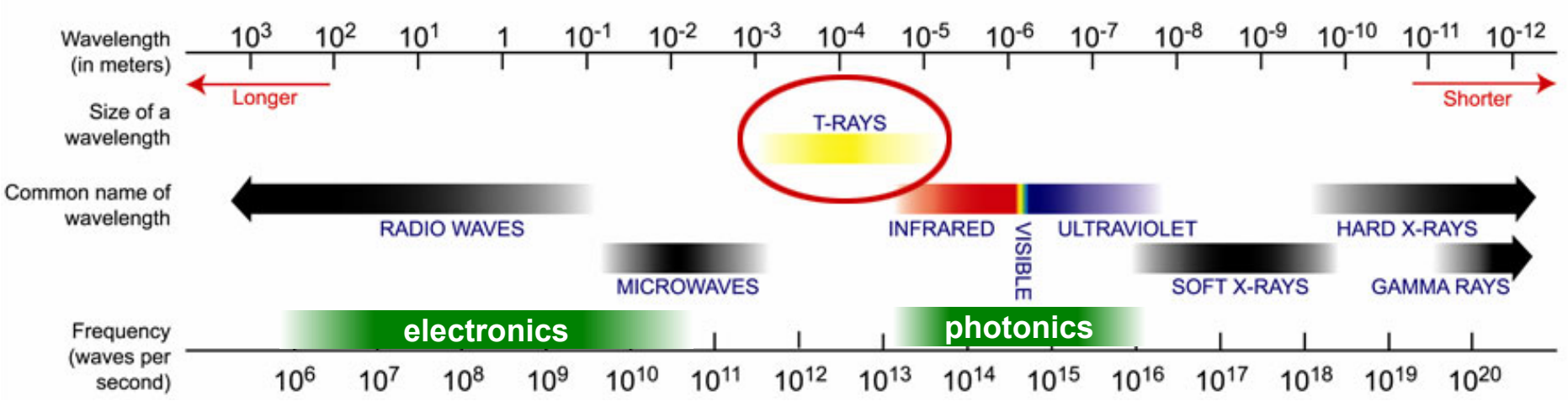

Frequencies between IR and THz (far-IR) are highly sensitive to

- **molecular vibrations → chemical composition**
- **crystal lattice vibrations → structural properties**
- **plasmons in doped semiconductors → electron properties**
- **…..**

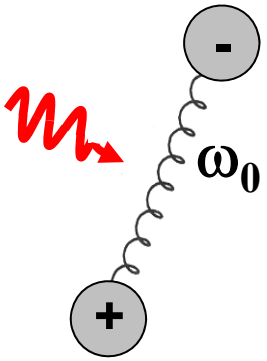

BUT: spatial resolution > $\lambda/2 \approx$ 10-100 μm

J. Aizpurua, Lecture given at SSOP Porquerolles, Sept. 2009

Theory predicts nanoscale confined THz fields

- Full electrodynamic calculation
- for 2.54 THz ($\lambda \approx 118$ µm) predicts field enhancement at tip apex
- Tip length: 1 µm ($\approx \lambda / 118$)
- 30 nm field confinement at tip apex, like for VIS or IR frequencies
- Mechanism: lightning-rod effect

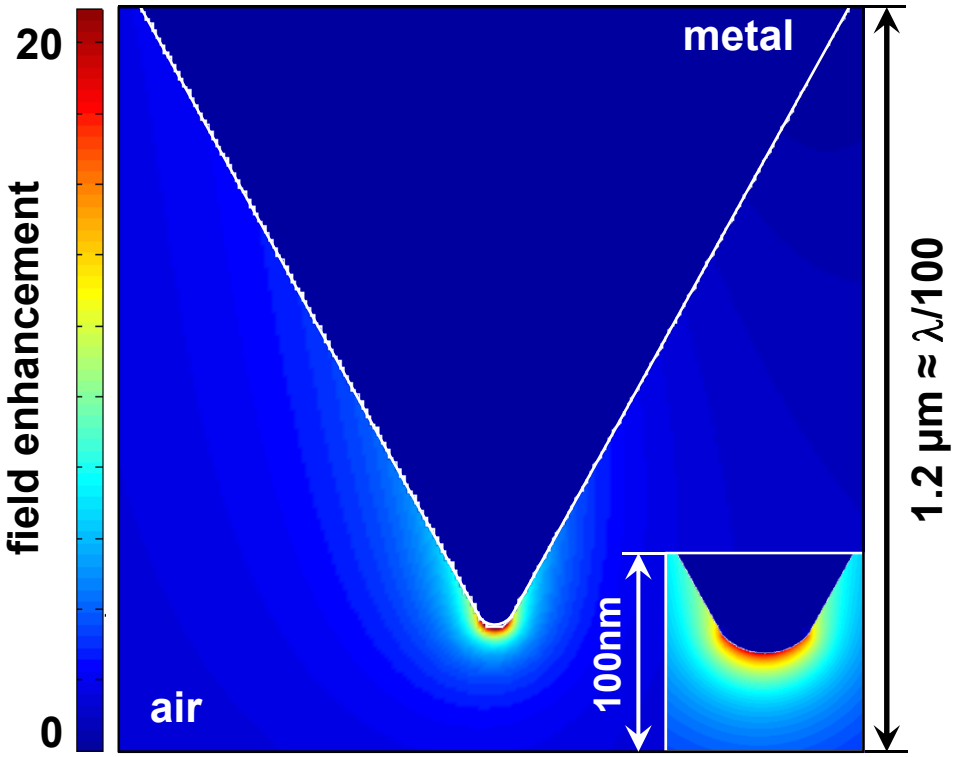

Boundary Element Method calculation

→ nanoscale confinement of THz fields can be achieved with metal tips much smaller than the wavelength, e.g. AFM tips

J. Aizpurua, Lecture given at SSOP Porquerolles, Sept. 2009

A. Huber et al. Nano Letters 8, 3766 (2008)

Lightning rod effect

- **Lightning rod effect**
  Needs:
  - **Geometric singularity**
  - **Proper polarization**
  - **Good conductor**

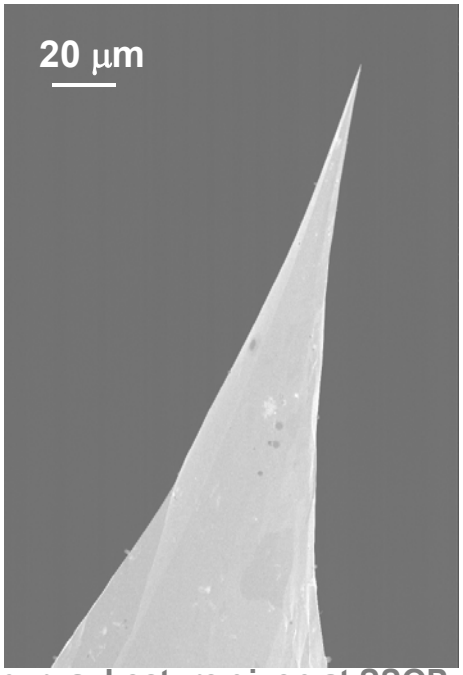

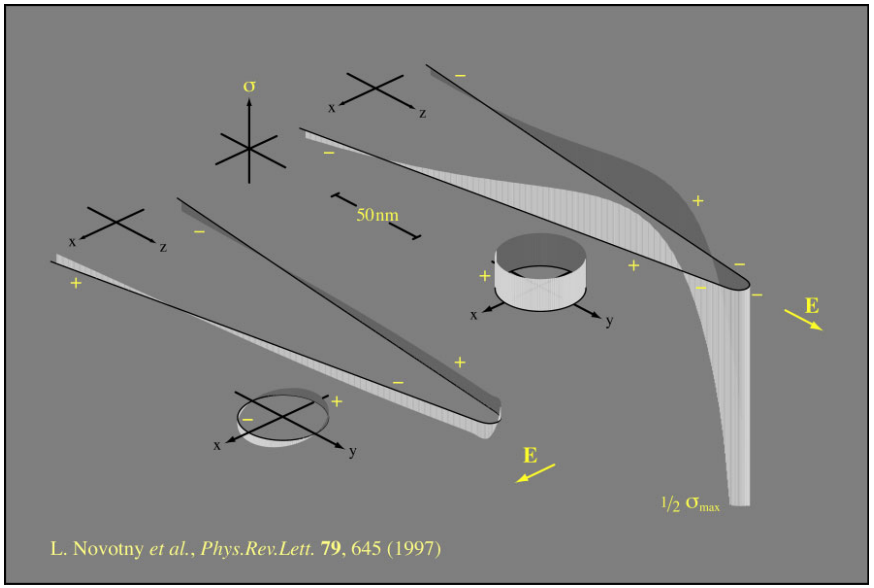

J. Aizpurua, Lecture given at SSOP Porquerolles, Sept. 2009

THz s-SNOM can map free carriers in semiconductor devices

SEM

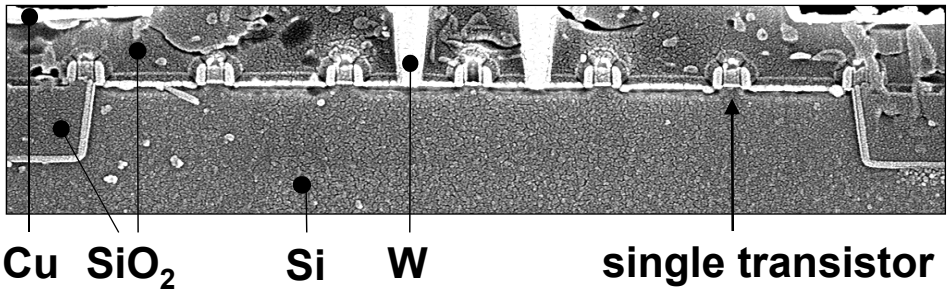

Infineon technologies

test structure containing transistors of 65 nm - technology

Topography

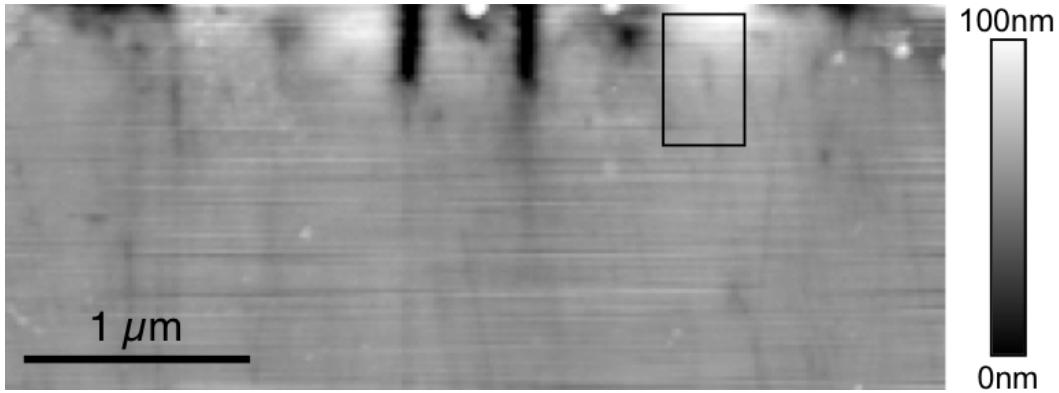

THz image

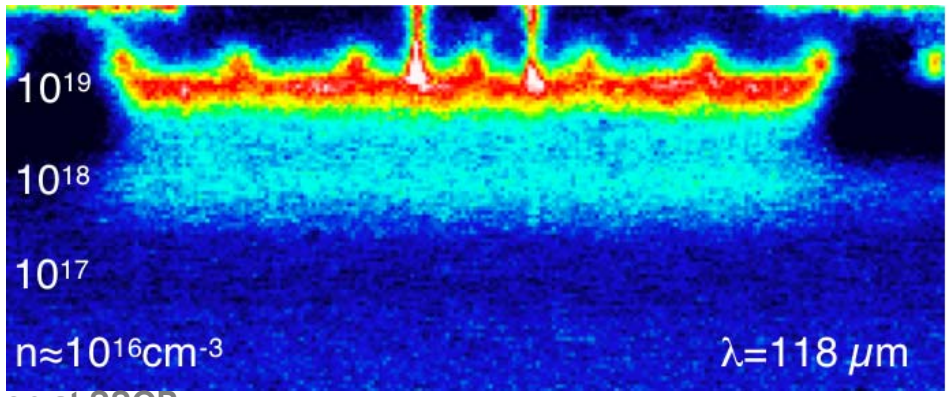

THz image exhibits material and free-carrier contrast

J. Aizpurua, Lecture given at SSOP Porquerolles, Sept. 2009

A. Huber et al. Nano Letters 8, 3766 (2008)

THz s-SNOM can map free carriers in semiconductor devices

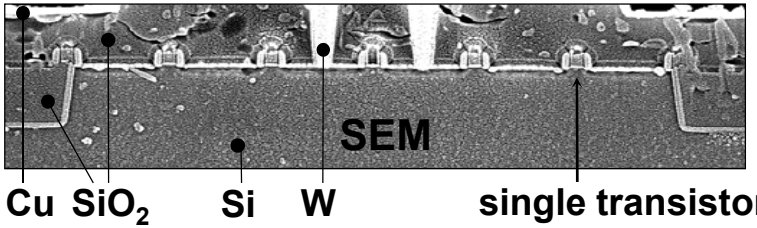

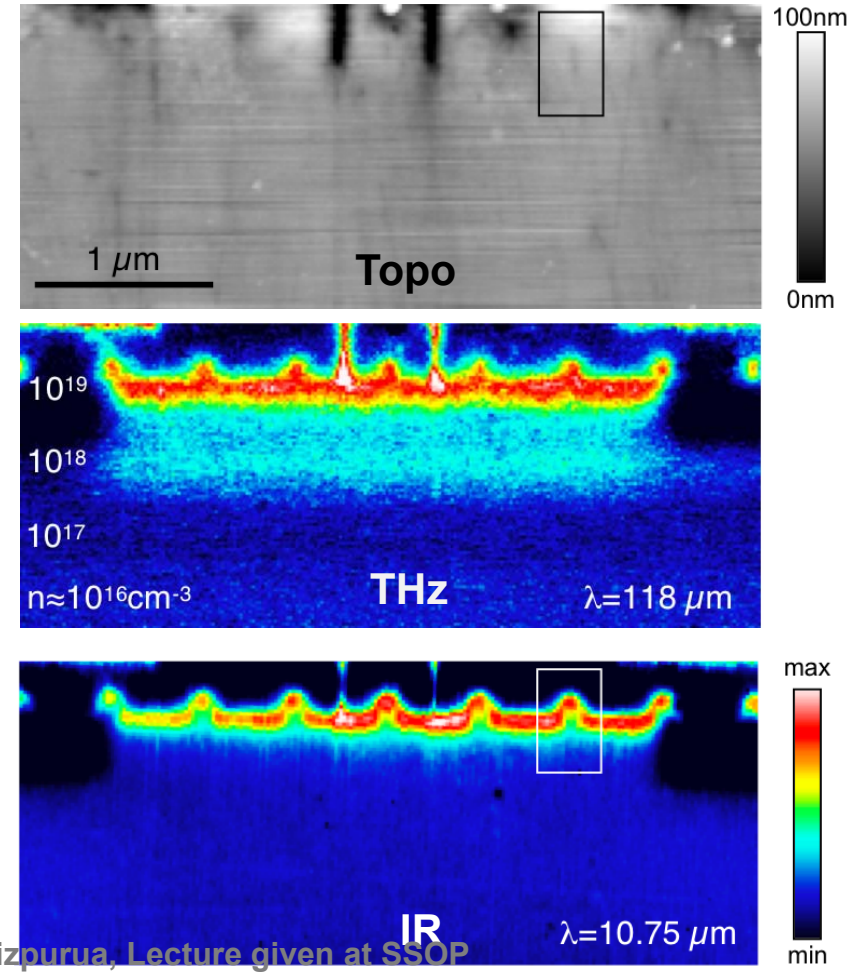

For doped semiconductors ε(ω) depends on concentration of free carriers:

$$\varepsilon(\omega) = \varepsilon_\infty \left(1 - \frac{\omega_P^2}{\omega^2 + i\gamma\omega}\right) \quad \text{with } \omega_P^2 = \frac{n\,e^2}{\varepsilon_0 \varepsilon_\infty m \cdot m_0}$$

Dipole model explains free-carrier contrast

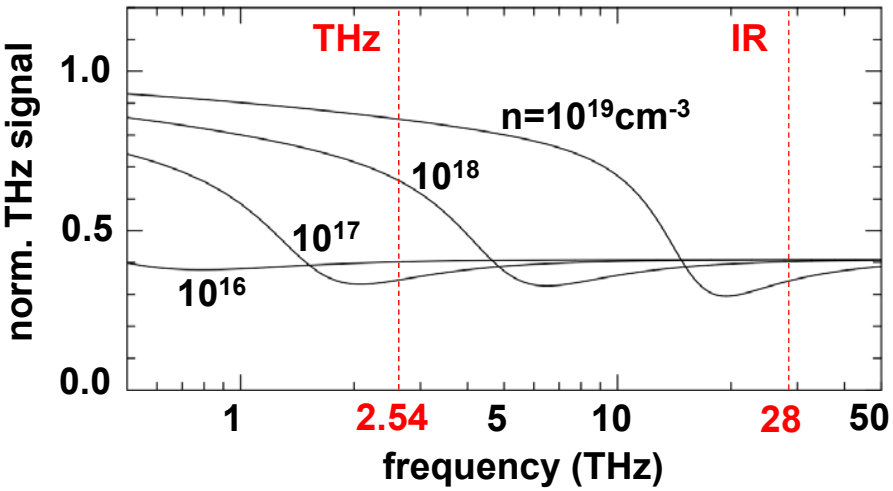

A. Huber et al. Nano Letters 8, 3766 (2008)